

**STRIPPING VOLTAMMETRIC PYROLYTIC  
GRAPHITE POLYANILINE SENSOR FOR  
SIMULTANEOUS DETERMINATION OF LEAD AND  
CADMIUM**

By

**PETER NAMUTALA WANYONYI**

Thesis submitted to the Board of Post Graduate Studies in partial fulfillment of the degree of

Master of Science in Chemistry of the University of Nairobi

**May 2014**

## DECLARATION

This thesis is my own original work and has not been submitted for examination in any other  
university

.....  
Wanyonyi Namutala Peter

156/72398/2008

Herewith our approval as supervisors

.....  
Prof. G.N. Kamau

Department of Chemistry, University of Nairobi

.....  
Dr. P.M. Guto

Department of Chemistry, University of Nairobi

## **DEDICATION**

I dedicate this work to my wife Sussy Nasimiyu, our two sons Denzel and Tervil. To all those who contributed towards the success of this work, Thank you.

## **ACKNOWLEDGEMENT**

I would like to thank Almighty God for giving me life, good health and determination to undertake this research. I wish to sincerely extend my gratitude to my supervisors Prof. G.N Kamau and Dr. Peter Guto for their guidance, patience, encouragement, academic and technical support during my research. I also wish to thank the entire Department of Chemistry especially the technical staff members Mr Amani, Mr Njoroge and Mr. Terere for their tireless effort and working closely with me during my research. I acknowledge the Department of Physics University of Nairobi for allowing me to use their potentiostat to carry out the analysis and ISP through Upsala University Sweden for donating the potentiostat. In particular I extend my sincere gratitude to Mr Muthoka and Mr Kamau for the support they rendered to me while I was working in the laboratory. To all, may God bless you abundantly.

## ABSTRACT

To improve sensitivity of a pyrolytic graphite electrode, a polyaniline thin film was coated on electrode substrate, via multipulse cyclic voltammetry electropolymerization to form pyrolytic graphite polyaniline sensor that was used successfully for simultaneous detection and determination of  $\text{Cd}^{2+}$  and  $\text{Pb}^{2+}$  ions. Various parameters were studied with reference to anodic stripping–square wave voltammetry signals. The experimental results depicted that the environment-friendly sensor had the ability to increase detection signal for  $\text{Cd}^{2+}$  and  $\text{Pb}^{2+}$  in the prepared solutions by 1.6 and 2.5 times respectively. Plots of peak current against deposition time, deposition potential, step potential, frequency and amplitude for a mixture of lead and cadmium ions showed high peak current for  $\text{Pb}(\text{NO})_3$  than  $\text{CdBr}_2$  solution. The highest peak current for the mixture was  $49.0\mu\text{A}$  obtained for  $\text{Pb}(\text{NO})_3$  solution, while that for  $\text{CdBr}_2$  solution was  $46.3\mu\text{A}$  at variable deposition time when other factors were held constant. A plot of peak current against frequency while other factors were held constant resulted in maximum peak current  $44\mu\text{A}$  and  $49\mu\text{A}$  at frequency of  $45\text{Hz}$  for  $\text{CdBr}_2$  and  $\text{Pb}(\text{NO})_3$  solution respectively. A similar plot of peak current against amplitude gave a maximum peak current of  $195\mu\text{A}$  and  $180\mu\text{A}$  at amplitude of  $0.12\text{V}$  for  $\text{CdBr}_2$  and  $\text{Pb}(\text{NO})_3$ . This amplitude was chosen for optimization of peak current. A plot of peak current against deposition potential gave optimized peak currents of  $46.3\mu\text{A}$  and  $48.8\mu\text{A}$  at deposition potential of  $0.05\text{V}$  for  $\text{CdBr}_2$  and  $\text{Pb}(\text{NO})_3$ , respectively. The plot of peak current against step potential gave two peaks at optimized potential of  $0.0405$ .

This suggested existence of inter-metallic bond formation between lead and cadmium ions. Competition between lead and cadmium on active sites of modified pyrolytic graphite electrode may also explain the observed peak suppression of cadmium. Lead seemed to outweigh cadmium for active sites because of its larger diffusivity. The calculation for the values of limits of detection (LOD) and limits of quantitation (LOQ) for cadmium bromide were higher than those of lead nitrate solution. The LOQ and LOD value for cadmium bromide solution was 0.908 ppm and 3.03 ppm respectively', while for  $\text{Pb}(\text{NO})_3$  solution, the calculated values were 0.11 ppm and 0.37 ppm in the same order.

## TABLE OF CONTENTS

DECLARATION .....	ii
DEDICATION .....	iii
ACKNOWLEDGEMENT .....	iv
ABSTRACT.....	v
LIST OF TABLES.....	xxi
LIST OF FIGURES .....	xxiv
<b>CHAPTER ONE</b> .....	<b>1</b>
1.0 INTRODUCTION .....	1
1.1 Background Information.....	1
1.2 Statement of the problem.....	4
1.3 Justification.....	5
1.4 Main Objectives .....	6
1.4.1 Specific objectives .....	6
<b>CHAPTER TWO</b> .....	<b>8</b>
2.0 LITERATURE REVIEW .....	8
2.1 Electrochemistry .....	8
2.2 Why Mercury free electrodes?.....	8
2.3 Electrochemical techniques .....	10

2.4	Linear sweep potential Voltammetry (LSPV) .....	13
2.4.1	Single – sweep voltammetry .....	14
2.4.2	Cyclic voltammetry.....	16
2.4.3	Anodic stripping -Square-Wave Voltammetry (AS-SWV) .....	21
2.4.4	Working electrode.....	23
2.4.5	Pyrolytic Graphite Electrode.....	23
2.4.6	Counter electrode .....	24
2.4.7	Reference electrode.....	25
2.4.8	Aqueous Reference Electrodes .....	26
2.4.9	Silver chloride electrode .....	27
2.4.10	Non-aqueous Reference Electrodes .....	30
2.4.11	Quasi-Reference Electrode (QRE).....	30
2.4.12	Pseudo-reference electrodes.....	31
<b>CHAPTER THREE</b> .....		<b>32</b>
3.0	METHODOLOGY AND INSTRUMENTATION.....	32
3.1	Reagents and Chemical solutions .....	32
3.2	Apparatus and procedure for cyclic Voltammetry.....	33
3.3	Apparatus and procedure for anodic stripping square wave voltammetry .....	34



3.3.1	Electrode modification protocol .....	35
3.3.2	Reagents and Chemical solutions .....	35
3.3.2.1	Apparatus and procedure for cyclic Voltammetry.....	36
3.3.2.2	Apparatus and procedure for anodic stripping square wave voltammetry .....	37
3.1.4	Electrode modification protocol .....	37
3.1.3.2	Procedure for optimization of deposition time for lead nitrate solution on un-modified pyrolytic graphite electrode .....	38
3.1.3.3	Procedure for optimization of frequency for lead nitrate solution on un-modified pyrolytic graphite electrode.....	38
3.1.3.4	Procedure for optimization of deposition potential for lead nitrate solution on un-modified pyrolytic graphite electrode .....	39
3.1.3.5	Procedure for optimization of step potential for lead nitrate solution on un-modified pyrolytic graphite electrode .....	39
3.1.3.6	Procedure for optimization of amplitude for lead nitrate solution on un-modified pyrolytic graphite electrode.....	39
3.1.4	Apparatus and procedure for anodic stripping-Anodic square wave voltammetry on un-modified pyrolytic graphite electrode for cadmium bromide solution .....	40
3.1.4.1	Procedure for optimization of deposition time for cadmium bromide solution on un-modified pyrolytic graphite electrode.....	40

3.1.4.2 Procedure for optimization of frequency for cadmium bromide solution on un-modified pyrolytic graphite electrode .....	40
3.1.4.3 Procedure for optimization of amplitude for cadmium bromide solution on un-modified pyrolytic graphite electrode .....	40
3.1.4.4 Procedure for optimization of deposition potential for cadmium bromide solution on un-modified pyrolytic graphite electrode.....	41
3.1.4.5 Procedure for optimization of step potential for Cadmium bromide solution on un-modified pyrolytic graphite electrode .....	41
3.1.5 Apparatus and procedure for Anodic stripping-square wave voltammetry on un-modified pyrolytic graphite electrode for a mixture of cadmium bromide and lead nitrate solution .....	42
3.1.5.1 Procedure for optimization of deposition time for a mixture of Lead nitrate and cadmium bromide solution on un-modified pyrolytic graphite electrode .....	42
3.1.5.2 Procedure for optimization of frequency for a mixture of Lead nitrate and cadmium bromide solution on un-modified pyrolytic graphite electrode .....	42
3.1.5.3 Procedure for optimization of Amplitude for a mixture of Lead nitrate and cadmium bromide solution on un-modified pyrolytic graphite electrode .....	42
3.1.5.4 Procedure for optimization of step potential for a mixture of Lead nitrate and cadmium bromide solution on un-modified pyrolytic graphite electrode .....	43
3.1.5.5 Procedure for optimization of deposition potential for a mixture of cadmium bromide solution on un-modified pyrolytic graphite electrode.....	43

3.1.6 Apparatus and procedure for Anodic stripping-square wave voltammetry on modified pyrolytic graphite electrode for a mixture of cadmium bromide and lead nitrate solution .....	43
3.1.7 Apparatus and procedure for determination of LOD and LOQ using Anodic stripping-square wave voltammetry on modified pyrolytic graphite electrode for a mixture of cadmium bromide and lead nitrate solution.....	44
3.1.8 Procedure for optimization of deposition time for lead nitrate solution on un-modified pyrolytic graphite electrode .....	44
3.1.9 Procedure for optimization of frequency for lead nitrate solution on un-modified pyrolytic graphite electrode.....	45
3.1.3.4 Procedure for optimization of deposition potential for lead nitrate solution on un-modified pyrolytic graphite electrode .....	45
3.1.3.5 Procedure for optimization of step potential for lead nitrate solution on un-modified pyrolytic graphite electrode .....	45
3.1.3.5 Procedure for optimization of amplitude for lead nitrate solution on un-modified pyrolytic graphite electrode.....	46
3.1.4 Apparatus and procedure for anodic stripping-Anodic square wave voltammetry on un-modified pyrolytic graphite electrode for cadmium bromide solution .....	46
3.1.4.1 Procedure for optimization of deposition time for cadmium bromide solution on un-modified pyrolytic graphite electrode.....	46

3.1.4.2 Procedure for optimization of frequency for cadmium bromide solution on un-modified pyrolytic graphite electrode .....	46
3.1.4.3 Procedure for optimization of amplitude for cadmium bromide solution on un-modified pyrolytic graphite electrode .....	47
3.1.4.4 Procedure for optimization of deposition potential for cadmium bromide solution on un-modified pyrolytic graphite electrode.....	47
3.1.4.5 Procedure for optimization of step potential for Cadmium bromide solution on un-modified pyrolytic graphite electrode .....	47
3.1.5 Apparatus and procedure for Anodic stripping-square wave voltammetry on un-modified pyrolytic graphite electrode for a mixture of cadmium bromide and lead nitrate solution .....	48
3.1.5.1 Procedure for optimization of deposition time for a mixture of Lead nitrate and cadmium bromide solution on un-modified pyrolytic graphite electrode .....	48
3.1.5.2 Procedure for optimization of frequency for a mixture of Lead nitrate and cadmium bromide solution on un-modified pyrolytic graphite electrode .....	48
3.1.5.3 Procedure for optimization of Amplitude for a mixture of Lead nitrate and cadmium bromide solution on un-modified pyrolytic graphite electrode .....	48
3.1.5.4 Procedure for optimization of step potential for a mixture of Lead nitrate and cadmium bromide solution on un-modified pyrolytic graphite electrode .....	49
3.1.5.5 Procedure for optimization of deposition potential for a mixture of cadmium bromide solution on un-modified pyrolytic graphite electrode.....	49

3.1.6 Apparatus and procedure for Anodic stripping-square wave voltammetry on modified pyrolytic graphite electrode for a mixture of cadmium bromide and lead nitrate solution .....	49
3.1.7 Apparatus and procedure for determination of LOD and LOQ using Anodic stripping-square wave voltammetry on modified pyrolytic graphite electrode for a mixture of cadmium bromide and lead nitrate solution.....	50
<b>CHAPTER FOUR</b> .....	<b>51</b>
4.0 RESULTS AND DISCUSSIONS.....	51
4.1 Cyclic voltammetry.....	51
4.1.1 Voltammetric study of 4.0mM ferrocene in 0.1M TEAB in acetonitrile/water (1:1) as a standard.....	51
4.1.2 Cyclic voltammetry of 5.0Mm Lead nitrate in 0.1M KCl using modified and un-modified pyrolytic graphite electrode .....	57
4.1.3 Cyclic voltammetry of 5.0mM cadmium bromide in 0.1M KCl using modified pyrolytic graphite electrode at different scan rate .....	61
4.2 Anodic stripping-square wave voltammetry on lead nitrate solution .....	62
4.2.1 The effect of deposition time on peak current obtained using Anodic stripping-square wave voltammetry on un-modified pyrolytic graphite electrode .....	63
4.2.2 The effect of frequency on peak current obtained using Anodic stripping-square wave voltammetry on un-modified pyrolytic graphite electrode .....	66

4.2.3	The effect of amplitude on peak current obtained using Anodic stripping-square wave voltammetry on un-modified pyrolytic graphite electrode .....	69
4.2.4	The effect of deposition potential on peak current obtained using Anodic stripping-square wave voltammetry (AS-SWV) on un-modified pyrolytic graphite electrode.....	72
4.2.5	The effect of step potential on peak current obtained using Anodic stripping-square wave voltammetry on un-modified pyrolytic graphite electrode .....	75
	Table 4-11: Peak current and step potential.....	76
4.3	Anodic stripping-square wave voltammetry on cadmium bromide solution.....	78
4.3.1	The effect of deposition time on peak current obtained using Anodic stripping-square wave voltammetry on un-modified pyrolytic graphite electrode .....	78
4.3.2	The effect of frequency on peak current obtained using Anodic stripping-square wave voltammetry on un-modified pyrolytic graphite electrode .....	81
4.3.3	The effect of wave amplitude on peak current obtained using Anodic stripping-square wave voltammetry on un-modified pyrolytic graphite electrode .....	84
4.3.4	The effect of deposition potential on peak current obtained using Anodic stripping-square wave voltammetry on un-modified pyrolytic graphite electrode.....	86
4.3.5	The effect of step potential on peak current obtained using Anodic stripping-square wave voltammetry on un-modified pyrolytic graphite electrode .....	89
4.4	Anodic stripping-square wave voltammetry on a mixture of lead nitrate and cadmium bromide solution using un-modified pyrolytic graphite electrode.....	91

4.4.1	The effect of deposition time on peak current obtained using Anodic stripping-square wave voltammetry on un-modified pyrolytic graphite electrode for 1 ppm mixture of lead nitrate and cadmium bromide .....	92
4.4.2	The effect of frequency on peak current obtained using Anodic stripping-square wave voltammetry on un-modified pyrolytic graphite electrode on 1 ppm mixture of lead nitrate and Cadmium bromide solution.....	95
4.4.3	The effect of amplitude on peak current obtained using Anodic stripping-square wave voltammetry on un-modified pyrolytic graphite electrode of 1 ppm mixture of lead nitrate and Cadmium bromide solution.....	98
4.4.4	The effect of deposition potential on peak current obtained using Anodic stripping-square wave voltammetry on un-modified pyrolytic graphite electrode of 1 ppm mixture of lead nitrate and Cadmium bromide solution.....	101
4.4.5	The effect of step potential on peak current obtained using Anodic stripping-square wave voltammetry on un-modified pyrolytic graphite electrode of 1 ppm mixture of lead nitrate and Cadmium bromide solution.....	104
4.5	Anodic stripping-square wave voltammetry on lead nitrate solution using modified pyrolytic graphite polyaniline sensor.....	107
4.5.1	The effect of deposition time on peak current obtained using Anodic stripping-square wave voltammetry on modified pyrolytic graphite electrode .....	107
4.5.2	The effect of frequency on peak current obtained using Anodic stripping-square wave voltammetry on modified pyrolytic graphite electrode for 30 ppm lead Nitrate.....	112

4.5.3	The effect of deposition potential on peak current obtained using Anodic stripping-square wave voltammetry on modified pyrolytic graphite electrode .....	115
4.5.4	The effect of Amplitude on peak current obtained using Anodic stripping-square wave voltammetry on modified pyrolytic graphite electrode. ....	118
4.5.5	The effect of step potential on peak current obtained using Anodic stripping-square wave voltammetry on modified pyrolytic graphite electrode .....	121
4.6	Anodic stripping-square wave voltammetry on a mixture of lead nitrate and cadmium bromide solution carried out using modified pyrolytic graphite electrode.....	124
4.6.1	The effect of deposition time on peak current obtained using Anodic stripping-square wave voltammetry on modified pyrolytic graphite electrode for 1 ppm mixture of lead nitrate and Cadmium bromide solution.....	124
4.6.2	The effect of frequency on peak current obtained using Anodic stripping-square wave voltammetry on modified pyrolytic graphite electrode for 1 ppm mixture of lead nitrate and Cadmium bromide solution.....	130
4.6.3	The effect of amplitude on peak current obtained using Anodic stripping-square wave voltammetry on modified pyrolytic graphite electrode of 1 ppm lead nitrate and cadmium bromide solution.....	132
4.6.4	The effect of deposition potential on peak current obtained using Anodic stripping-square wave voltammetry on modified pyrolytic graphite electrode.....	135



4.6.5	The effect of step potential on peak current obtained using Anodic stripping-square wave voltammetry on modified pyrolytic graphite electrode .....	138
4.7	Comparative analysis of peak currents obtained using modified and un-modified pyrolytic electrode for lead nitrate solutions.....	141
4.7.1	The effect of deposition time on peak current obtained using Anodic stripping-square wave voltammetry on modified and un-modified pyrolytic graphite electrode for lead nitrate solution.....	141
4.7.2	The effect of frequency on peak current obtained using Anodic stripping-square wave voltammetry on modified and un-modified pyrolytic graphite electrode for lead nitrate solution.....	144
4.7.3	The effect of amplitude on peak current obtained using Anodic stripping-square wave voltammetry on modified and un-modified pyrolytic graphite electrode for lead nitrate solution.....	146
4.7.4	The effect of deposition potential on peak current obtained using Anodic stripping-square wave voltammetry on modified and un-modified pyrolytic graphite electrode for lead nitrate solution.....	147
4.7.5	The effect of step potential on peak current obtained using Anodic stripping-square wave voltammetry on modified and un-modified pyrolytic graphite electrode for lead nitrate solution.....	150
4.8	Comparative analysis of peak currents obtained using modified and un-modified pyrolytic electrode for a mixture of 1 ppm lead nitrate and cadmium bromide solutions .....	152

4.8.1	The effect of deposition time on peak current obtained using Anodic stripping-square wave voltammetry on modified and un-modified pyrolytic graphite electrode for a mixture of 1 ppm lead nitrate and cadmium bromide solutions.....	152
4.8.2	The effect of frequency on peak current obtained using Anodic stripping-square wave voltammetry on modified and un-modified pyrolytic graphite electrode for a mixture of 1 ppm lead nitrate and cadmium bromide solutions.....	154
4.8.3	The effect of amplitude on peak current obtained using Anodic stripping-square wave voltammetry on modified and un-modified pyrolytic graphite electrode for a mixture of 1 ppm lead nitrate and cadmium bromide solutions.....	157
4.8.4	The effect of deposition potential on peak current obtained using Anodic stripping-square wave voltammetry on modified and un-modified pyrolytic graphite electrode for a mixture of 1 ppm lead nitrate and cadmium bromide solutions.....	160
4.8.5	The effect of step potential on peak current obtained using Anodic stripping-square wave voltammetry on modified and un-modified pyrolytic graphite electrode for a mixture of 1 ppm lead nitrate and cadmium bromide solutions.....	162
4.9	Determination of Limits of Detection (LOD) and Limits of Quantitation (LOQ) .....	164
4.9.1	LOD and Limits of Quantitation (LOQ) for cadmium bromide.....	165
4.9.2	Limits of detection (LOD) and Limits of Quantitation (LOQ) for lead nitrate solution ....	168
<b>CHAPTER FIVE....</b> .....		172
<b>CONCLUSIONS AND RECOMMENDATIONS</b> .....		172

5.1	CONCLUSIONS.....	172
5.1.1	Cyclic voltammetry.....	172
5.1.2	Anodic stripping-square wave voltammetry.....	172
5.2	Recommendations.....	174
	REFERENCES .....	175

## ABBREVIATIONS

ASV	Anodic stripping- voltammetry
CSV	Cathodic stripping-voltammetry
DDAB	Didecyldimethylammonium bromide
$E_p$	Peak potential
HMDE	Hanging Mercury-Drop Electrode
MFEs	Mercury, in the form of mercury-film electrodes
SCE	Saturated Calomel electrode
SV	Stripping voltammetry
SWV	Square wave voltammetry
TBAP	Tetrabutylammonium perchlorate
TEAB	Tetraethylammoniumbromide
AS-SWV	Anodic stripping -square wave voltammetry
PVS	Polyvinyl sulfonate
LOD	Limit of detection
LOD	Limit of quantitation
TBABF	Tetrabutylammonium tetrafluoroborate
QRE	Quasi-Reference Electrode (QRE)

## LIST OF TABLES

<b>Table 2–1:</b> The potential of a silver chloride reference electrode with respect to the standard hydrogen electrode (SHE).....	29
<b>Table 4-1:</b> Scan rate studies of 0.4 mM ferrocene in 0.1 M TEAB in acetonitrile/water (1:1).....	52
<b>Table 4-2:</b> Square root of Scan rate against peak current for ferrocene in 0.1 M TEAB, acetonitrile/water (1:1).....	53
<b>Table 4-3:</b> Scan rate against peak current for ferrocene in 0.1 M TEAB, acetonitrile/water (1:1). .....	55
<b>Table 4-4:</b> Anodic and cathodic peak currents for 5mM lead nitrate. ....	58
<b>Table 4-5:</b> Anodic peak current versus square root of scan rate for Lead Nitrate for modified electrode.....	59
<b>Table 4-6:</b> Scan rate studies of cadmium bromide in 0.1 M KCl. ....	61
<b>Table 4-7:</b> Peak current and deposition time. ....	64
<b>Table 4-8:</b> Peak current and Frequency using un-modified pyrolytic graphite electrode.....	67
<b>Table 4-9:</b> Peak current and amplitude. ....	70
<b>Table 4-10:</b> Peak current and deposition potential obtained using un-modified electrode.....	73
<b>Table 4-11:</b> Peak current and step potential.....	76
<b>Table 4-12:</b> Peak current and deposition time. ....	80
<b>Table 4-13:</b> Peak current and frequency. ....	82
<b>Table 4-14:</b> Peak current and Phase amplitude.....	85
<b>Table 4-15:</b> Peak current and deposition potential.....	87
<b>Table 4-16:</b> Peak current and step potential.....	90

<b>Table 4-17:</b> Peak current and deposition time. ....	94
<b>Table 4-18:</b> Peak current and Frequency. ....	97
<b>Table 4-19:</b> Peak current and amplitude. ....	100
<b>Table 4-20:</b> Peak current and deposition potential.....	102
<b>Table 4-21:</b> Peak current and Step potential. ....	105
<b>Table 4-22:</b> Peak and deposition time.....	111
<b>Table 4-23:</b> Peak current and Frequency. ....	114
<b>Table 4-24:</b> Peak current and deposition potential.....	117
<b>Table 4-25:</b> Peak current and Phase amplitude.....	120
<b>Table 4-26:</b> Peak current and step up potential.....	123
<b>Table 4-27:</b> Peak current and deposition time. ....	127
<b>Table 4-28:</b> Peak current and frequency. ....	131
<b>Table 4-29:</b> Peak current and Phase amplitude.....	134
<b>Table 4-30:</b> Peak current and Deposition potential.....	137
<b>Table 4-31:</b> Peak current and Step potential. ....	140
<b>Table 4-32:</b> Peak current and deposition time for modified and un-modified electrode. ....	142
<b>Table 4-33:</b> Peak current and Frequency for modified and un-modified electrode.....	145
<b>Table 4-34:</b> Peak current and amplitude for modified and un-modified electrode.....	147
<b>Table 4-35:</b> Peak current and deposition potential for modified and un-modified electrode. ....	148
<b>Table 4-36:</b> Peak current and step potential for modified and un-modified electrode. ....	150
<b>Table 4-37:</b> Deposition time for modified and un-modified electrode. ....	153
<b>Table 4-38:</b> Peak current and frequency for modified and un-modified electrode.....	155

<b>Table 4-39:</b> Peak current and phase amplitude for modified and un-modified electrode.....	158
<b>Table 4-40:</b> Peak current and deposition potential for modified and un-modified electrode. ....	161
<b>Table 4-41:</b> Peak current and step potential for modified and un-modified electrode. ....	163
<b>Table 4-42:</b> Peak current and concentration. ....	165
<b>Table 4-43:</b> Summary output for $\text{CdBr}_2$ .....	166
<b>Table 4-44:</b> Summary Output for $\text{Pb}(\text{NO})_3$ .....	169

## LIST OF FIGURES

<b>Figure 1.1:</b> Repeat unit of the emeraldine oxidation state of polyaniline in the undoped, base form (top) and the fully doped, acid form (bottom). .....	2
<b>Figure 2.1:</b> cyclic voltammogram of reversible analyte. ....	18
<b>Figure 2. 2:</b> Plot of peak currents against various parameters. ....	22
<b>Figure 2.3:</b> Sheets of pyrolytic carbon.....	23
<b>Figure 2.4:</b> Silver chloride electrodes.....	27
<b>Figure 3.1:</b> Three electrode system, Potentialstat and the computer. ....	33
<b>Figure 4.1:</b> Cyclic voltammogram of 4mM ferrocene in 0.1 M TEAB in acetonitrile/water (1:1) at a scan rate of 0.010 VS <sup>-1</sup> .....	53
<b>Figure 4.2:</b> A plot of anodic peak current versus square root of scan rate for ferrocene.....	54
<b>Figure 4.3:</b> A plot of peak anodic current versus square root of scan rate for ferrocene.....	55
<b>Figure 4.4:</b> Cyclic voltammogram of 5.0mM Lead nitrate in 0.1M KCl using un-modified pyrolytic graphite electrode at scan rate of 0.035 Vsec-1.....	57
<b>Figure 4. 5:</b> Cyclic voltammogram of 5.0mM lead nitrate in 0.1M KCl using modified pyrolytic graphite electrode at scan rate of 0.010 Vs <sup>-1</sup> .....	58
<b>Figure 4. 6:</b> A plot of peak anodic current versus square root of scan rate for Lead nitrate on modified electrode. ....	60
<b>Figure 4.7:</b> Resultant Voltammogram of Cadmium bromide obtained at scan rate of 0.05 VS <sup>-1</sup> using pyrolytic graphite as working electrode.....	62
<b>Figure 4.8:</b> Square wave voltammogram for 30 ppm Lead nitrate solution obtained at 120 seconds deposition time using un-modified Pyrolytic graphite as working electrode. ....	63



**Figure 4.9:** A plot of peak current against deposition time for lead nitrate solution. .... 65

**Figure 4.10:** Square wave voltammogram for 0.1M KCl (Blank) solution obtained at Frequency of 15 Hz using bare Pyrolytic graphite as working electrode. .... 66

**Figure 4.11:** Square wave voltammogram for 30 ppm Lead nitrate solution obtained at Frequency of 20 Hz using un-modified Pyrolytic graphite as working electrode. .... 67

**Figure 4. 12:** A plot of peak current against Frequency for 30ppm lead nitrate solution. .... 68

**Figure 4. 13:** Square wave voltammogram for 30 ppm Lead nitrate solution obtained at amplitude of 0.08 Volts using un-modified Pyrolytic graphite as working electrode. .... 69

**Figure 4. 14:** A plot of peak current against Change in phase amplitude using un-modified pyrolytic graphite electrode. .... 71

**Figure 4. 15:** Square wave voltammogram for 30 ppm Lead nitrate solution obtained at deposition potential 0.05 Volts using un-modified Pyrolytic graphite as working electrode. .... 72

**Figure 4. 16:** A plot of peak current against deposition potential..... 74

**Figure 4. 17:** Square wave voltammogram for 30 ppm Lead nitrate solution obtained at step potential of 0.00605 Volts using un-modified Pyrolytic graphite as working electrode. .... 75

**Figure 4. 18:** A plot of peak current against step potential..... 77

**Figure 4. 19:** Voltammogram of 0.1M KCl (Blank) obtained at 120 seconds deposition time using un-modified Pyrolytic graphite as working electrode. .... 78

**Figure 4. 20:** Square wave voltammogram for 1 ppm Cadmium bromide solution obtained at 120 seconds deposition time using un-modified Pyrolytic graphite as working electrode..... 79

**Figure 4. 21:** A plot of peak current against deposition time for 1 ppm cadmium bromide solution. .... 80

<b>Figure 4. 22:</b> Square wave voltammogram for 1 ppm Cadmium bromide solution obtained at frequency of 35 Hz using un-modified Pyrolytic graphite as working electrode. ....	82
<b>Figure 4. 23:</b> A plot of peak current against Frequency. ....	83
<b>Figure 4. 24:</b> Square wave voltammogram for 1 ppm cadmium bromide solution obtained at amplitude of 0.12 Volts using un-modified Pyrolytic graphite as working electrode. ....	84
<b>Figure 4. 25:</b> A plot of peak current against Change in phase amplitude. ....	85
<b>Figure 4. 26:</b> Square wave voltammogram for 1 ppm Cadmium bromide solution obtained at deposition potential of 0.05 Volts using bare Pyrolytic graphite as working electrode. ....	87
<b>Figure 4. 27:</b> A plot of peak current against deposition potential. ....	88
<b>Figure 4. 28:</b> Square wave voltammogram for 1 ppm cadmium bromide solution obtained at scan rate 0.00405 Volts using un-modified Pyrolytic graphite as working electrode. ....	89
<b>Figure 4. 29:</b> A plot of peak current against step potential for 1 ppm cadmium bromide solution. ....	90
<b>Figure 4. 30:</b> Square wave voltammogram of 0.1M KCl (Blank) obtained at 120 seconds deposition time using un-modified Pyrolytic graphite as working electrode. ....	92
<b>Figure 4. 31:</b> Square wave voltammogram for 1 ppm mixture of lead and cadmium bromide solution obtained at deposition potential of 120 s using un-modified Pyrolytic graphite as working electrode. ....	93
<b>Figure 4. 32:</b> A plot of peak current against deposition time for 1 ppm mixture of Lead nitrate and Cadmium Bromide solutions. ....	94
<b>Figure 4. 33:</b> Square wave voltammogram for 1 ppm mixture of Cadmium bromide and Lead Nitrate solution obtained at frequency of 15 Hz using un-modified Pyrolytic graphite as working electrode. ....	96

<b>Figure 4. 34:</b> A plot of peak current against Frequency. ....	97
<b>Figure 4. 35:</b> Square wave voltammogram for 1 ppm mixture of cadmium bromide and Lead Nitrate solution obtained at amplitude 0.02 Volts using un-modified Pyrolytic graphite as working electrode.....	99
<b>Figure 4.36:</b> A plot of peak current against Change in phase amplitude.....	100
<b>Figure 4. 37:</b> Square wave voltammogram for 1 ppm mixture Lead nitrate and Cadmium Bromide solution obtained at deposition potential 0.05 Volts using bare Pyrolytic graphite as working electrode.....	102
<b>Figure 4. 38:</b> A plot of peak current versus deposition potential.....	103
<b>Figure 4. 39:</b> Square wave voltammogram for 1 ppm mixture Lead nitrate and Cadmium Bromide solution obtained at a step potential 0.0805 Volts, using non modified Pyrolytic graphite as working electrode. ....	104
<b>Figure 4. 40:</b> A plot of peak current versus step potential for 1 ppm mixture of lead nitrate and cadmium bromide solution. ....	106
<b>Figure 4. 41:</b> Cyclic voltammogram for aniline mixture using modified Pyrolytic graphite as working electrode.....	108
<b>Figure 4. 42:</b> Square wave voltammogram for 0.1M KCl (Blank) obtained at 120 seconds deposition time using modified Pyrolytic graphite as working electrode.....	109
<b>Figure 4. 43:</b> Square wave voltammogram for 30 ppm lead Nitrate obtained at 420 seconds deposition time using modified Pyrolytic graphite as working electrode.....	110
<b>Figure 4. 44:</b> Plot of peak current against deposition time on modified pyrolytic graphite electrode .....	111

<b>Figure 4. 45:</b> Square wave voltammogram for 30ppm lead nitrate solution obtained at 70 Hz frequency using modified Pyrolytic graphite as working electrode. ....	113
<b>Figure 4. 46:</b> A plot of peak current against Frequency. ....	114
<b>Figure 4. 47:</b> Square wave voltammogram for 30 ppm lead nitrate solution obtained at 0.075 V deposition potential using modified Pyrolytic graphite as working electrode.....	116
<b>Figure 4. 48:</b> A plot of peak current against the deposition potential.....	117
<b>Figure 4. 49:</b> Square wave voltammogram for 30 ppm lead nitrate obtained at 0.04 Volts using modified Pyrolytic graphite as working electrode. ....	119
<b>Figure 4. 50:</b> A plot of peak current against amplitude on modified Pyrolytic graphite as working electrode. ....	120
<b>Figure 4. 51:</b> Square wave voltammogram for 30 ppm lead nitrate solution obtained at 0.00605 step up potential using modified Pyrolytic graphite as working electrode.....	122
<b>Figure 4. 52:</b> A plot of peak current against step potential on modified Pyrolytic graphite as working electrode.....	123
<b>Figure 4. 53:</b> Voltammogram obtained after electropolymerization of polyaniline on the surface using modified Pyrolytic graphite as working electrode. ....	125
<b>Figure 4. 54:</b> Square wave voltammogram for 0.1M KCl (Blank) obtained at 120 seconds deposition time using modified Pyrolytic graphite as working electrode.....	126
<b>Figure 4. 55:</b> Square wave voltammogram for 1 ppm mixture of lead Nitrate and cadmium bromide mixture obtained at 240 seconds deposition time using modified Pyrolytic graphite as working electrode.....	127

<b>Figure 4. 56:</b> A plot of peak current against deposition time for Lead nitrate and Cadmium Bromide solution carried out on modified pyrolytic graphite. ....	128
<b>Figure 4. 57:</b> Square wave voltammogram for 1 ppm mixture of Cadmium bromide and Lead Nitrate solution obtained at frequency of 20 Hz using modified Pyrolytic graphite as working electrode. ....	130
<b>Figure 4. 58:</b> A plot of peak current against frequency. ....	131
<b>Figure 4. 59:</b> Square wave voltammogram for 1 ppm mixture of cadmium bromide and Lead Nitrate solution obtained at amplitude 0.08 Volts using Modified Pyrolytic graphite as working electrode. ....	133
<b>Figure 4. 60:</b> A plot of peak current against Change in phase amplitude. ....	134
<b>Figure 4. 61:</b> Square wave voltammogram for 1 ppm mixture Lead nitrate and Cadmium Bromide solution obtained at deposition potential 0.15 Volts using modified Pyrolytic graphite as working electrode. ....	136
<b>Figure 4. 62:</b> A plot of peak current against deposition potential. ....	137
<b>Figure 4. 63:</b> Square wave voltammogram for 1 ppm mixture of cadmium bromide and Lead Nitrate solution obtained at scan rate 0.02 Volts using modified Pyrolytic graphite as working electrode. ....	139
<b>Figure 4. 64:</b> A plot of peak current against step potential. ....	140
<b>Figure 4. 65:</b> A plot of peak current against deposition time for modified and un-modified electrode. ....	143
<b>Figure 4. 66:</b> A plot of peak current against frequency for modified and un-modified electrode. ....	145

<b>Figure 4. 67:</b> A plot of peak current against deposition potential for modified and un-modified electrode.....	149
<b>Figure 4. 68:</b> A plot of peak current against step potential for modified and un-modified electrode. .....	151
<b>Figure 4. 69:</b> A plot of peak current against deposition potential for modified and un-modified electrode.....	153
<b>Figure 4. 70:</b> A plot of peak current against frequency for modified and un-modified electrode.	156
<b>Figure 4. 71:</b> A plot of peak current versus amplitude for modified and un-modified electrode.	159
<b>Figure 4.72:</b> A plot of peak current against amplitude for modified and un-modified electrode.	162
<b>Figure 4. 73:</b> A plot of peak current against step for modified and un-modified electrode. ....	164
<b>Figure 4. 74:</b> A plot of peak current against concentration for $\text{CaBr}_2$ . ....	166
<b>Figure 4. 75:</b> A plot of peak current against concentration for $\text{Pb}(\text{NO})_3$ . ....	168

# CHAPTER ONE

## 1.0 INTRODUCTION

### 1.1 Background Information

Since the discovery that conjugated polymers can be made to conduct electricity through doping, a tremendous amount of research has been carried out in the field of conducting polymers. Polyaniline is a unique conjugated polymer that can be tailored for specific applications through a non-redox acid/base doping process. The electrically conductive form of polyaniline is known as the emeraldine Oxidation state (Figure 1.1 below), which, when doped in an acid, protonates the imine nitrogen's on the polymer backbone and induces charge carriers. The conductivity of polyaniline increases with doping from the undoped insulating emeraldine base form ( $\sigma < 10^{-10} \text{ Scm}^{-1}$ ) to the fully doped, conducting emeraldine salt form ( $\sigma > 1 \text{ Scm}^{-1}$ ). Dopants can be removed by the interaction of the emeraldine salt form with common bases such as ammonium hydroxide [Wiley-VCH Verlag GmbH&Co., Weinheim (2004) Nanostructured Polyaniline Sensors, Chem. Eur. J. 2004, 10, 1314-1319].

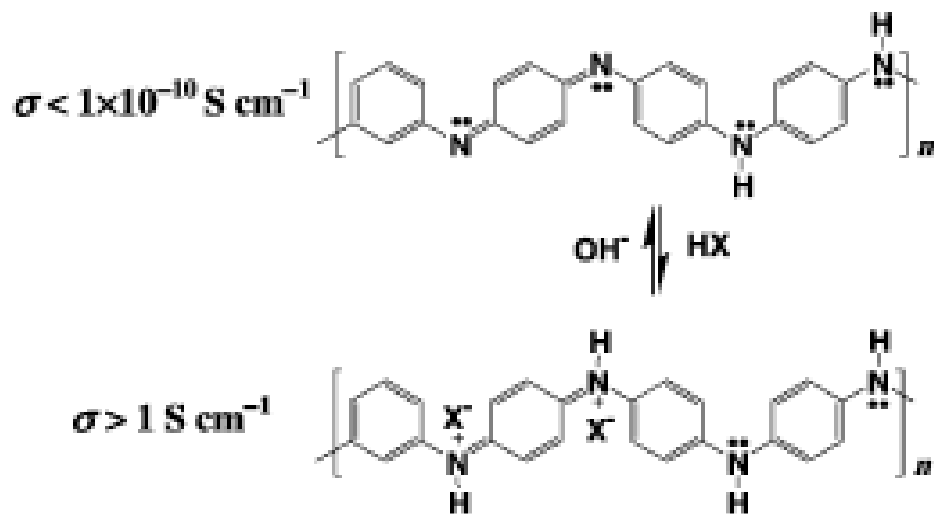


**Figure 1.1: Repeat unit of the emeraldine oxidation state of polyaniline in the undoped, base form (top) and the fully doped, acid form (bottom).**

Doping can be carried out with any strong acid, HX, where X serves as the counter ion to maintain charge balance. Dedoping can be accomplished with any strong base, OH<sup>-</sup>. Conductivity of polyaniline depends on both its ability to transport charge carriers along the polymer backbone and for the carriers to hop between polymer chains, any interaction with polyaniline that alters either of these processes will affect its conductivity. This is the underlying chemical principle enabling polyaniline to be used as the selective layer in a chemical-vapor sensor, such as resistance type detectors known as chemiresistors. Due to their room temperature sensitivity, the ease of deposition on to a wide variety of substrates and the rich chemistry of structural modifications, polyaniline as well as other conducting polymers are becoming attractive materials for sensor applications. A polyaniline chemiresistor typically consists of a substrate, electrodes, and the polymer selective layer changes in conductivity of the polymer film



upon exposure. Heavy metals is a term which is used to define metals with elemental densities above  $5 \text{ g/ cm}^3$ .

As many other metals can be found on the Earth's shell, human body contains a small amount of these substances. Mainly they get to the organisms via food, drinking water and air. Some heavy metals (copper, selenium and zinc) are involved in the metabolism of the human body (so called essential elements) but at very low concentrations. If the concentration of a heavy metal in the environment exceeds certain amount it can be toxic. The source of heavy metal poisoning from metals contained in water pipes, drinking polluted water or air emissions from factories. Bioaccumulation of heavy metals in biological organisms is faster than its decomposition and thus has led to a great demand for determination of heavy metals in the environment [ Znoeva Anna Viladmirovna (2006), Msc thesis, " The Improvement of anodic stripping voltammetric (ASV) method of cadmium and mercury determination"]. Analytical techniques must accomplish a number of requisites like sensitivity, cost, suitability for studies in the field, applicability to a wide range of substances, and the capability of determining more than one species. Heavy metals monitoring as result of their high toxicity over human health has a special importance. Due to the remarkable sensitivity attributed to its unique built – in pre-concentration (electro deposition) step, the stripping techniques are the most used methods for heavy metals analysis. The performance of these techniques is strongly affected by the working electrode material. Composite electrodes can often be fabricated with great flexibility in size and shape of the material, permitting easy adaptation to a variety of electrode configurations (conventional, flow-through, screen-printed et cetera). The electrode can be smoothed or polished to provide fresh active surface ready to be used in a new assay (an interesting issue for biosensor devices). Each

new surface yields reproducible results because all individual compounds are homogeneously dispersed or compressed in the bulk of the composite.

Mercury, in the form of mercury-film electrodes (MFEs) or the hanging mercury-drop electrode (HMDE), has been the traditional working electrode material in anodic stripping voltammetry (ASV) owing to the advantageous analytical properties of mercury in the negative potential range. However, the general trend for more environmentally friendly analytical methods and the extreme toxicity of metallic mercury and mercury salts have led to a growing interest in the use of mercury free electrodes.

## **1.2 Statement of the problem**

There is a great demand for determination of heavy metals in the environment due to health concerns. Among toxic heavy metals, lead (Pb) and cadmium (Cd) continues to be the most problematic. Mercury electrode has been used widely as a sensitive electrode in anodic stripping owing to the advantageous analytical properties of mercury in the negative potential range. Globally there has been an increasing concern about the negative impact of mercury on the environment. For example, the Swedish government banned its use in 1993 and replaced mercury with other products by end of year 2000. Another internationally known example occurred in Japan between 1932-55. In 1932 “Chisso’s chemicals” built a plant for sodium alkali production by amalgam process on Minimata Bay in Japan. Sewerage of the plant contained mercury and were released onto Minimata Bay. The mercury was consumed by sea creatures and especially by fish. In 1952, strange illness caused the death of dozens of people and animals.

In total 500 victims were recorded. The reason was identified later. It appeared to be mercury poisoned fish which was consumed in great amounts by population of Minimata Bay. The utilization of mercury-free electrodes for anodic stripping-square wave voltammetry is an attempt to perform environmentally friendly electro-analysis and hence practically addresses global health concerns. Mercury from the Environment enters living organisms. It's not naturally found in food stuffs but, but it can spread within food chain through humans, for instance food. Through vegetable that are spread by Insecticides containing Mercury, it can enter human bodies. It causes a number of effects on human such as, disruption of the nervous system, damage of brain functions, [ Znoeva Anna Viladmirovna (2006), Msc thesis " The Improvement of anodic stripping voltammetric (ASV) method of cadmium and mercury determination" ].

### **1.3 Justification**

Currently, expensive Instruments like AAS are required to detect concentration of heavy metals in water samples. AAS requires heavy maintenance, however the use of modified electrodes will involve simple and cost effective use of the potentiostat that requires low maintenance. Polyaniline is a unique conjugated polymer in that it can be tailored for specific applications through a non-Redox acid/base doping process on appropriate surface. Polyaniline, being conductive is expected to enhance the electrode sensitivity better than the detection limit of non modified (bare) electrode. Anodic stripping- square wave voltammetry has been shown to have the following advantages over other electrochemical techniques with respect to heavy metal analysis; specificity for target metal ions, enhanced measurement frequency, enhanced precision, Robustness, ability to be automated and easy regeneration of the surface (sensors).

It has also high detection sensitivity due to the combination of the built-in preconcentration step with an extremely favorable signal-to-noise ratio (S/N)[Wiley-VCH Verlag GmbH&Co., Weinheim (2004) Nanostructured Polyaniline Sensors, Chem. Eur. J. 2004, 10, 1314-1319].

## **1.4 Main Objectives**

The overall objective of the research work was to prepare a pyrolytic graphite polyaniline sensor and optimize conditions for determination of mixtures of cadmium and lead solutions.

### **1.4.1 Specific objectives**

1. To study the behavior of ferrocyanide as a prototype standard system on pyrolytic graphite electrode and obtain the relevant electrochemical parameters.
2. To modify the surface of pyrolytic graphite electrode by depositing thin film of polyaniline using cyclic voltammetry.
3. To evaluate the characteristic of voltammograms with respect to i-E curve versus scan rate.
4. To study the behavior of modified and un-modified pyrolytic graphite electrode using anodic stripping-square wave voltammetry for prepared solutions of lead nitrate and cadmium bromide.

5. To optimize the factors affecting anodic stripping-square wave voltammetry, aimed at obtaining the best square wave factors for analysis of lead nitrate and cadmium bromide solutions in a given environment.
6. To explore the possibility of  $\text{Pb}^{2+}(\text{aq})$  suppressing the stripping peaks of  $\text{Cd}^{2+}(\text{aq})$  in prepared solutions
7. To determine Limits of Detection and Limits of Quantitation

## **CHAPTER TWO**

### **2.0 LITERATURE REVIEW**

#### **2.1 Electrochemistry**

Electrochemistry is a branch of chemistry that enables one to study chemical reactions which take place in a solution at the interface of an electron conductor or electrode (a metal or a semiconductor) and an ionic conductor (the electrolyte), and which involve electron transfer between the electrode and the electrolyte or chemical species of interest in solution.

If a chemical reaction is driven by an external applied voltage, as in electrolysis, or if a voltage is created by a chemical reaction as in a battery, it is an electrochemical reaction. Chemical reactions where electrons are transferred between molecules are called oxidation/reduction (redox) reactions. In general, electrochemistry deals with situations where oxidation and reduction reactions are separated in space or time, connected by an external electric circuit to understand each process [William et al. 2004].

#### **2.2 Why Mercury free electrodes?**

The principle of electrochemistry is based on redox reactions where an electron is transferred to or from a molecule or ion and thus changing its oxidation state. This reaction can occur through the application of an external voltage (electrolytic cell) or through the release of chemical energy (galvanic cell).

The term redox comes from the two concepts of reduction and oxidation. It can be explained in simple terms [Brown et al. 2003]: Oxidation describes the loss of electrons / hydrogen or gain of oxygen / increase in oxidation.

The universal working electrodes for stripping analysis are the stationary mercury electrodes, namely the hanging mercury drop electrode (HMDE) and the electrochemically generated mercury film electrode (MFE). In some cases, carbon-based electrodes as well as the noble platinum and gold metals are used when mercury electrodes pose some complications.

Globally, there has been an increasing concern on the use of mercury in all aspects of human activities and its negative impact on the environment. The Swedish government, for instance, banned its use in 1993 and put measures to replace mercury with other products by the year 2000. The utilization of mercury-free electrodes for Anodic stripping- square wave voltammetry is an attempt to perform environmentally friendly electro-analysis and hence practically addresses global health concerns [Swain et al.2004]. The advent of anodic stripping voltammetry has improved the performance of analytical voltammetry to a considerable extent. The enhanced sensitivity and lower detection limits can be achieved in this technique by enrichment of the analyte prior to voltammetric determination. The common enrichment processes include reduction of metal ions through formation of metal films or amalgams, reductive or oxidative formation of sparingly soluble salts with or without reagent addition, and adsorptive accumulation of chelates or complexes onto the electrode surface. Recently, there has been a growing interest in the area of chemically modified electrodes for trace metal analysis. Prompted by environmental issues, these investigations are also aimed at the development of mercury-free electrodes for electro-analysis in which lead is of significant concern.

In this study we report a totally mercury-free Voltammetric stripping technique for the analysis of Lead and Cadmium ions using a conducting polymer modified electrode.

### **2.3 Electrochemical techniques**

Electrochemical techniques refer to methods in which there is an interaction between electrical power and matter. Electro-analytical methods in particular are methods where electricity is used to analyze matter. Electrochemical measurements on chemical systems are used by chemists for different purposes. These include obtaining thermodynamic data about a reaction, generating unstable intermediates so as to study the rate of decay or spectroscopic properties, analyzing trace amount of some species of interest and synthesizing new compounds or to decompose a given chemical species, among others.

Electro-analytical techniques involve a great variety of methods each differing from each other by the phenomenon occurring within the electrochemical cell [Sawyer et al. (1974)]. They include but not limited to:

- (i) Potentiometry in which the potential energy (E) is measured as a function of the reactant concentration at currents which are constant or approaching zero,
- (ii) Chronopotentiometry, where potential (E) versus time (t) is measured at constant current, electrogravimetry the amount of metal oxide deposited on an electrode by either reduction or oxidation is measured while either the potential (E) or current (i) is controlled,



- (iii) Conductometry where the measurement of conductance versus volume of the reagent are done at constant potential,
- (iv) Voltammetry where the current is measured as a function of the potential at constant concentrations and making use of microelectrodes,
- (v) Amperometry where measurement of current versus volume of reagent is done at fixed potential. It's an application of voltammetry;
- (vi) Controlled potential coulometry and controlled current coulometry. Whereby the quantity of electricity(coulombs) is measured at controlled potential and current respectively, and
- (vii) Anodic stripping square wave voltammetry, a method whereby metal is concentrated on micro electrode by electro-deposition followed by anodic Reoxidation to produce large current. Polarography is a volumetric method where dropping mercury(DME) is used as a working electrode and includes DC Polarography and controlled potential coulometry using stationary electrodes.

Electrochemical methods can be grouped into two categories according to

1. equilibrium methods (non-polarized) [Willard et. al .1986].; In this case the solution is stirred vigorously or electrode is rotated or both the concentration gradients at the electrode are or nearly eliminated. This ensures equilibrium effectively.
2. Transient or dynamic (polarized or diffusion controlled) method. In this case, both the electrode and solution are static thus after electrolysis the concentration gradient at the electrode surface become time independent or diffusion controlled .They include

techniques such as Voltammetry, chronopotentiometry and chronoamperometry. In a transient method, the substrate or species of interest is brought to the surface of electrode by the influence of concentration gradient unlike in equilibrium method where such movement is influenced by combination of gradient in electrical and chemical potential and both natural and forced convection (mass transport). Mass transport is the process by which species of interest move from one location of the solution to another from the bulk solution to the electrode surface or vice versa this is according to Bard and Faulkner (1980).

Mass transfer processes include (a) migration, which is the movement of charged species under influence of applied field; (b) convection which is brought about by agitation of electrode or stirring of the solution causing fluid to flow because of natural convection caused by density gradient and forced convection; and (c) diffusion which is the movement of the species of interest under the influence of gradient of chemical potential (concentration gradient). In voltammetry electrical migration is minimized by the use of high concentration of inert supporting electrolyte (at least 10 times concentrated) e.g.  $\text{KNO}_3$ . This was highlighted by Scogg et al. 1988.

When a current is applied the ions of the electrolyte migrate thus hindering the chemical species of interest from migrating. The high concentrated inert ions eliminate attraction or repulsion forces between the electrode and the analyte and instead the inert ions are attracted or repulsed but they are not electrolyzed. On the other hand convection is minimized by using transient electrochemical method [Willard et al. 1986]. Mass transfer to an electrode is governed by Nernst-Planck equation, which is written for one dimensional mass transfer along x-axis:

$$E_{\text{cell}} = E_{\text{cell}}^{\ominus} - \frac{RT}{zF} \ln Q \quad \dots\dots\dots 2.1$$

Where:

$E_{\text{cell}}$  is the cell potential (electromotive force) or applied potential.

$E_{\text{cell}}^{\ominus}$  is the standard cell potential.

R is the universal gas constant:  $R = 8.314\ 472(15)\ \text{J K}^{-1}\ \text{mol}^{-1}$ .

T is the absolute temperature (K).

F is the Faraday constant, the number of coulombs per mole of electrons:

$F = 9.648\ 533\ 99(24) \times 10^4\ \text{C mol}^{-1}$ .

Z is the number of electrons transferred in the cell reaction or half-reaction

Q is the reaction quotient.

## 2.4 Linear sweep potential Voltammetry (LSPV)

Voltammetry technique uses a microelectrode for microanalysis to enhance polarization. It comprises electro-analytical methods in which analysis is achieved by the measurement of the current  $i$ , as a function of the applied potential,  $E_{\text{app}}$ , during electrolysis performed under conditions that encourage polarization of the electrode [Bard and Faulkner, 1980]. A complete concentration polarization exists when the current in an electrochemical cell is limited by the rate of mass transfer of the reactant to the electrode surface [Bard and Faulkner, 1980]. As  $E_{\text{app}}$  is

scanned, the dilute solution of the analyte produce a limiting current at a given potential which is independent of  $E_{app}$  but depends on the rate at which the reactant is brought to the electrode surface. Since the reactions are steady state, the only process involved in mass transport is diffusion and thus such a current is called diffusion-controlled limiting current or diffusion controlled,  $i_d$ , [Willard et al 1986]. The decomposition by such a current does not alter the concentration of the reactant significantly when the voltammogram is being obtained [Pletcher, 1975].

### 2.4.1 Single – sweep voltammetry

In this technique a rapidly changing ramp of potential (from  $E_i$  to  $E_f$ ) is applied to working electrode as a function of time and the resulting current is then measured as a function of the applied potential. The electrode reaction is carried out in un-stirred solution, hence mass transport is as a result of diffusion alone [Bard and Faulkner, 1980]. The rate of reaction increases as the potential is increased towards the potential where reduction or oxidation occurs. However, since the solution is un-stirred, the region in the vicinity of the working electrode is depleted off the species of interest. A potential is reached where the increase in rate balances the depletion effect and thus a current plateau is recorded. The  $i$ - $e$ , curve for a simple electrode process shows a marked current peak instead of the smooth s-shaped for an equilibrium technique for reversible system [Sawyer et al. 1974]. The following reaction occurs.



The potential,  $E_p$  is given by:

$$E_p = E_{1/2} - 1.109(RT/nF) \dots \dots \dots (2.3)$$

At 25°C,

$$E_p = E_{1/2} - 0.285/nV \dots \dots \dots (2.4)$$

Where  $E_p$  is the peak potential and  $E_{1/2}$  is the potential at which the current is half the diffusion limited value ( $1/2i_d$ ).

The peak current,  $i_p$ , in amperes is given by

$$I_p = 0.4463 n F A C_0 (nF/RT)^{1/2} v^{1/2} D_0^{1/2} \dots \dots \dots (2.5)$$

Where:

A is the electrode area (cm<sup>2</sup>)

n is the number of electrons transferred,

$C_0$  is the concentration of the oxidized species O in cm<sup>3</sup> mol<sup>-1</sup>,

v is the scan rate in Vsec<sup>-1</sup>

$D_0$  is the diffusion coefficient of the oxidized species O in cm<sup>2</sup> sec<sup>-1</sup>

F is the faradaic constant

R is the gas constant

T(K) is the absolute temperature

Since the peak is slightly broad, causing difficulties in determining peak potential  $E_p$ , its sometimes convenient to report the potential at half  $i_p$ , called half peak potential,  $E_{p/2}$ . This however has no direct thermodynamic significance.

$$E_{p/2} = E_{1/2} + 1.09 RT/nF \dots\dots\dots (2.6)$$

At 25<sup>0</sup>C,

$$E_{p/2} = E_{1/2} + (0.0285/n)V \dots\dots\dots (2.7)$$

The potential  $E_{1/2}$  occurs about midway between  $E_p$  and  $E_{p/2}$ , thus for Nernstian wave

$$E_p - E_{p/2} = 2.2 (RT/nF)V \dots\dots\dots (2.8)$$

At 25<sup>0</sup>C,

$$E_p - E_{p/2} = (0.0565/n)V \dots\dots\dots (2.9)$$

This shows that the reversible wave  $E_p$  is independent of the scan rate and of  $i_p$  as well as current at any point on the wave but  $I_p$  is proportional to the square root of the scan rate [Bard and Faulkner, 1980]. For irreversible systems the  $i$ - $E$  relationship is not simple and contains terms relating the electron transfer characteristic of the reaction process. Deviations from linearity in the plot of  $i$  vs.  $V^{1/2}$  sometimes indicate that the redox event is associated with other processes, such as association of ligand, dissociation of ligand, or change in geometry or related chemical reactions [Bard and Faulkner,2001].

### 2.4.2 Cyclic voltammetry

Cyclic voltammetry (CV) is a type of potentiodynamic electrochemical measurement. In a cyclic voltammetry experiment the working electrode potential is ramped linearly versus time like linear sweep voltammetry. Cyclic voltammetry takes the experiment a step farther than linear sweep voltammetry which ends when it reaches a set potential. When cyclic voltammetry

reaches the switching potential, the working electrode's potential ramp is inverted. This inversion can happen multiple times during a single experiment. The current at the working electrode is plotted versus the applied voltage to give the cyclic voltammogram trace. Cyclic voltammetry is generally used to study the electrochemical properties of an analyte in solution [Allen et al. 2000].

In cyclic voltammetry, the electrode potential ramps linearly versus time. This ramping is known as the experiment's scan rate (V/s). The potential is measured between the reference electrode and the working electrode and the current is measured between the working electrode and the counter electrode. This data is then plotted as current ( $i$ ) vs. potential ( $E$ ). As the waveform shows, the forward scan produces a current peak for any analyte that can be reduced (or oxidized depending on the initial scan direction) through the range of the potential scanned. The current will increase as the potential reaches the reduction potential of the analyte, but then drops as the concentration of the analyte is depleted close to the electrode surface. If the redox couple is reversible then when the applied potential is reversed, it will reach the potential that will re-oxidize the product formed in the first reduction reaction, and produce a current of reverse polarity from the forward scan. This oxidation peak will usually have a similar shape to the reduction peak. As a result, information about the redox potential and electrochemical reaction rates of the compounds is obtained. For instance if the electronic transfer at the surface is fast and the current is limited by the diffusion of species to the electrode surface, then the current peak will be proportional to the square root of the scan rate. This relationship is described by the Cottrell equation [Bard, A. J. and Faulkner, 2001].

The utility of cyclic voltammetry is highly dependent on the analyte being studied. The analyte has to be redox active within the experimental potential window. It is also highly desirable for the analyte to display a reversible wave.

A reversible wave is when an analyte is reduced or oxidized on a forward scan and is then reoxidized or reduced in a predictable way on the return scan as shown in Figure 2.1 below.

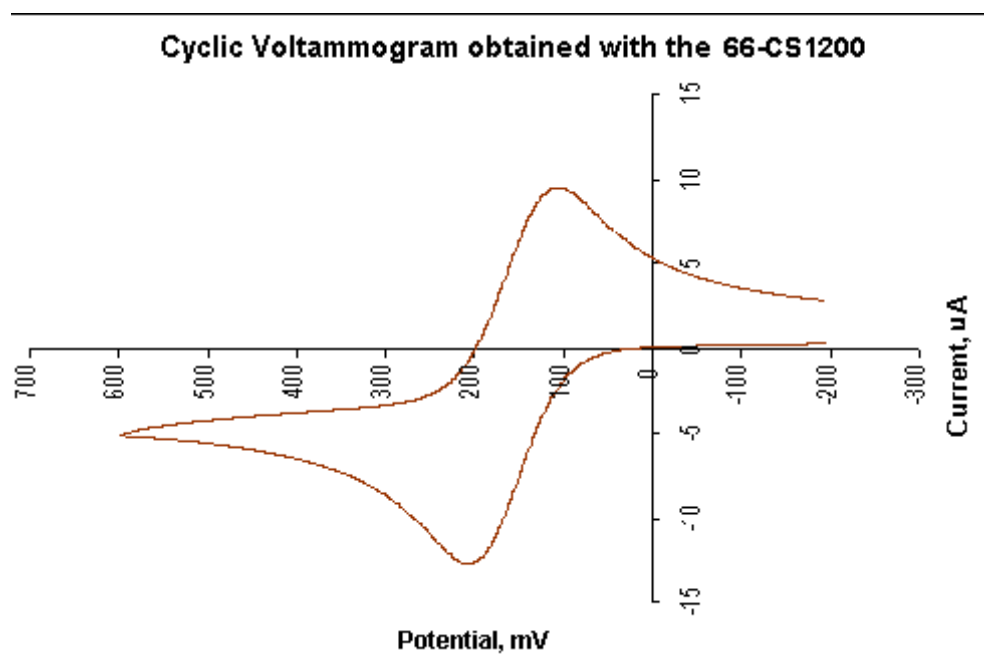


**Figure 2.1: cyclic voltammogram of reversible analyte.**

The waveform of the voltage applied to the working electrode versus the reference electrode is triangular shaped. Since this voltage varies linearly with time, the slope is referred to as the scan rate (V/s). On the reverse scan, the ferricyanide, formed during the forward scan, is reduced back to ferrocyanide. The peak shape of the oxidative and reverse current-potential (I-E) curve in Figure 2.1 is typical for an electrode reaction in which the rate is governed by diffusion to a planar electrode surface.



That is, the rate of the electron transfer step is relatively fast compared to that of diffusion. In such a case the peak current,  $I_p$ , is governed by the Randle-Sevcik relationship[Larry and Faulkner, 1983]:

$$I_p = k n^{3/2} A D^{1/2} C V^{1/2} \dots\dots\dots(2.10)$$

Where :

$I_p$  is peak current,

constant, k, has a value of  $2.72 \times 10^5$  ;

n is the mole of electrons transferred per mole of electro active species,

A is the area of the electrode in  $\text{cm}^2$  ,

D is the diffusion coefficient in  $\text{cm}^2/\text{s}$  ,

C is concentration in  $\text{mole}/\text{cm}^3$  and

V is the scan rate of the potential in volt/s.

The  $I_p$  is linearly proportional to the bulk concentration, C, of the electroactive species and the square root of the scan rate,  $V^{1/2}$ . Thus, an important diagnostic is a plot of the  $I_p$  vs.  $V^{1/2}$ . If the plot is linear, it is reasonably safe to say that the electrode reaction is controlled by diffusion, which is the mass transport of electroactive species to the surface of the electrode across a concentration gradient. The thickness, d, of the "diffusion" layer can be approximated by:  $d \sim [Dt]^{1/2}$ , where D is the diffusion coefficient and t is time in seconds. A "quiet" i.e. unstirred

solution is required. The presence of supporting electrolyte, such as the KCl in the example, is required to eliminate movement of the charged electroactive species due to migration in the electric field gradient. Reversible peaks have a distinct absolute potential difference between the

reduction ( $E_{pc}$ ) and oxidation peak ( $E_{pa}$ ). In an ideal system,  $|E_{pc} - E_{pa}| = \frac{57 \text{ mV}}{n}$  for one electron process [Nicholson and Irving, 1964]. In addition, the ratio of the currents passed at reduction ( $i_{pc}$ ) and end oxidation ( $i_{pa}$ ) is near unity ( $1 = i_{pa}/i_{pc}$ ) for a reversible peaks.

When such reversible peaks are observed, thermodynamic information in the form of half cell potential  $E_{1/2}^0$  can be determined. When waves are semi-reversible such as when  $i_{pa}/i_{pc}$  is less than or greater than 1, it can be possible to determine even more information especially kinetic processes like following chemical reaction.

When waves are non-reversible it is impossible to determine what their thermodynamic  $E_{1/2}^0$  with cyclic voltammetry. When a wave is non-reversible cyclic voltammetry cannot determine if the wave is at its thermodynamic potential or shift to a more extreme potential by some form of over potential. The couple could be irreversible because of a following chemical process; a common example for transition metals is a shift in the geometry of the coordination sphere. If this is the case, then higher scan rates may show a reversible wave. It is also possible that the wave is reversible due to a physical process most commonly some form of precipitation

[ Bosch et al. 2007].

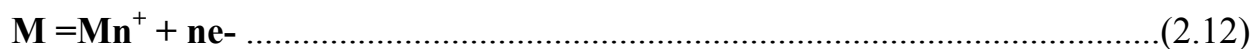
### 2.4.3 Anodic stripping -Square-Wave Voltammetry (AS-SWV)

The excitation signal in AS-SWV consists of a symmetrical square-wave pulse of amplitude  $E_{sw}$  superimposed on a staircase waveform of step height  $\Delta E$ , where the forward pulse of the square wave coincides with the staircase step. The net current,  $i_{net}$ , is obtained by taking the difference between the forward and reverse currents ( $i_{for} - i_{rev}$ ) and is centered on the redox potential. The peak height is directly proportional to the concentration of the electroactive. Square-wave voltammetry has several advantages. Among these are its excellent sensitivity and the rejection of background currents. Another is the speed (for example, its ability to scan the voltage range over one drop during polarography with the DME). This speed, coupled with computer control and signal averaging, allows for experiments to be performed repetitively and increases the signal to-noise ratio. Applications of square-wave voltammetry include the study of electrode kinetics with regard to preceding, following, or catalytic homogeneous chemical reactions, determination of some species at trace levels.

Anodic stripping-square wave voltammetry is one of the numerous voltammetric techniques. It's commonly used for metal detection. It has two steps involved. First metal ions are accumulated on the electrode at suitable potential. This potential is called "deposition potential". The deposition potential continues during appropriate time called "deposition time". The solution is stirred during accumulation to maximize on the amount of metal deposited [Znoeva ,2006]



Second, the metal deposits are dissolved in the solution. During this stripping step the potential is scanned at a certain rate. The measuring of the limiting current in contrast to ordinary Voltammetry is carried out at this step.



The curves obtained using such method and ordinary Voltammetry look alike. The method is applicable to simultaneous detection of several metal ions. If solution contains two or more compounds the curve will have two or more current peak on it in the order of their deposition peak values see Figure 2.2 below

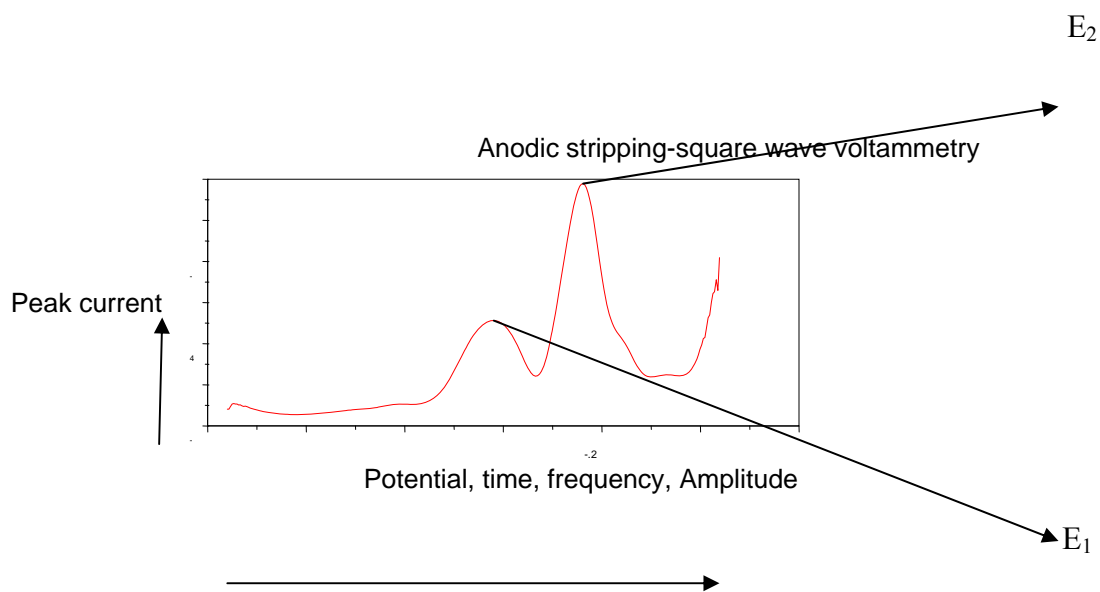


**Figure 2. 2: Plot of peak currents against various parameters.**

#### **2.4.4 Working electrode**

Common materials for working electrodes include Pyrolytic graphite, glassy carbon, platinum, and gold. These electrodes are generally encased in a rod of inert insulator with a disk exposed at one end. A regular working electrode has a radius within an order of magnitude of 1 mm. Having a controlled surface area with a defined shape is important for interpreting cyclic voltammetry results. In the present research work, pyrolytic carbon working electrode was used [ Kissinger et al. 1996].

#### **2.4.5 Pyrolytic Graphite Electrode**

Pyrolytic carbon is a material similar to graphite, but with some covalent bonding between its graphene sheets as are result of imperfection during production.

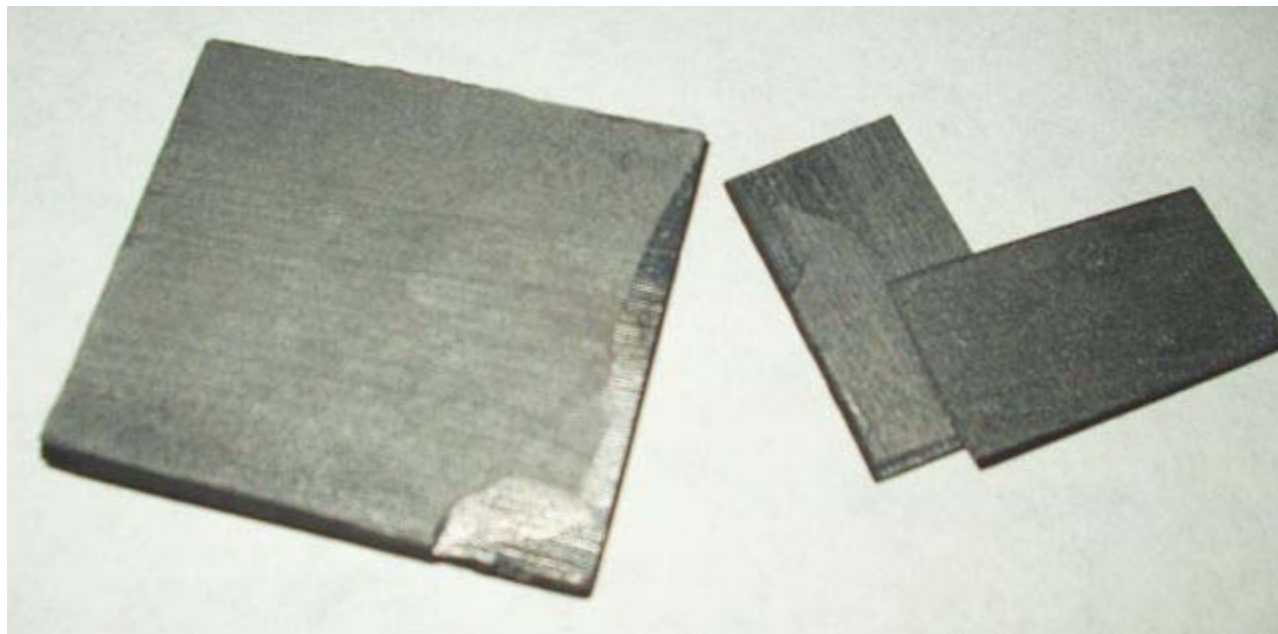


**Figure 2.3: Sheets of pyrolytic carbon.**

Generally it is produced by heating a hydrocarbon nearly to its decomposition temperature and permitting the graphite to crystallize (pyrolysis). One method is to heat synthetic fibers in a vacuum. Another method is to place seeds or a plate in the very hot gas to collect the graphite coating [Cook, et al. 1999].

Pyrolytic carbon samples usually have a single cleavage plane, similar to mica, because the graphene sheets crystallize in a planar order, as opposed to graphite, which forms microscopic randomly-oriented zones. Because of this, pyrolytic carbon exhibits several unusual anisotropic properties. It is more thermally conductive along the cleavage plane than graphite, making it one of the best planar thermal conductors available. It is also more diamagnetic against the cleavage plane, exhibiting the greatest diamagnetism of any room temperature (by weight) diamagnet. Cook et al. 1999 further suggested that it is even possible to levitate reasonably pure and sufficiently ordered samples over rare earth permanent magnets.

#### **2.4.6 Counter electrode**

The counter electrode, also known as the auxiliary or second electrode, can be any material which conducts easily and won't react with the bulk solution and made of inert materials such as gold, platinum, or carbon. Reactions occurring at the counter electrode surface are unimportant as long as it continues to conduct current well. To maintain the observed current the counter electrode will often oxidize or reduce the solvent or bulk electrolyte. The auxiliary electrode's potential is opposite in sign to that of the working electrode, but its current and potential are not measured. Rather, it is used to ensure that current does not run through the reference electrode (three electrode system), which would disturb the reference electrode's potential. The auxiliary

electrode often has a surface area much larger than that of the working electrode to ensure that the reactions occurring on the working electrode are not surface area limited by the auxiliary electrode.

When using a three electrode cell system to perform electro- analytical chemistry, the auxiliary electrode is often isolated from the working electrode using a glass frit. Such isolation prevents any byproducts generated at the auxiliary electrode from contaminating the main test solution and interfering with the analytical measurement being made at the working electrode [Zoski and Cynthia, 2007].

#### **2.4.7 Reference electrode**

A Reference electrode is an electrode which has a stable and well-known electrode potential. The high stability of the electrode potential is usually reached by employing a redox system with constant (buffered or saturated) concentration of each participant of the redox reaction [Allen J et al. 2000]. The ideal reference electrode should possess the following properties:

- It should be reversible and obey the Nernst equation with respect to some species in the electrolyte.
- Its potential should be stable with time.
- Its potential should return to the equilibrium potential after small currents are passed through the electrode.
- If it is an electrode like the Ag/AgCl reference electrode, the solid phase must not be appreciably soluble in the electrolyte.

- It should show low hysteresis with temperature cycling.

There are many ways reference electrodes are used. The simplest is when the reference electrode is used as a half cell to build an electrochemical cell. This allows the potential of the other half cell to be determined. An accurate and practical method to measure an electrode's potential in isolation (absolute electrode potential) has yet to be developed. There are four kinds of reference electrode: Aqueous Reference Electrodes, non aqueous Reference Electrodes, Quasi-Reference Electrode (QRE), Pseudo-reference electrodes.

#### **2.4.8 Aqueous Reference Electrodes**

According to Gritzner and Kuta,1984 the common reference electrodes and potential with respect to the standard hydrogen electrode are:

- Standard hydrogen electrode (SHE) ( $E=0.000\text{ V}$ ) also known as "normal hydrogen electrode" (NHE).
- Reversible hydrogen electrode (RHE) ( $E=0.000\text{ V} + 0.0591 \cdot \text{pH}$ ).
- Saturated calomel electrode (SCE) ( $E=+0.242\text{ V}$  saturated).
- Copper-copper(II) sulfate electrode ( $E=+0.314\text{ V}$ ).
- Silver chloride electrode ( $E=+0.197\text{ V}$  saturated).
- pH-electrode (in case of pH buffered solutions, see buffer solution)
- Palladium-hydrogen electrode.



### 2.4.9 Silver chloride electrode

A silver chloride electrode is a type of reference electrode, commonly used in electrochemical measurements. For example, it is usually the internal reference electrode in pH meters. As another example, the silver chloride electrode is the most commonly used reference electrode for testing cathodic protection and corrosion control systems in sea water environments. The above reference electrodes consist of a plastic tube electrode body. The electrode is a silver wire that is coated with a thin layer of silver chloride, either physically by dipping the wire in molten silver chloride, or chemically by electroplating the wire in concentrated hydrochloric acid. A porous plug on one end allows contact between the field environments with the silver chloride electrolyte. An insulated lead wire connects the silver rod with measuring instruments.

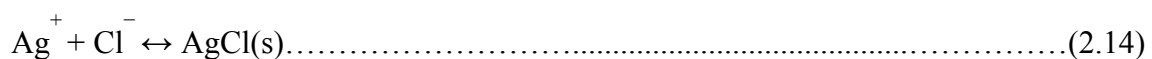


**Figure 2.4: Silver chloride electrodes.**

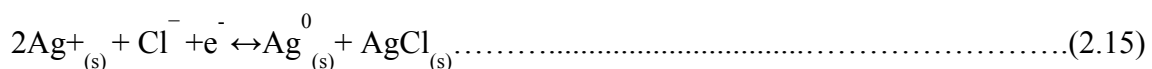
A voltmeter negative lead is connected to the test wire. The reference electrode contains potassium to stabilize the silver chloride concentration.

The electrode functions as a redox electrode and the reaction is between the silver metal (Ag) and its salt — silver chloride (AgCl, also called silver (I) chloride).

The corresponding reactions can be presented as follows:



or an overall reaction can be written:



This reaction characterized by fast electrode kinetics, meaning that a sufficiently high current can be passed through the electrode with the 100% efficiency of the redox reaction (dissolution of the metal or cathodic deposition of the silver-ions). The reaction has been proved to obey these equations in solutions with pH's of between 0 and 13.5.

Dependence of potential on the electrolyte is shown in Table 2–1.

**Table 2–1: The potential of a silver chloride reference electrode with respect to the standard hydrogen electrode (SHE).**

Reference Electrode Potentials		
Electrode	Potential $E^0 + E_j$	Temperature Coef.
	(V) at 25 °C	(mV/°C) at around 25 °C
SHE	0.000	+0.87
Ag/AgCl/Sat. KCL	+0.197	-1.01
Ag/AgCl mol/kg KCL	+0.205	-0.73
Ag/AgCl/1.0 mol/kg KCL	+0.235	+0.25
Ag/AgCl/0.6 mol/kg KCL	+0.25	
Ag/AgCl (Seawater)	+0.266	

The electrode has many features and advantages making it suitable for use in the field. These range from simple to construct, inexpensive to manufacture, stable potential, and non-toxic components.

It is usually manufactured with saturated potassium chloride electrolyte, but can be used with lower concentrations such as 1 mol/kg potassium chloride. As noted above, changing the electrolyte concentration changes the electrode potential. Silver chloride is slightly soluble in strong potassium chloride solutions, so it is sometimes recommended that the potassium chloride be saturated with silver chloride to avoid stripping the silver chloride off the silver wire.

#### **2.4.10 Non-aqueous Reference Electrodes**

The SHE might seem to be a reasonable reference for non-aqueous work, as it turns out the platinum is rapidly poisoned by many solvents including acetonitrile causing uncontrolled drifts in potential. Both the SCE and saturated Ag/AgCl are aqueous electrodes based around saturated aqueous solution. While for short periods it may be possible to use such aqueous electrodes as references with non-aqueous solutions the long-term results are not trustworthy. Using aqueous electrodes introduces undefined, variable, and unmeasurable junction potentials to the cell in the form of a liquid-liquid junction as well as different ionic composition between the reference compartment and the rest of the cell [Pavlishchuk et al. 2000]. The best argument against using aqueous reference electrodes with non-aqueous systems, as mentioned earlier, is that potentials measured in different solvents are not directly comparable [Geiger and William, 2007].

#### **2.4.11 Quasi-Reference Electrode (QRE)**

A Quasi-Reference Electrode (QRE) avoids the issues mentioned above. A QRE with Ferrocene or similar internal standard (Cobaltocene) is ideal for nonaqueous work. Since the early 1960s ferrocene has been gaining acceptance as the standard reference for nonaqueous work for a

number of reasons. In 1984 IUPAC recommend ferrocene (II/III) as a standard redox couple [Gritzner and Kuta, 1984]. The preparation of the QRE electrode is simple allowing a fresh reference to be prepared with each set of experiments. Since QREs are made fresh there is also no concern of improper storage or maintenance of the electrode. QREs are also more affordable than other reference electrodes.

#### **2.4.12 Pseudo-reference electrodes**

A pseudo-reference electrode is a term that is not well defined and borders on having multiple meanings since pseudo and quasi are often used interchangeably. There are a class of electrodes named pseudo-reference electrodes because they do not maintain a constant potential but vary predictably with conditions. If the conditions are known, the potential can be calculated and the electrode can be used as a reference. Most electrode work over a limited range of conditions, such as pH or temperature, outside of this range the electrodes behavior becomes unpredictable. The advantage of a pseudo-reference electrode is that the resulting variation is factored into the system allowing researchers to accurately study systems over a wide range of conditions [Bosch. et al. 2007].

## CHAPTER THREE

### 3.0 METHODOLOGY AND INSTRUMENTATION

#### 3.1 Reagents and Chemical solutions

Ferrocene (98%), and tetraethylammoniumbromide [TEAB] (98%), Were obtained from Aldrich Chemical Co. Acetonitrile was supplied by Kobian Chemical Co. All the chemicals were analytical reagent grade and were used as received. Distilled water supplied by the Chemistry department was used. Solutions of 1, 2, 3, 4, 5mM Ferrocene in (1:1) acetonitrile-water was prepared freshly for each procedure.

The following are reagents used for cyclic voltammetry; 0.1 M KCl as an electrolyte, Cadmium Nitrate 5mM, Cadmium Bromide, 100mM, 10mM, 1mM, 0.1mM, 0.01 mM Lead Nitrate 5mM, 100mM, 10mM, 1mM, 0.1mM, 0.01 mM, Alumina paste for cleaning the pyrolytic graphite electrode. All chemicals were obtained from Aldrich Chemical Co., supplied by Kobian chemical Co ltd in Kenya.

The chemicals used for anodic stripping square wave voltammetry were as follows: 1ppm mixture Cadmium bromide and Lead Nitrate, Alumina for cleaning the electrode, Distilled water, pure aniline, 1M HCl, 1.00 mL, Polyvinyl sulfonate (PVS) solution, Nitrogen gas, Cadmium bromide 1ppm, Cadmium bromide 30 ppm.

### 3.2 Apparatus and procedure for cyclic Voltammetry

The Autolab Princeton applied research (PAR) analyzer, a three electrode potentiostat, was used to control the potential for all the electrochemical experiments and all potential were referred to saturated calomel electrode (SCE). Platinum wire was employed as the counter electrode and pyrolytic graphite electrode was used as working electrode. The pyrolytic graphite was polished for about 2 minutes with alumina slurry before each potential scan. All the electrolytic solutions were de-aerated for at least 25 minutes by passing Nitrogen gas through them before carrying out the experiment. All experiments took place at room temperature.



**Figure 3.1: Three electrode system, Potentialstat and the computer.**

The pyrolytic graphite carbon electrode was polished for about 2 minutes. with alumina slurry before each potential scan. All the electrolytic solutions were de-aerated for at least 25 min by passing Nitrogen gas through them before carrying out the study. All experiments were done at

room temperature ( $20-25^{\circ}\text{C}$ ). The electrochemical cell was washed with distilled water and rinsed. This cell preparation was done in same way for cyclic voltammetry and anodic stripping square wave voltammetry.

The pyrolytic graphite electrode was polished with aluminium slurry. The solution of 0.1M TEAB in acetonitrile water was first run to establish the working window. Concentration Studies of Ferrocene 1, 2, 3, 4 and 5 mM were done at a scan rate  $0.025\text{Vsec}^{-1}$ . The potential was swept from -1.250V to 0.750V and back to -1.250V.

- i. The electrochemical cell was washed with distilled water and rinsed thoroughly
- ii. The pyrolytic graphite electrode was polished with aluminium slurry and rinsed well.
- iii. Cyclic voltammetry studies of 10mL 0.4 M ferrocene in homogeneous acetonitrile water (1:1) solvent was with 0.1 M TEAB as a supporting electrolyte. The potential was swept from -0.250 to 0.750 V and back to 0.250V at various scan rate of 0.010,0.015,0.020,0.025,0.030,0.035,0.040,0.045 and 0.050.
- iv. The procedure (iii) was repeated for 5.0 mM lead nitrate solution using 0.1M KCl as the electrolyte on modified and un-modified electrode.
- v. The procedure (iii) was repeated for 5.0mM cadmium bromide solution using 0.1M KCl as the electrolyte on modified pyrolytic graphite electrode.

### **3.3 Apparatus and procedure for anodic stripping square wave voltammetry**

The method used same apparatus as cyclic Voltammetry



### 3.3.1 Electrode modification protocol

Pyrolytic graphite electrode was polished on slurry of 0.5 mm alumina and rinsed with distilled water. Then electrodes were dipped in an electrochemical cell containing 93mL pure aniline, 3.9 mL 1M HCl and 1.00 mL PVS solution. The cell was purged for 20 minutes with Nitrogen gas prior to obtaining the experimental data.

Polyaniline films were grown electrochemically on the electrode surface by multiple cyclic Voltammetry scanning at  $100 \text{ mVs}^{-1}$  from -500 to 1100mV and back for 30 cycles at room temperature. The modified electrode was then used to perform the anodic stripping square wave voltammetry studies on solution prepared.

### 3.3.2 Reagents and Chemical solutions

Ferrocene (98%), and Tetraethylammoniumbromide [TEAB] (98%), were obtained from Aldrich Chemical Co. Acetonitrile was supplied by Kobian Chemical Co. All the chemicals were analytical reagent grade and were used as received. Distilled water supplied by the Chemistry department was used. Solutions of 1, 2, 3, 4, 5mM Ferrocene in (1:1) acetonitrile-water was prepared freshly for each procedure.

The following are reagents used for cyclic voltammetry; 0.1 M KCl as an electrolyte, Cadmium Nitrate 5mM, Cadmium Bromide, 100mM, 10mM, 1mM, 0.1mM, 0.01 mM Lead Nitrate 5mM, 100mM, 10mM, 1mM, 0.1mM, 0.01 mM, Alumina paste for cleaning the pyrolytic graphite electrode. All chemicals were obtained from Aldrich Chemical Co., supplied by Kobian chemical Co ltd in Kenya.

The chemicals used for anodic stripping square wave voltammetry were as follows: 1ppm mixture Cadmium bromide and Lead Nitrate ,Alumina for cleaning the electrode, Distilled water, pure aniline,1M HCl,1.00 mL ,Polyvinyl sulfonate (PVS) solution ,Nitrogen gas, Cadmium bromide 1ppm, Cadmium bromide 30 ppm.

### **3.3.2.1 Apparatus and procedure for cyclic Voltammetry**

The Autolab Princeton applied research (PAR) analyzer, a three electrode potentiostat, was used to control the potential for all the electrochemical experiments and all potential were referred to saturated calomel electrode (SCE). Platinum wire was employed as the counter electrode and pyrolytic graphite electrode was used as working electrode. The pyrolytic graphite was polished for about 2 minutes with alumina slurry before each potential scan. All the electrolytic solutions were de-aerated for at least 25 minutes by passing Nitrogen gas through them before carrying out the experiment. All experiments took place at room temperature.

The pyrolytic graphite carbon electrode was polished for about 2 minutes with alumina slurry before each potential scan. All the electrolytic solutions were de-aerated for at least 25 min by passing Nitrogen gas through them before carrying out the study. All experiments were done at room temperature (20-25<sup>o</sup> C).The electrochemical cell was washed with distilled water and rinsed. This cell preparation was done in same way for cyclic voltammetry and anodic stripping square wave voltammetry.

The pyrolytic graphite electrode was polished with aluminium slurry. The solution of 0.1M TEAB in acetonitrile water was first run to establish the working window. Concentration Studies of Ferrocene 1, 2, 3, 4 and 5 mM were done at a scan rate  $0.025\text{Vsec}^{-1}$ . The potential was swept from -1.250V to 0.750V and back to -1.250V.

- i. The electrochemical cell was washed with distilled water and rinsed thoroughly
- ii. The pyrolytic graphite electrode was polished with aluminium slurry and rinsed well.
- iii. Cyclic voltammetry studies of 10mL 0.4 M ferrocene in homogeneous acetonitrile water (1:1) solvent was with 0.1 M TEAB as a supporting electrolyte. The potential was swept from -0.250 to 0.750 V and back to 0.250V at various scan rate of 0.010,0.015, 0.020,0.025,0.030,0.035,0.040,0.045 and 0.050.
- iv. The procedure (iii) was repeated for 5.0 mM lead nitrate solution using 0.1M KCl as the electrolyte on modified and un-modified electrode.
- v. The procedure (iii) was repeated for 5.0mM cadmium bromide solution using 0.1M KCl as the electrolyte on modified pyrolytic graphite electrode.

### **3.3.2.2 Apparatus and procedure for anodic stripping square wave voltammetry**

The method used same apparatus as cyclic Voltammetry

#### **3.1.4 Electrode modification protocol**

Pyrolytic graphite electrode was polished on slurry of 0.5 mm alumina and rinsed with distilled water. Then electrodes were dipped in an electrochemical cell containing 93mL pure aniline, 3.9

mL 1M HCl and 1.00 mL PVS solution. The cell was purged for 20 minutes with Nitrogen gas prior to obtaining the experimental data.

Polyaniline films were grown electrochemically on the electrode surface by multiple cyclic Voltammetry scanning at  $100 \text{ mVs}^{-1}$  from -500 to 1100mV and back for 30 cycles at room temperature. The modified electrode was then used to perform the anodic stripping square wave voltammetry studies on solution prepared.

### **3.1.3.2 Procedure for optimization of deposition time for lead nitrate solution on un-modified pyrolytic graphite electrode**

The pyrolytic graphite carbon electrode was polished for about 2 minutes with alumina slurry before each potential scan. All the electrolytic solutions were de-aerated for at least 25 min by passing Nitrogen gas through them before carrying out the study. All experiments were done at room temperature ( $20\text{-}25^{\circ}\text{C}$ ). The electrochemical cell was washed with distilled water and rinsed. A scan of the blank (0.1M KCl) was done.

All the measurements were carried out in square wave anodic stripping mode. The equipment set-up was as follows: frequency 15 Hz, deposition time 60 to 480 seconds, deposition potential 0.05V, Initial Potential 0.5 EV, final potential -1.25, Step up potential was 0.00405 EV and amplitude 0.01995 EV. The values of peak current were obtained by varying the deposition time.

### **3.1.3.3 Procedure for optimization of frequency for lead nitrate solution on un-modified pyrolytic graphite electrode**

The cell preparation was carried out as described in procedure for optimization of deposition time in un-modified electrode. All the measurements were carried out in square wave anodic

stripping mode. The equipment set-up was as follows: frequency 15 to 60 Hz, deposition time 120 seconds, deposition potential 0.05V, Initial Potential 0.5 V, Final potential -1.25 V, Step up potential 0.00405 V and amplitude 0.01995 V. The values of peak current were obtained by varying the frequency.

#### **3.1.3.4 Procedure for optimization of deposition potential for lead nitrate solution on un-modified pyrolytic graphite electrode**

The measurements were carried out in square wave anodic stripping mode. The equipment set-up was as follows: Frequency 30 Hz, deposition potential 0.05 to 0.075 V, deposition time 120 s, Initial Potential 0.5 V, Final potential -1.25 V, Step up potential 0.00405 EV Amplitude 0.01995 volts. The values of peak current were obtained by varying the deposition time.

#### **3.1.3.5 Procedure for optimization of step potential for lead nitrate solution on un-modified pyrolytic graphite electrode**

All the measurements were carried out in square wave anodic stripping mode. The equipment set-up was as follows: Frequency 30 Hz, deposition potential 0.05 V, deposition time 120 s, Initial Potential 0.5 V, final potential -1.25 V, step up potential 0.00405 to 0.00705 EV and amplitude 0.08 volts. The values of peak current were obtained by varying the step potential.

#### **3.1.3.6 Procedure for optimization of amplitude for lead nitrate solution on un-modified pyrolytic graphite electrode**

The measurements obtained were carried out in square wave anodic stripping mode. The equipment set-up was as follows: Frequency 30 Hz, deposition time 120 s, Initial Potential 0.5V,

final potential -1.25, Step up potential 0.00405 V and amplitude 0.02 to 0.14 V. The values of peak current were obtained by varying the amplitude.

### **3.1.4 Apparatus and procedure for anodic stripping-Anodic square wave voltammetry on un-modified pyrolytic graphite electrode for cadmium bromide solution**

#### **3.1.4.1 Procedure for optimization of deposition time for cadmium bromide solution on un-modified pyrolytic graphite electrode**

The measurements were carried out in square wave anodic stripping mode. The equipment set-up was as follows: frequency 15 Hz, deposition time 60 to 420 seconds deposition potential 0.05V, Initial Potential 0.5V, final potential -1.25 Step up potential 0.00405 V and amplitude 0.01995 V. The values of peak current were obtained by varying the deposition time.

#### **3.1.4.2 Procedure for optimization of frequency for cadmium bromide solution on un-modified pyrolytic graphite electrode**

All the measurements were carried out in square wave anodic stripping mode. The equipment set-up was as follows: frequency 15 to 45 Hz, deposition time 120 seconds, deposition potential 0.05V Initial Potential 0.5 V, Final potential -1.25, Step up potential 0.00405 V and amplitude 0.01995 V. The values of peak current were obtained by varying the frequency.

#### **3.1.4.3 Procedure for optimization of amplitude for cadmium bromide solution on un-modified pyrolytic graphite electrode**

The measurements were carried out in square wave anodic stripping mode. The equipment set-up was as follows: Frequency 30 Hz, deposition time 120 s, Initial Potential 0.5, final potential -1.25

V, Step up potential 0.00405 V and amplitude 0.02 to 0.14 V. The values of peak current were obtained by varying the amplitude.

#### **3.1.4.4 Procedure for optimization of deposition potential for cadmium bromide solution on un-modified pyrolytic graphite electrode**

All the measurements were carried out in square wave anodic stripping mode. The equipment set-up was as follows: Frequency 30 Hz, deposition potential 0.05 to 0.35 V, deposition time 120 s, Initial Potential 0.5 V, Final potential -1.25 V, Step up potential 0.00405 V Amplitude 0.01995 volts. The values of peak current were obtained by varying the deposition potential.

#### **3.1.4.5 Procedure for optimization of step potential for Cadmium bromide solution on un-modified pyrolytic graphite electrode**

All the measurements were carried out in square wave anodic stripping mode. The equipment set-up was as follows: Frequency 30 Hz, deposition potential 0.05 V, deposition time 120 s, Initial Potential 0.5 V, final potential -1.25 V ,step up potential 0.00405 to 0.02405 V and amplitude 0.08 volts. The values of peak current were obtained by varying the step potential.

### **3.1.5 Apparatus and procedure for Anodic stripping-square wave voltammetry on un-modified pyrolytic graphite electrode for a mixture of cadmium bromide and lead nitrate solution**

#### **3.1.5.1 Procedure for optimization of deposition time for a mixture of Lead nitrate and cadmium bromide solution on un-modified pyrolytic graphite electrode**

The measurements were carried out in square wave anodic stripping mode. The equipment set-up was as follows: frequency 15 Hz, deposition time 60 to 420 seconds deposition potential 0.05V, Initial Potential 0.5 V, final potential -1.25 V step up potential 0.00405 V and amplitude 0.01995 V. The values of peak current were obtained by varying the time

#### **3.1.5.2 Procedure for optimization of frequency for a mixture of Lead nitrate and cadmium bromide solution on un-modified pyrolytic graphite electrode**

All the measurements were carried out in square wave anodic stripping mode. The equipment set-up was as follows: frequency 15 to 45 Hz, deposition time 120 seconds, deposition potential 0.05V Initial Potential -1.25 V, Final potential 0.5, Step up potential 0.00405 V and amplitude 0.01995 V. The values of peak current were obtained by varying the frequency.

#### **3.1.5.3 Procedure for optimization of Amplitude for a mixture of Lead nitrate and cadmium bromide solution on un-modified pyrolytic graphite electrode**

The measurements were carried out in square wave anodic stripping mode. The equipment set-up was as follows: Frequency 30 Hz, deposition time 120 s, Initial Potential 0.5 V, final potential -



1.25 V, Step up potential 0.00405 V and amplitude 0.02 to 0.12 V. The values of peak current were obtained by varying the amplitude.

#### **3.1.5.4 Procedure for optimization of step potential for a mixture of Lead nitrate and cadmium bromide solution on un-modified pyrolytic graphite electrode**

All the measurements were carried out in square wave anodic stripping mode. The equipment set-up was as follows: Frequency 30 Hz, deposition potential 0.05 V, deposition time 120 s, Initial Potential 0.5V, final potential -1.25V, step up potential 0.00405 to 0.02005 V and amplitude 0.01995 V. The values of peak current were obtained by varying the step potential.

#### **3.1.5.5 Procedure for optimization of deposition potential for a mixture of cadmium bromide solution on un-modified pyrolytic graphite electrode**

The measurements were carried out in square wave anodic stripping mode. The equipment set-up was as follows: Frequency 30 Hz, deposition potential 0.05 to 0.35 V, deposition time 120 s, Initial Potential 0.5 V, Final potential -1.25 V, Step up potential 0.00405 V Amplitude 0.01995 volts. The values of peak current were obtained by varying the deposition potential.

#### **3.1.6 Apparatus and procedure for Anodic stripping-square wave voltammetry on modified pyrolytic graphite electrode for a mixture of cadmium bromide and lead nitrate solution**

The modified electrode was used to perform Anodic stripping-square wave voltammetry on 1ppm mixture Lead Nitrate and Cadmium bromide solution. A scan of the blank (0.1M KCl) was done. The modified electrode was used to perform experiments on optimization of factors

affecting the peak current namely, deposition time, frequency, phase amplitude, deposition potential and step potential. The equipment set up for the experiments was same as that of the non modified electrode. The values of peak current were obtained by varying this factors.

### **3.1.7 Apparatus and procedure for determination of LOD and LOQ using Anodic stripping-square wave voltammetry on modified pyrolytic graphite electrode for a mixture of cadmium bromide and lead nitrate solution**

In this experiment the modified electrode was used to perform Anodic stripping-square wave voltammetry. The LOD and LOQ values were determined by measuring the peak currents of prepared solutions of 0.1, 0.2, 0.3, 0.4 and 0.5 ppm mixture of lead nitrate and cadmium bromide. Plots of peak current against concentration was done. From the plots values of the y-intercept and calibration standard error were obtained.

### **3.1.8 Procedure for optimization of deposition time for lead nitrate solution on unmodified pyrolytic graphite electrode**

The pyrolytic graphite carbon electrode was polished for about 2 minutes with alumina slurry before each potential scan. All the electrolytic solutions were de-aerated for at least 25 min by passing Nitrogen gas through them before carrying out the study. All experiments were done at room temperature (20-25 °C ).The electrochemical cell was washed with distilled water and rinsed. A scan of the blank (0.1M KCl) was done.

All the measurements were carried out in square wave anodic stripping mode. The equipment set-up was as follows: frequency 15 Hz, deposition time 60 to 480 seconds, deposition potential 0.05V, Initial Potential 0.5 EV, final potential -1.25, Step up potential was 0.00405 EV and

amplitude 0.01995 EV. The values of peak current were obtained by varying the deposition time.

### **3.1.9 Procedure for optimization of frequency for lead nitrate solution on un-modified pyrolytic graphite electrode**

The cell preparation was carried out as described in procedure for optimization of deposition time in un-modified electrode. All the measurements were carried out in square wave anodic stripping mode. The equipment set-up was as follows: frequency 15 to 60 Hz, deposition time 120 seconds, deposition potential 0.05V, Initial Potential 0.5 V, Final potential -1.25 V, Step up potential 0.00405 V and amplitude 0.01995 V. The values of peak current were obtained by varying the frequency.

#### **3.1.3.4 Procedure for optimization of deposition potential for lead nitrate solution on un-modified pyrolytic graphite electrode**

The measurements were carried out in square wave anodic stripping mode. The equipment set-up was as follows: Frequency 30 Hz, deposition potential 0.05 to 0.075 V, deposition time 120 s, Initial Potential 0.5 V, Final potential -1.25 V, Step up potential 0.00405 EV Amplitude 0.01995 volts. The values of peak current were obtained by varying the deposition time.

#### **3.1.3.5 Procedure for optimization of step potential for lead nitrate solution on un-modified pyrolytic graphite electrode**

All the measurements were carried out in square wave anodic stripping mode. The equipment set-up was as follows: Frequency 30 Hz, deposition potential 0.05 V, deposition time 120 s, Initial Potential 0.5 V, final potential -1.25 V, step up potential 0.00405 to 0.00705 EV and amplitude 0.08 volts. The values of peak current were obtained by varying the step potential.

### **3.1.3.5 Procedure for optimization of amplitude for lead nitrate solution on un-modified pyrolytic graphite electrode**

The measurement obtained were carried out in square wave anodic stripping mode. The equipment set-up was as follows: Frequency 30 Hz, deposition time 120 s, Initial Potential 0.5V, final potential -1.25, Step up potential 0.00405 V and amplitude 0.02 to 0.14 V. The values of peak current were obtained by varying the amplitude.

### **3.1.4 Apparatus and procedure for anodic stripping-Anodic square wave voltammetry on un-modified pyrolytic graphite electrode for cadmium bromide solution**

#### **3.1.4.1 Procedure for optimization of deposition time for cadmium bromide solution on un-modified pyrolytic graphite electrode**

The measurements were carried out in square wave anodic stripping mode. The equipment set-up was as follows: frequency 15 Hz, deposition time 60 to 420 seconds deposition potential 0.05V, Initial Potential 0.5V, final potential -1.25 Step up potential 0.00405 V and amplitude 0.01995 V. The values of peak current were obtained by varying the deposition time.

#### **3.1.4.2 Procedure for optimization of frequency for cadmium bromide solution on un-modified pyrolytic graphite electrode**

All the measurements were carried out in square wave anodic stripping mode. The equipment set-up was as follows: frequency 15 to 45 Hz, deposition time 120 seconds, deposition potential 0.05V Initial Potential 0.5 V, Final potential -1.25, Step up potential 0.00405 V and amplitude 0.01995 V. The values of peak current were obtained by varying the frequency.

#### **3.1.4.3 Procedure for optimization of amplitude for cadmium bromide solution on un-modified pyrolytic graphite electrode**

The measurements were carried out in square wave anodic stripping mode. The equipment set-up was as follows: Frequency 30 Hz, deposition time 120 s, Initial Potential 0.5, final potential -1.25 V, Step up potential 0.00405 V and amplitude 0.02 to 0.14 V. The values of peak current were obtained by varying the amplitude.

#### **3.1.4.4 Procedure for optimization of deposition potential for cadmium bromide solution on un-modified pyrolytic graphite electrode**

All the measurements were carried out in square wave anodic stripping mode. The equipment set-up was as follows: Frequency 30 Hz, deposition potential 0.05 to 0.35 V, deposition time 120 s, Initial Potential 0.5 V, Final potential -1.25 V, Step up potential 0.00405 V Amplitude 0.01995 volts. The values of peak current were obtained by varying the deposition potential.

#### **3.1.4.5 Procedure for optimization of step potential for Cadmium bromide solution on un-modified pyrolytic graphite electrode**

All the measurements were carried out in square wave anodic stripping mode. The equipment set-up was as follows: Frequency 30 Hz, deposition potential 0.05 V, deposition time 120 s, Initial Potential 0.5 V, final potential -1.25 V, step up potential 0.00405 to 0.02405 V and amplitude 0.08 volts. The values of peak current were obtained by varying the step potential.

### **3.1.5 Apparatus and procedure for Anodic stripping-square wave voltammetry on un-modified pyrolytic graphite electrode for a mixture of cadmium bromide and lead nitrate solution**

#### **3.1.5.1 Procedure for optimization of deposition time for a mixture of Lead nitrate and cadmium bromide solution on un-modified pyrolytic graphite electrode**

The measurements were carried out in square wave anodic stripping mode. The equipment set-up was as follows: frequency 15 Hz, deposition time 60 to 420 seconds deposition potential 0.05V, Initial Potential 0.5 V, final potential -1.25 V step up potential 0.00405 V and amplitude 0.01995 V. The values of peak current were obtained by varying the time

#### **3.1.5.2 Procedure for optimization of frequency for a mixture of Lead nitrate and cadmium bromide solution on un-modified pyrolytic graphite electrode**

All the measurements were carried out in square wave anodic stripping mode. The equipment set-up was as follows: frequency 15 to 45 Hz, deposition time 120 seconds, deposition potential 0.05V Initial Potential -1.25 V, Final potential 0.5, Step up potential 0.00405 V and amplitude 0.01995 V. The values of peak current were obtained by varying the frequency.

#### **3.1.5.3 Procedure for optimization of Amplitude for a mixture of Lead nitrate and cadmium bromide solution on un-modified pyrolytic graphite electrode**

The measurements were carried out in square wave anodic stripping mode. The equipment set-up was as follows: Frequency 30 Hz, deposition time 120 s, Initial Potential 0.5 V, final potential -

1.25 V, Step up potential 0.00405 V and amplitude 0.02 to 0.12 V. The values of peak current were obtained by varying the amplitude.

#### **3.1.5.4 Procedure for optimization of step potential for a mixture of Lead nitrate and cadmium bromide solution on un-modified pyrolytic graphite electrode**

All the measurements were carried out in square wave anodic stripping mode. The equipment set-up was as follows: Frequency 30 Hz, deposition potential 0.05 V, deposition time 120 s, Initial Potential 0.5V, final potential -1.25V, step up potential 0.00405 to 0.02005 V and amplitude 0.01995 V. The values of peak current were obtained by varying the step potential.

#### **3.1.5.5 Procedure for optimization of deposition potential for a mixture of cadmium bromide solution on un-modified pyrolytic graphite electrode**

The measurements were carried out in square wave anodic stripping mode. The equipment set-up was as follows: Frequency 30 Hz, deposition potential 0.05 to 0.35 V, deposition time 120 s, Initial Potential 0.5 V, Final potential -1.25 V, Step up potential 0.00405 V Amplitude 0.01995 volts. The values of peak current were obtained by varying the deposition potential.

#### **3.1.6 Apparatus and procedure for Anodic stripping-square wave voltammetry on modified pyrolytic graphite electrode for a mixture of cadmium bromide and lead nitrate solution**

The modified electrode was used to perform Anodic stripping-square wave voltammetry on 1ppm mixture Lead Nitrate and Cadmium bromide solution. A scan of the blank (0.1M KCl) was done. The modified electrode was used to perform experiments on optimization of factors

affecting the peak current namely, deposition time, frequency, phase amplitude, deposition potential and step potential. The equipment set up for the experiments was same as that of the non modified electrode. The values of peak current were obtained by varying these factors.

### **3.1.7 Apparatus and procedure for determination of LOD and LOQ using Anodic stripping-square wave voltammetry on modified pyrolytic graphite electrode for a mixture of cadmium bromide and lead nitrate solution**

In this experiment the modified electrode was used to perform Anodic stripping-square wave voltammetry. The LOD and LOQ values were determined by measuring the peak currents of prepared solutions of 0.1, 0.2, 0.3, 0.4 and 0.5 ppm mixture of lead nitrate and cadmium bromide. Plots of peak current against concentration was done. From the plots values of the y-intercept and calibration standard error were obtained.



## CHAPTER FOUR

### 4.0 RESULTS AND DISCUSSIONS

#### 4.1 Cyclic voltammetry

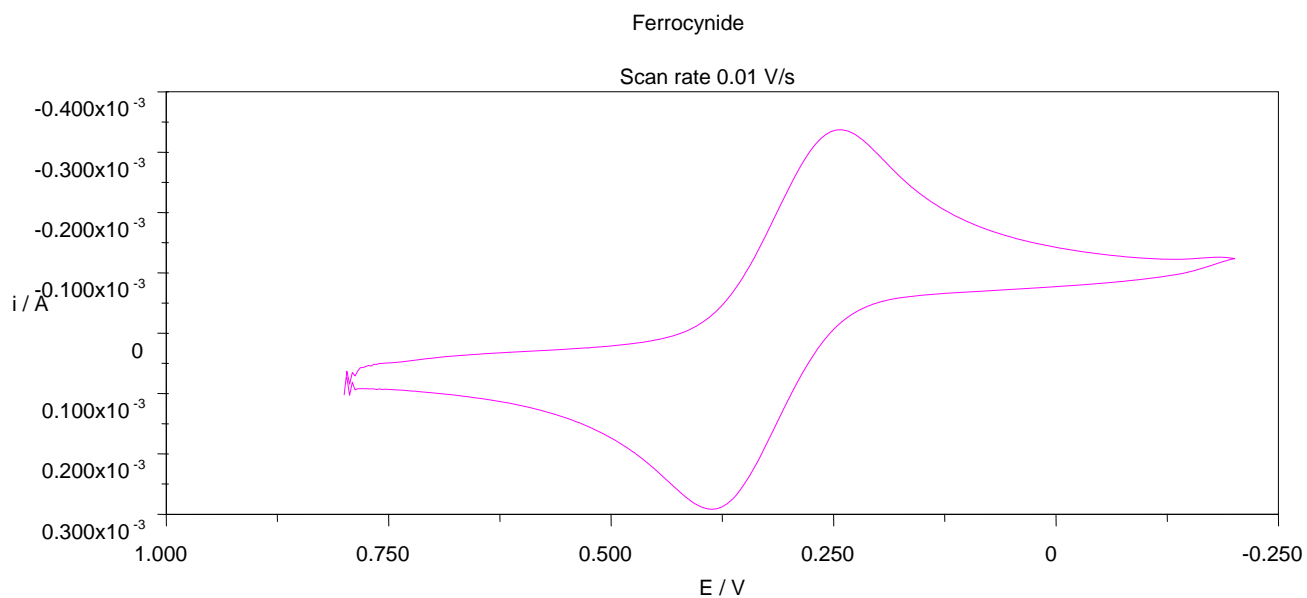
##### 4.1.1 Voltammetric study of 4.0mM ferrocene in 0.1M TEAB in acetonitrile/water (1:1) as a standard

Ferrocene is popularly used as standard for the study of electrode processes [Hinman et al. 1985], [Kamau et. al, (1994)]. Ferrocene (bis-cyclopentadienyl iron),  $(C_5H_5)_2Fe$ , has the iron atom symmetrically placed between two cyclopentadienyl rings. Each of the anion forms a covalent bond to the ferrous ion symmetrically; it is readily oxidized to Ferrocenium ion [Wilkinson et al. 1952]. The results of the voltammetric studies of ferrocene in 0.1 M TEAB in acetonitrile/water (1:1) are given in Table 4–1 below:

**Table 4-1: Scan rate studies of 0.4 mM ferrocene in 0.1 M TEAB in acetonitrile/water (1:1).**

Scan rate Volts/seconds	$E_{Pa}$ V/s SCE	$I_{pa}, \mu A$	$E_{pc}$ Volts, V/s SCE	$I_{pc}, \mu A$	$\Delta E_p$ Volts	$I_{pa}/ I_{pc}$
0.010	0.388	50	0.317	50	0.071	1
0.015	0.389	59	0.317	59	0.072	1
0.020	0.383	69	0.317	69	0.072	1
0.030	0.400	96	0.320	96	0.080	1
0.04	0.390	104	0.310	104	0.080	1

Cyclic voltammetry studies on 0.4 mM ferrocene in 0.1M Tetraethylammoniumbromide (TEAB) gave one peak for each of the anodic and cathodic potential scans. Both peaks were of similar shape as shown in Figure 4.1:



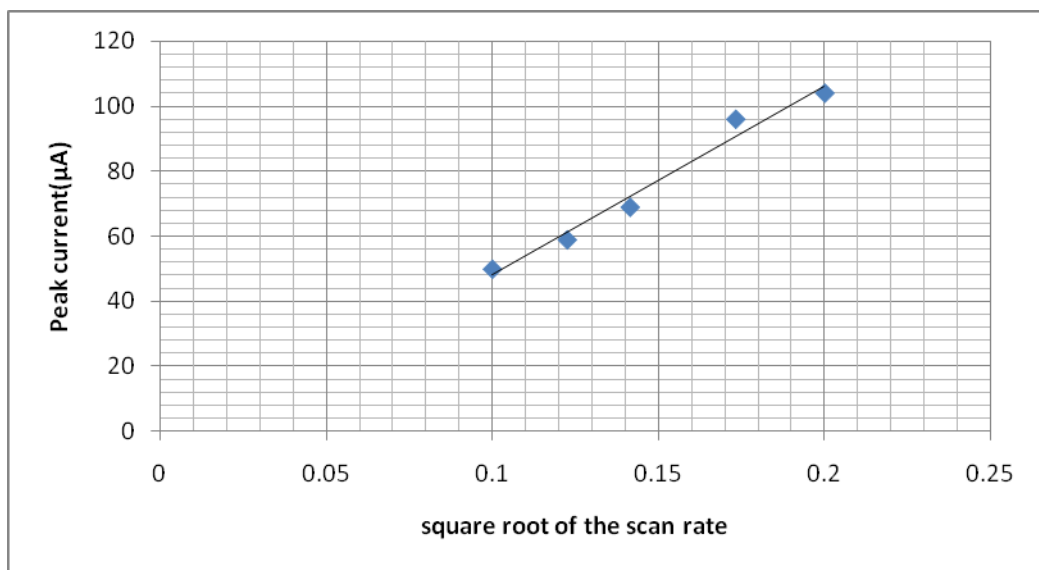
**Figure 4.1: Cyclic voltammogram of 4mM ferrocene in 0.1 M TEAB in acetonitrile/water (1:1) at a scan rate of 0.010 VS<sup>-1</sup>.**

Table 4.2 below show the scan rate in Volts/seconds, square root of scan rate and corresponding ( $I_{pa}$ ) in micro amperes ( $\mu A$ ).

**Table 4-2: Square root of Scan rate against peak current for ferrocene in 0.1 M TEAB, acetonitrile/water (1:1).**

Scan rate Volts/seconds	Square root of the Scan rate Volts/seconds	$I_{pa}, \mu A$
0.01	0.100	50
0.015	0.1225	59
0.020	0.1414	69
0.030	0.1732	96
0.040	0.2	104

A plot of peak current versus square root of scan rate (Figure 4.2 ) gave a straight line, suggesting diffusion controlled electrode reaction as expected for this system. This is similar to what was previously reported by [Kamau et al (1994)].



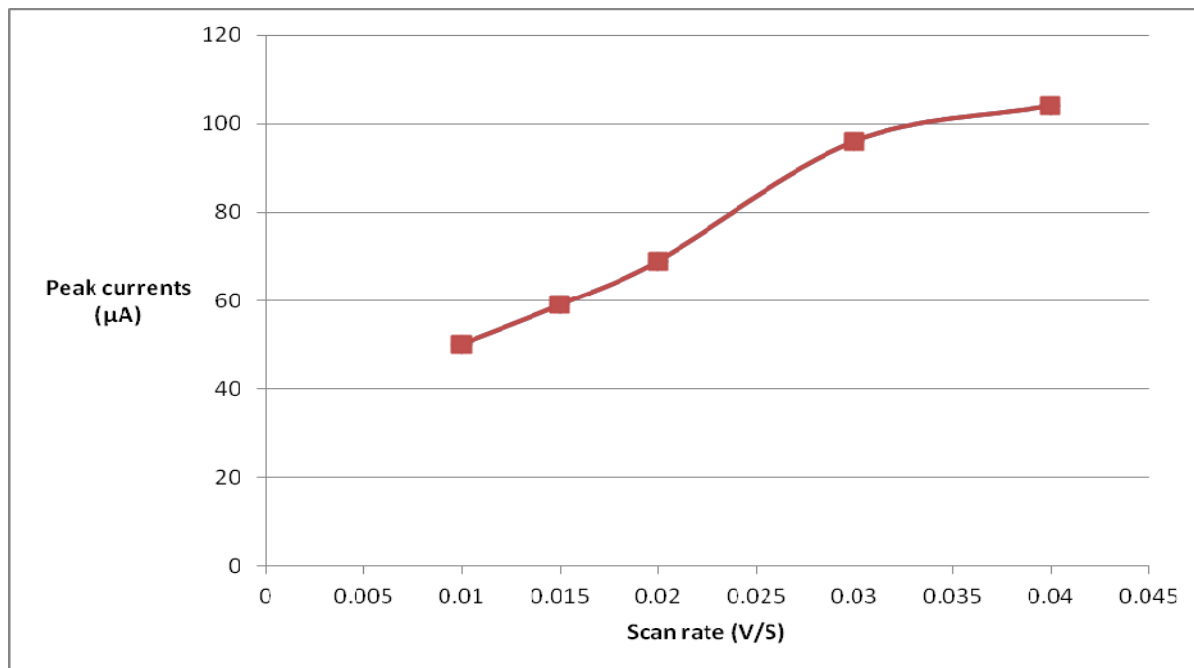
**Figure 4.2: A plot of anodic peak current versus square root of scan rate for ferrocene.**

Table 4-3 below shows the variation of measured current with increase in scan rate for the ferrocene compound. on un-modified pyrolytic graphite as working electrode

**Table 4-3: Scan rate against peak current for ferrocene in 0.1 M TEAB, acetonitrile/water (1:1).**

Scan rate Volts/seconds	$I_{pa}, \mu A$
0.01	50
0.015	59
0.020	69
0.030	96
0.040	104

On the other hand, non linear cases was observed for a plot of peak current versus scan rate as expected (Figure 4.3 ) for the ferrocene-acetonitrile-water system.



**Figure 4.3: A plot of peak anodic current versus square root of scan rate for ferrocene.**

The above plots (Figure 4.2 and 4.3) were expected for a reversible system [Christopher and Ana Maria, 1993]. The fact that  $i_{pa}$  is proportional to the square root of scan rate indicates diffusion controlled electrode process [ Bard et al. 2001]. The ratio of anodic peak current to cathodic peak current (Table 4.1) was unity ( $i_{pa}/i_{pc}=1$ ), which implied a diffusion- controlled electrode process [Nicholson and Irving 1964]. The anodic peak potential,  $E_{pa}$ , was  $0.390 \pm 0.006V$  vs SCE for five different scan rate while the cathodic peak potential,  $E_{pc}$ , was  $0.22 V \pm 0.003 V$  vs SCE for five different scan rates. The values of  $E_{pa}$  ( $0.390 \pm 0.006$ ) were within experimental error compared to  $0.354 \pm 0.09 V$  in tetrabutylammonium tetrafluoroborate ( $TBABF_4$ ) reported by Mirriam, (1998). The increase in anodic peak potential with increase of the scan rate (Table 4.1) agrees with the result observed by Mirriam (1996) and by Iwunze et al. (1990) for ferrocene in 21% DDAB microemulsions and Kamau et al (1994).

The anodic to cathodic peak potential separation observed for the five scan rates was  $170 mV \pm 0.006 mV$  vs.SCE as expected for nearly reversible one electron transfer system [Nicholson and Irving, 1964]. The increase of peak separation with increase in scan rate observed at higher scan rates (Table 4.1) is consistent with what has been reported for 1.0 mM ferrocene in 21% DDAB microemulsions [Iwunze et al.1999], 0.4mM ferrocene in 0.1M tetrabutylammonium perchlorate [Kadish et al 1984] and 0.1 mM ferrocene in 0.1 M TBAP/CHCN using platinum electrode [Hinman et al.1985]. Such an increase may be attributed to uncompensated resistance (IR) or the quasi-reversible behavior (non-linear diffusion) of oxidation of ferrocene at higher scan rate as reported by Hague et al. The effect of solution resistance and uneven potential distribution (resistivity and electrode radius or shift in reference electrode potential) on linear sweep

voltammetry was shown experimentally to cause a displacement of the anodic peak potential towards a positive potential while the reverse was observed for the cathodic peak [Hinman et al. 1985]. Even under optimum conditions for the reduction, uncompensated resistance (IR) may still remain [Kadish et al 1984].

#### 4.1.2 Cyclic voltammetry of 5.0mM Lead nitrate in 0.1M KCl using modified and un-modified pyrolytic graphite electrode

Cyclic voltammetry studies of 5mM lead nitrate in 0.1M potassium chloride (KCl) gave one peak for each of the anodic and cathodic potential scans. Both peaks were of similar shape as shown in Figure 4.4 and 4.5 below:

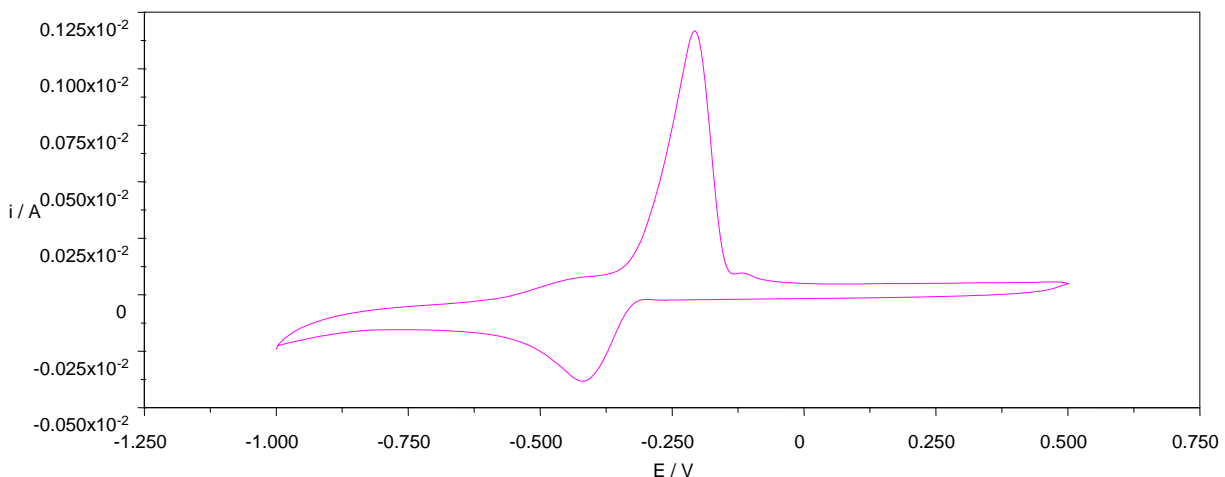


**Figure 4.4: Cyclic voltammogram of 5.0mM Lead nitrate in 0.1M KCl using un-modified pyrolytic graphite electrode at scan rate of 0.035 Vsec-1.**

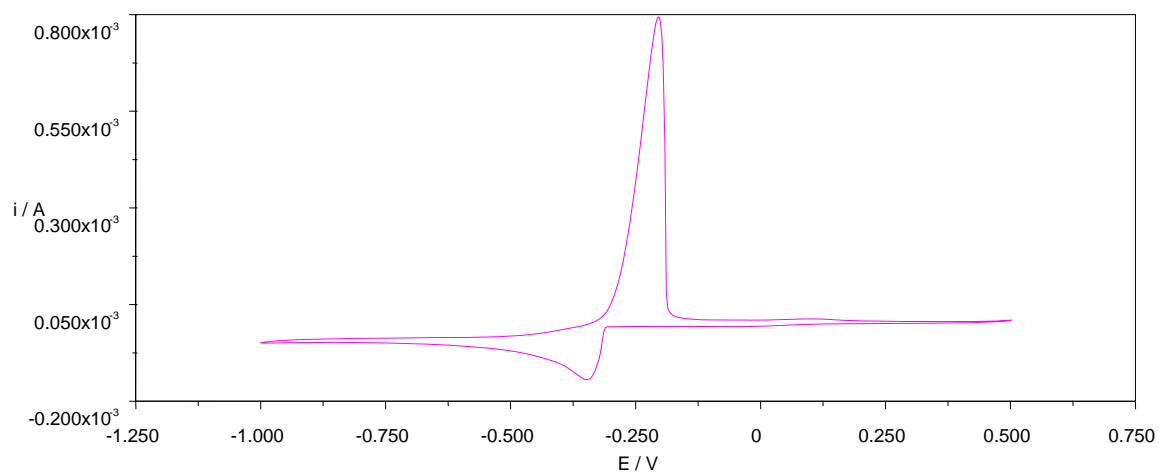


**Figure 4. 5: Cyclic voltammogram of 5.0mM lead nitrate in 0.1M KCl using modified pyrolytic graphite electrode at scan rate of 0.010 Vs<sup>-1</sup>.**

Table 4-4 highlights the effects of scan rate on the measured current.

**Table 4-4: Anodic and cathodic peak currents for 5mM lead nitrate.**

Table :Scan Rate Volts/Sec	Un-modified electrode		Modified electrode		Ratio of Anodic current (Modified/un-modified)
	Anodic peak current(μA)	Cathodic peak current	Anodic peak current	Cathodic peak current	
0.01	675	175	875	1250	1.3
0.015	825	237.5	875	1250	1.1
0.020	830	250	975	200	1.2
0.025	875	313	1125	250	1.3
0.030	875	313	1125	250	1.3
0.035	1125	375	1200	375	1.1
0.040	1193	375	1250	375	1.1
0.045	1250	443	1250	125	1.0
0.05	1250	443	1380	375	1.1



The ratio of anodic peak current for modified and non modified electrode was greater than unity as shown in Table 4-4. This is a clear demonstration of an increase in the sensitivity of the modified electrode in the detection of lead. Conjugated polymers can be made to conduct electricity through doping and polyaniline is such example. The electrically conductive form of polyaniline ( emeraldine ) when doped with an acid, protonates the imine nitrogens on the polymer backbone and induces charge carriers. The conductivity of polyaniline increases with doping from the undoped insulating emeraldine base form ( $\sigma < 10^{-10} \text{ Scm}^{-1}$ ) to the fully doped, conducting emeraldine salt form ( $\sigma > 1 \text{ Scm}^{-1}$ ) [ Wiley-VCH, et. al, 2004.] Table 4.5 shows the scan rate in Volts/seconds, square root of scan rate and corresponding  $I_{pa}$ ,  $\mu\text{A}$  for modified electrode.

**Table 4-5: Anodic peak current versus square root of scan rate for Lead Nitrate for modified electrode.**

Scan rate(V/S)	Square root of V/S	Current $I_{pa}$ , $\mu\text{A}$
0.01	0.10	875
0.015	0.12	875
0.020	0.14	975
0.025	0.16	1125
0.030	0.17	1125
0.035	0.19	1200
0.040	0.2	1250
0.045	0.21	1250
0.050	0.22	1380

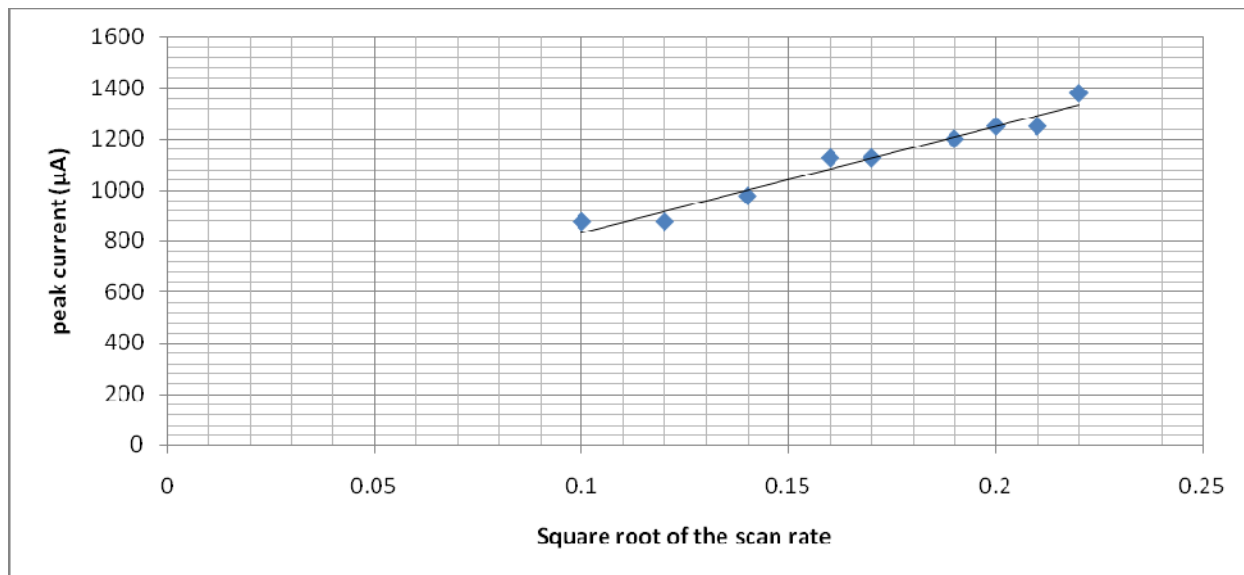


**Figure 4. 6: A plot of peak anodic current versus square root of scan rate for Lead nitrate on modified electrode.**

The anodic peak potential,  $E_{pa}$ , was  $0.42 \text{ V} \pm 0.006 \text{ V}$  vs. Ag / AgCl for nine different scan rates. The values of  $E_{pa}$  ( $0.42 \pm 0.006$ ) were within experimental error compared to  $0.354 \pm 0.09 \text{ V}$  in tetrabutylammonium tetrafluoroborate ( $\text{TBABF}_4$ ), reported by Mirriam, (1998) and also  $0.34 \text{ V}$  in 21% DDAB microemulsions reported by Iwunze et al. (1990),  $0.304 \pm 0.002 \text{ v/s SCE}$  in  $0.2 \text{ LiCl}_4/\text{CH}_3\text{CN}/\text{H}_2\text{O}$ , at highly polished glassy carbon electrode reported by Kamau et al (1994). The increase in anodic peak potential with increase of the scan rate (Table 4-5) agrees with the result observed by Mirriam (1996) and by Iwunze et al. (1990) for ferrocene in 21% DDAB microemulsions.

### 4.1.3 Cyclic voltammetry of 5.0mM cadmium bromide in 0.1M KCl using modified pyrolytic graphite electrode at different scan rate

Cyclic voltammetry studies on 5mM cadmium bromide in 0.1M potassium chloride (KCl) gave one peak for each of the anodic and cathodic potential scans. Both peaks were of similar shape as shown in Table 4-6 and Figure 4.7:

**Table 4-6: Scan rate studies of cadmium bromide in 0.1 M KCl.**

Scan rate in Volts/sec	$E_{pc}$ Volts V/s SCE	$I_{pa}$ , $\mu A$	$E_{pa}$ Volts V/s SCE	$I_{pc}$ , $\mu A$	$\Delta E_p$ Volts V/s SCE	$I_{pa}/I_{pc}$
0.05	0.45	1230	0.525	880	0.075	1.3
0.045	0.50	350	0.69	250	0.20	1.4
0.04	0.50	410	0.670	290	0.17	1.4
0.035	0.50	410	0.630	290	0.13	1.4
0.025	0.50	400	0.630	290	0.13	1.4

This suggests that the oxidized ions on the surface of the electrode are not stable [Bard et al. 2000]. The ratio of anodic peak current to cathodic peak current (Table 4.6) was unity ( $i_{pa}/i_{pc}=1$ ), which implied a diffusion- controlled electrode process [Nicholson and Irving 1964]. The anodic peak potential,  $E_{pa}$ , was  $0.490 \pm 0.006$  V vs Ag/AgCl for five different scan rates while the cathodic peak potential,  $E_{pc}$ , was  $0.63 \pm 0.006$  V vs SCE for five different scan rates.

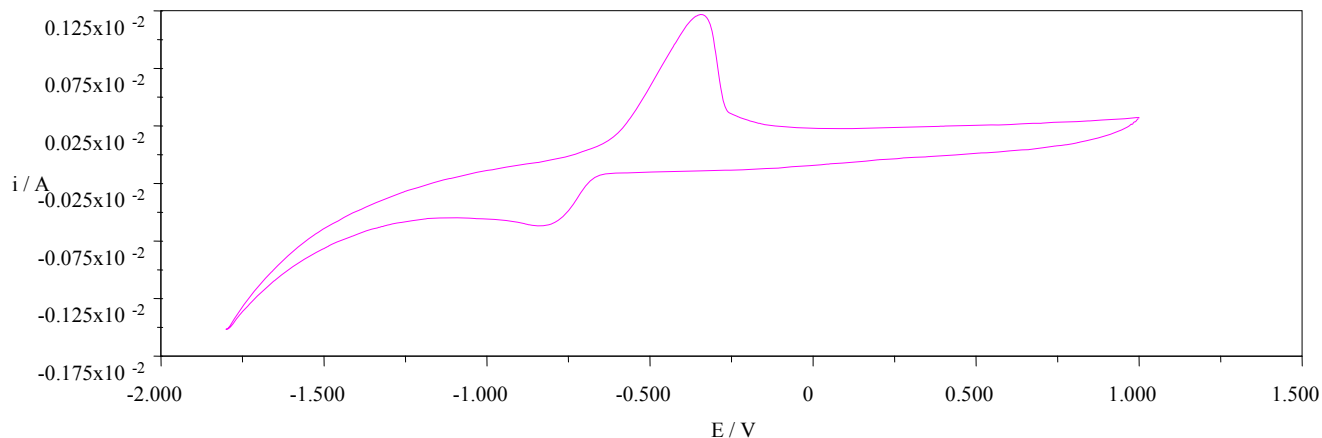
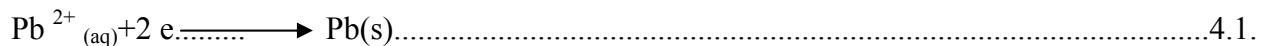


**Figure 4.7: Resultant Voltammogram of Cadmium bromide obtained at scan rate of 0.05 VS<sup>-1</sup> using pyrolytic graphite as working electrode.**

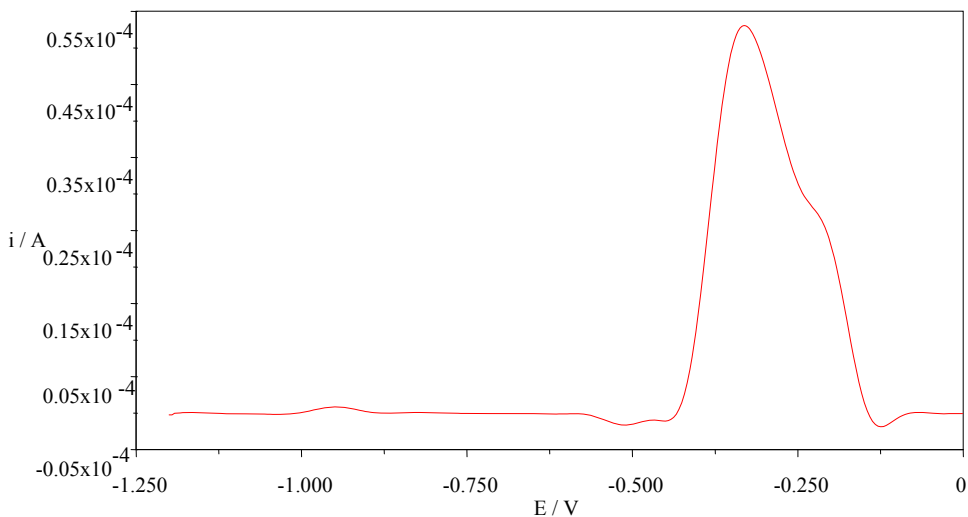
#### **4.2 Anodic stripping-square wave voltammetry on lead nitrate solution**

The cyclic voltammogram of 5ppm Pb<sup>2+</sup> in 0.1M KCl solution as a supporting electrolyte was recorded (Figure. 1.8). Reduction/oxidation processes were clearly exhibited. The reduction peak appeared 0.42V. When the scan rate was reversed, the oxidation peak occurred at 0.025 V. The scan was from 0.750V to -1.250 V which was high enough to drive the reduction of Pb<sup>2+</sup>. Lead ions in the solution gain electrons to become Pb metal at the surface of the electrode.



#### 4.2.1 The effect of deposition time on peak current obtained using Anodic stripping-square wave voltammetry on un-modified pyrolytic graphite electrode

Electroanalysis has made it possible the detection of trace levels of heavy metals in aqueous samples at an affordable cost. Anodic stripping-square wave voltammetry (AS-SWV) can provide detection limits for heavy metals in the low parts-per-billion (ppb) concentration range. The pyrolytic graphite electrode has been widely used with ASV. Numerous applications in trace metal analysis involve the use of modified electrodes. Parameters such as frequency, deposition potential, step potential and amplitude were held constant. Fig 4.8 shows voltammogram obtained when AS-SWV was carried out on 30 ppm lead nitrate solution at 120 s deposition time.



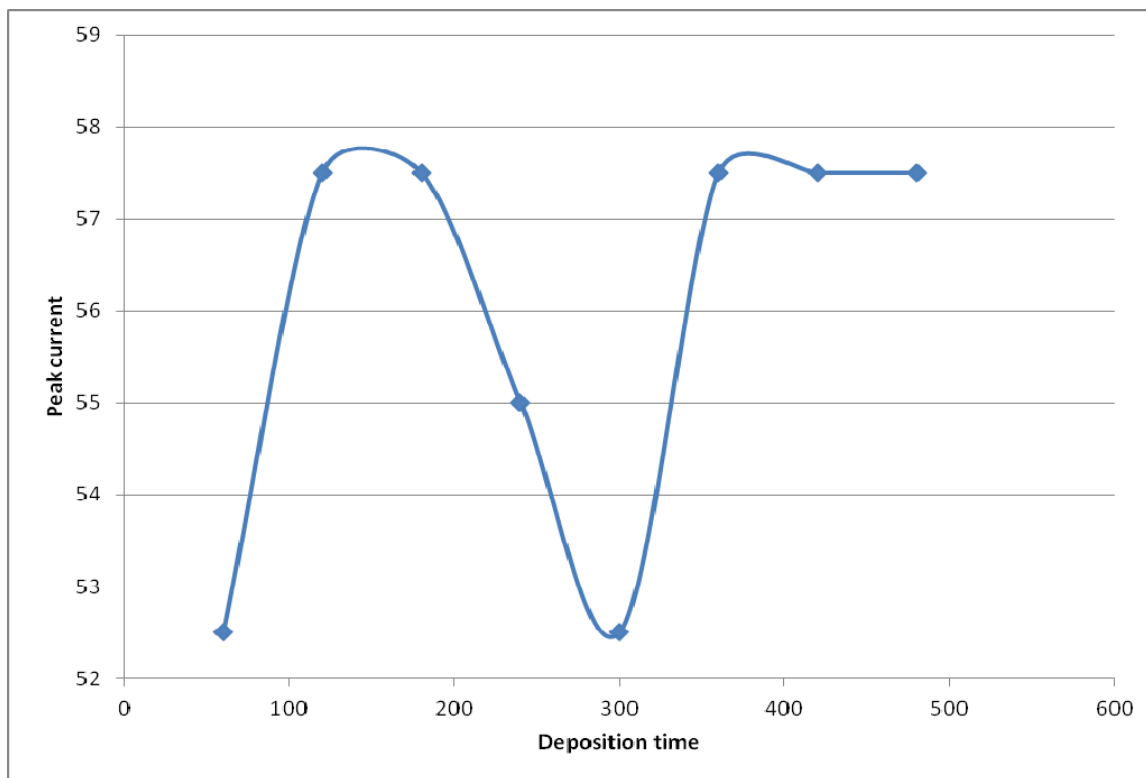
**Figure 4.8: Square wave voltammogram for 30 ppm Lead nitrate solution obtained at 120 seconds deposition time using un-modified Pyrolytic graphite as working electrode.**

Table 4-7 below shows the effect of deposition time on the peak currents. This is an important parameter for stripping techniques and has a substantial influence on the sensitivity of the technique. The effect of deposition time on stripping current for lead ions was studied from 60 to 480 seconds .

**Table 4-7: Peak current and deposition time.**

Deposition time	Current( $\mu$ A)
60	52.5
120	57.5
180	57.5
240	55
300	52.5
360	57.5
420	57.5
480	57.5

The Figure 4.9 below show a plot of peak current against deposition time. From the cyclic voltammetry carried on out  $Pb^{2+}_{(ag)}$  earlier in the research, the midpoint for the forward and backward wave was 0.313 V, This is a confirmation that peaks obtained at almost same V using anodic stripping-square wave voltammetry are for  $Pb^{2+}$  ions. It can be seen from Fig 4.9, the peak current increased as the deposition time increased up to 120 seconds, dropped, rose and remained constant.

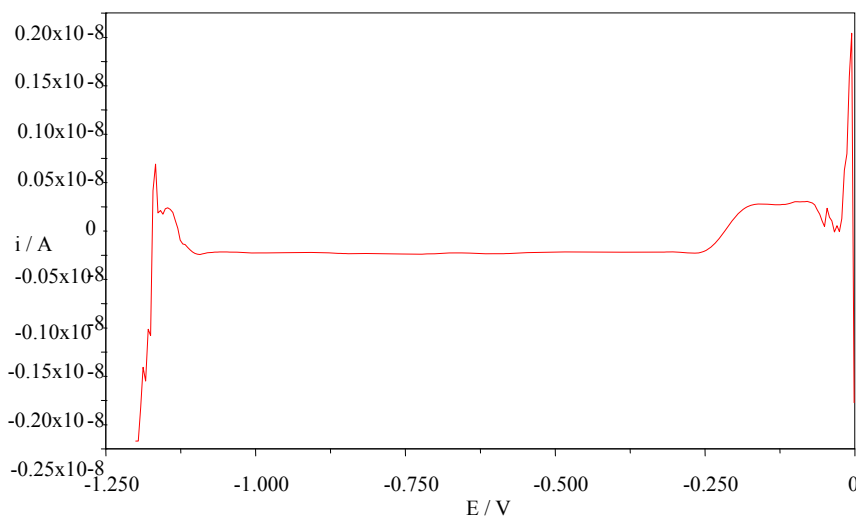


**Figure 4.9: A plot of peak current against deposition time for lead nitrate solution.**

Improving the deposition time more and more lead ions accumulated on the surface of the electrode. This had significant increase on the peak current. The drop in peak current at 300 seconds is un expected, however, the peak current remain constant. This is expected since the surface of the electrode get saturated with lead ions. In this work 120 seconds deposition time was selected as the deposition time. The scan of the blank solution never gave absorption peaks at -0.313 V see Figure 4.10.A similar experiment was carried out by [Pipat et al., 2010]. In this experiment 600 s was employed for subsequent experiments". The peak current obtained in this case was 40.8 $\mu$ A, This was less than 57.5  $\mu$ A obtained in present research work, in this two studies different electrodes and electrolyte was employed which may accounted for the differences in observed peak currents .

#### 4.2.2 The effect of frequency on peak current obtained using Anodic stripping-square wave voltammetry on un-modified pyrolytic graphite electrode

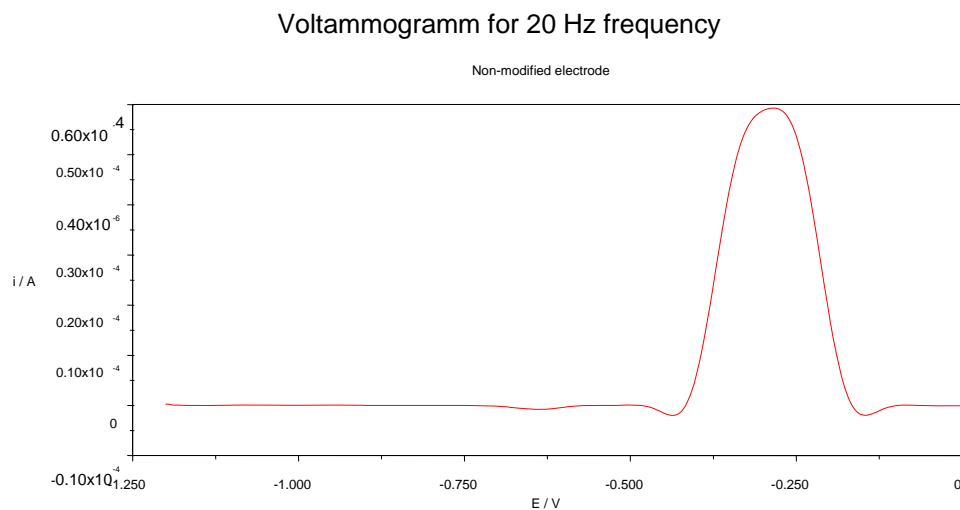
The anodic stripping performed here was aimed at optimizing the frequency in order to obtain maximum peak current for detection of lead ions in prepared solution while other parameters such as deposition potential, deposition time, step potential and amplitude were held constant. The voltammogram obtained for the blank did not show absorption at reduction potential for lead ions (Figure 4.10).



**Figure 4.10: Square wave voltammogram for 0.1M KCl (Blank) solution obtained at Frequency of 15 Hz using bare Pyrolytic graphite as working electrode.**



Figure 4.11 shows voltammogram obtained when AS-SWV was carried out on 30 ppm lead nitrate solution at a frequency of 20Hz using un-modified pyrolytic graphite electrode. The electrolyte used was 0.1M KCl.



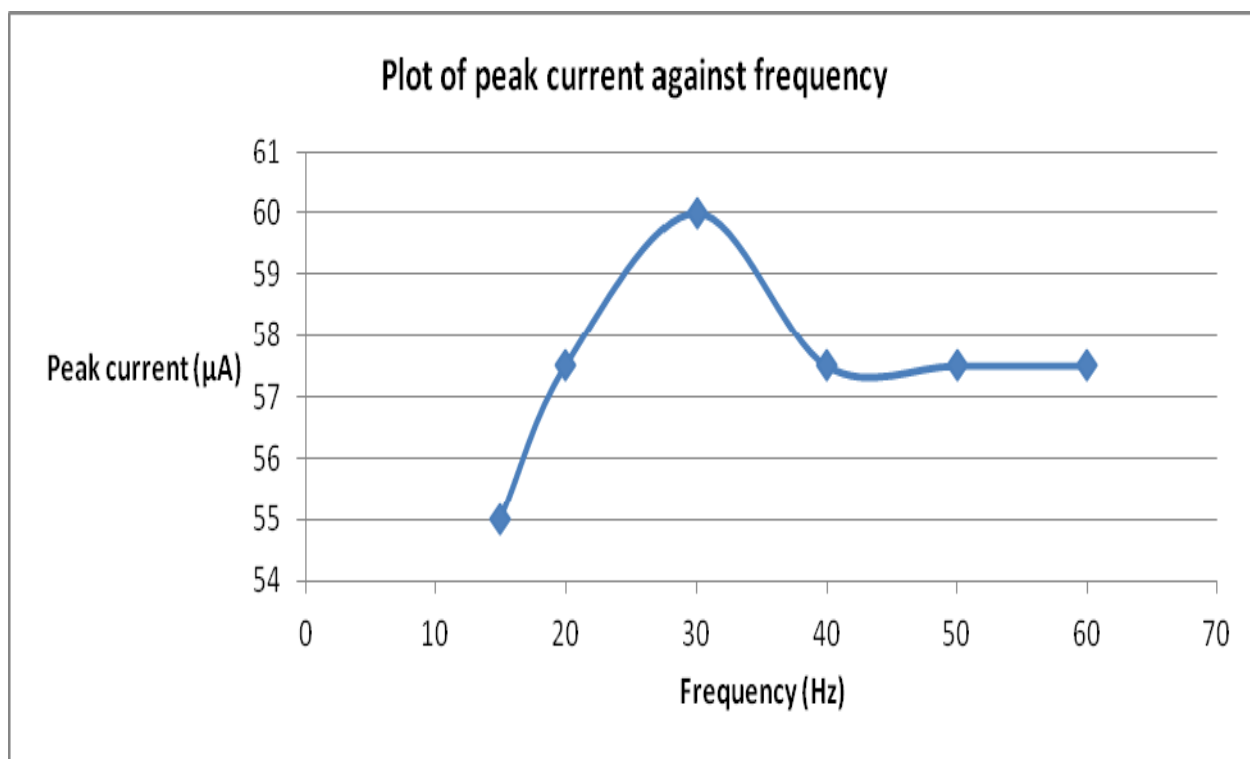
**Figure 4.11: Square wave voltammogram for 30 ppm Lead nitrate solution obtained at Frequency of 20 Hz using un-modified Pyrolytic graphite as working electrode.**

Table 4–8 below shows frequency and corresponding peak current obtained using non-modified pyrolytic graphite as working electrode.

**Table 4-8: Peak current and Frequency using un-modified pyrolytic graphite electrode.**

Frequency(Hz)	Current( $\mu$ A)
15	55
20	57.5
30	60
40	57.5
50	57.5
60	57.5

Figure 4.12 shows a plot of peak current against frequency for 30ppm lead nitrate solution, obtained using un-modified pyrolytic graphite electrode as working electrode. Frequency was varied from 15 to 60 Hz. The corresponding peak currents increased as frequency reached 30 Hz. It was observed from the voltammograms that the peak size started broadening beyond frequency of 30 Hz. The maximum peak current was obtained at frequency of 30 Hz. This frequency was chosen for the experiment. Beyond this frequency the peak current dropped and then leveled off. The stripping potential for this experiment was -0.313V.

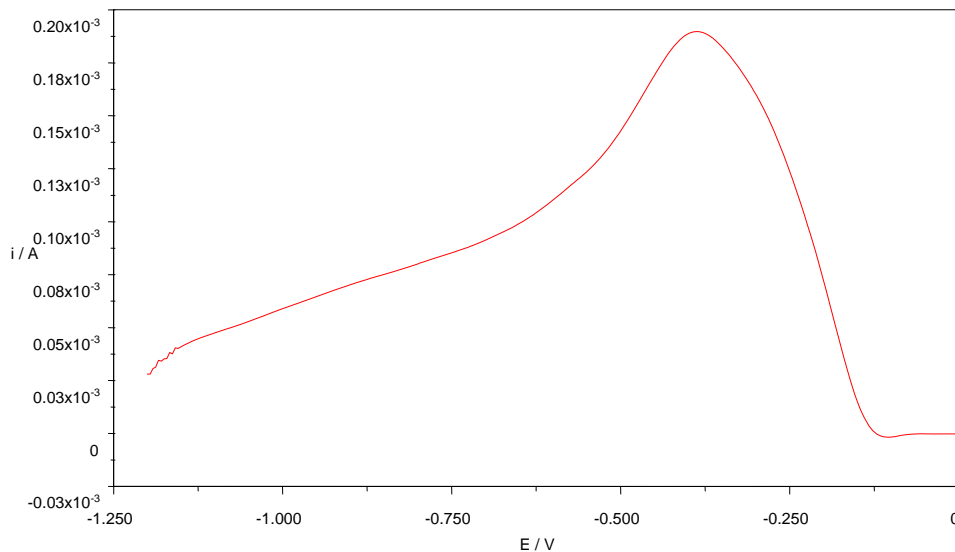


**Figure 4. 12: A plot of peak current against Frequency for 30ppm lead nitrate solution.**

A similar experiment was carried out by Pipat et al., 2010. The stripping potential was -0.450, which is comparable to the stripping potential obtained in the current research above.

#### 4.2.3 The effect of amplitude on peak current obtained using Anodic stripping-square wave voltammetry on un-modified pyrolytic graphite electrode

The anodic stripping performed here was aimed at optimizing the amplitude in order to obtain maximum peak current for detection of lead ions in prepared solution while other parameters such as frequency, deposition time, step potential and deposition potential were held constant. Figure 4.13 shows voltammogram obtained when AS-SWV was carried out on 30 ppm lead nitrate solution at amplitude of 0.08 V using un-modified pyrolytic graphite electrode as working electrode. The electrolyte used was 0.1M KCl.



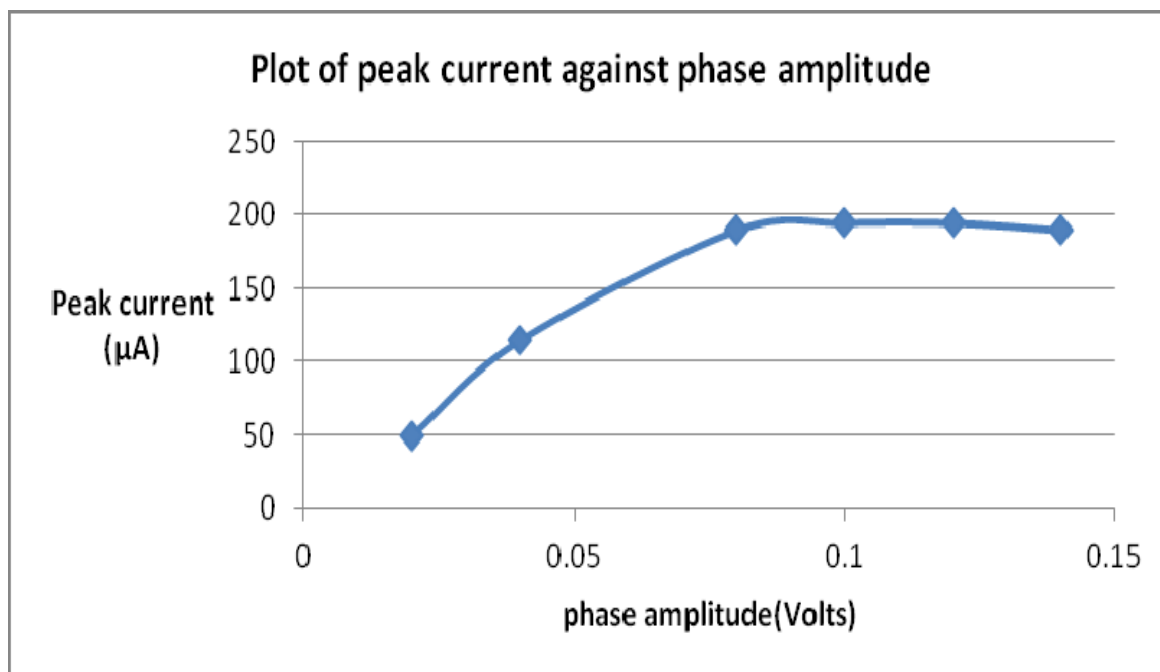
**Figure 4. 13: Square wave voltammogram for 30 ppm Lead nitrate solution obtained at amplitude of 0.08 Volts using un-modified Pyrolytic graphite as working electrode.**

Table 4-9 shows amplitude and corresponding peak current obtained using un-modified pyrolytic graphite as working electrode.

**Table 4-9: Peak current and amplitude.**

Phase amplitude (volts)	Current( $\mu$ A)
0.02	50
0.04	115
0.08	190
0.10	195
0.12	195
0.14	190

**Figure 4.14 shows a plot of peak current against amplitude obtained using un-modified pyrolytic graphite as working electrode.**



**Figure 4. 14: A plot of peak current against Change in phase amplitude using un-modified pyrolytic graphite electrode.**

The amplitude was varied from 0.02 to 0.14 volts. From the geometry of the voltammograms, the peak current increased as the phase amplitude was raised from 0.02 to 0.1 Volts. The amplitude of 0.08 Volts gave a fairly symmetrical peak. Beyond this amplitude the peak started to broaden with lower stability. Therefore, amplitude phase of 0.08 Volts was chosen for further studies. A repeat of the scan at low amplitude of 0.008 and 0.006 gave even broader peaks.

#### 4.2.4 The effect of deposition potential on peak current obtained using Anodic stripping-square wave voltammetry (AS-SWV) on un-modified pyrolytic graphite electrode

Deposition potential is an important parameter for stripping techniques and it has a substantial influence on the sensitivity determination. The electrochemical analysis performed here was aimed at optimizing the deposition potential in order to obtain maximum peak current for detection of lead ions in prepared solution while other parameters such as frequency, deposition time, step potential and amplitude were held constant. Figure 4.15 shows voltammogram obtained when AS-SWV was carried out on 30 ppm lead nitrate solution at deposition potential of 0.05 V using un-modified pyrolytic graphite electrode as working electrode.

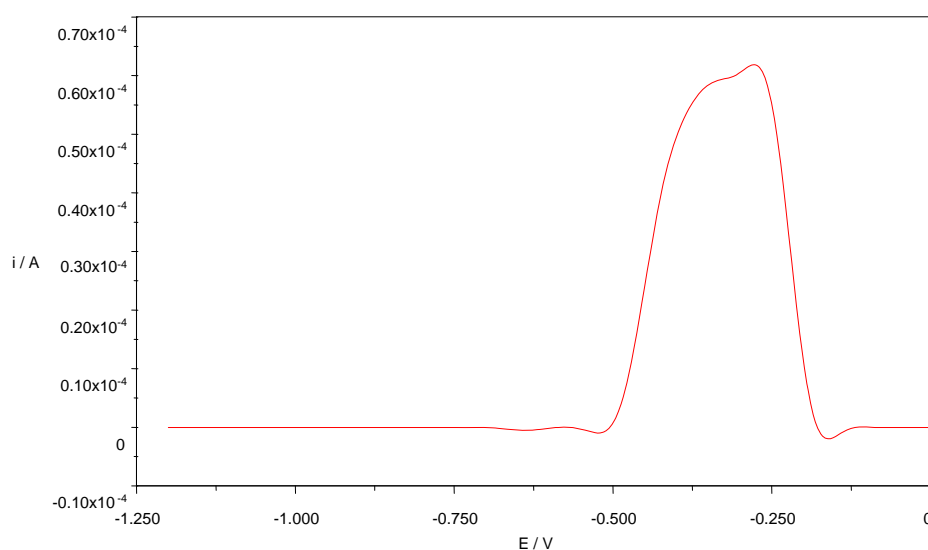


**Figure 4. 15: Square wave voltammogram for 30 ppm Lead nitrate solution obtained at deposition potential 0.05 Volts using un-modified Pyrolytic graphite as working electrode.**

Table 4–10 shows deposition potential and corresponding peak current obtained using un-modified pyrolytic graphite as working electrode.

**Table 4-10: Peak current and deposition potential obtained using un-modified electrode.**

Deposition potential (Volts)	Current( $\mu$ A)
0.05	62.5
0.055	57.5
0.060	57.5
0.065	57.5
0.070	57.5
0.075	57.5

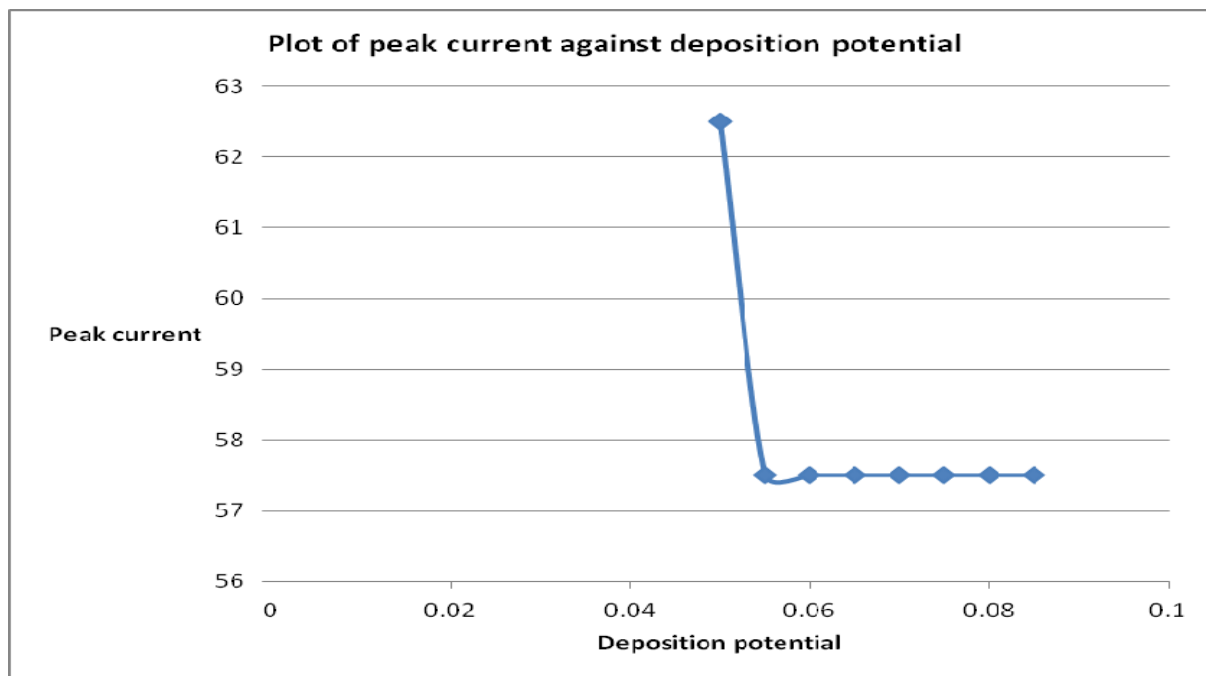


**Figure 4. 16: A plot of peak current against deposition potential.**

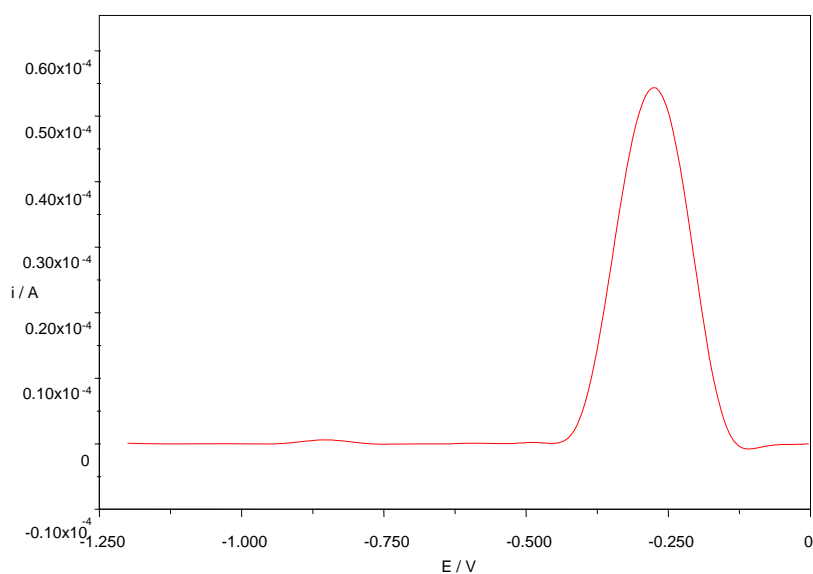
The effect of deposition potentials on the stripping peak currents of  $Pb^{2+}$  is shown in Figure. 4.16. The deposition potential was varied from 0.05 to 0.085 V with a constant deposition time of 120 s. Therefore, the optimum value of the deposition potential used in this work was 0.05V. This value gave the highest peak current, there after the peak current dropped and leveled off. In this experiment the stripping peak was observed at -0.3125 Volts. This shows that at deposition potential of 0.05 volts all the lead ions are reduced and more negative potential is unnecessary.



#### 4.2.5 The effect of step potential on peak current obtained using Anodic stripping-square wave voltammetry on un-modified pyrolytic graphite electrode

The anodic stripping performed here was aimed at optimizing the step potential in order to obtain maximum peak current for detection of lead ions in prepared solution while other parameters such as frequency, deposition time, amplitude and deposition potential were held constant.

Figure 4.17 shows voltammogram obtained when AS-SWV was carried out on 30 ppm lead nitrate solution at step potential of 0.00605 V using un-modified pyrolytic graphite electrode as working electrode.



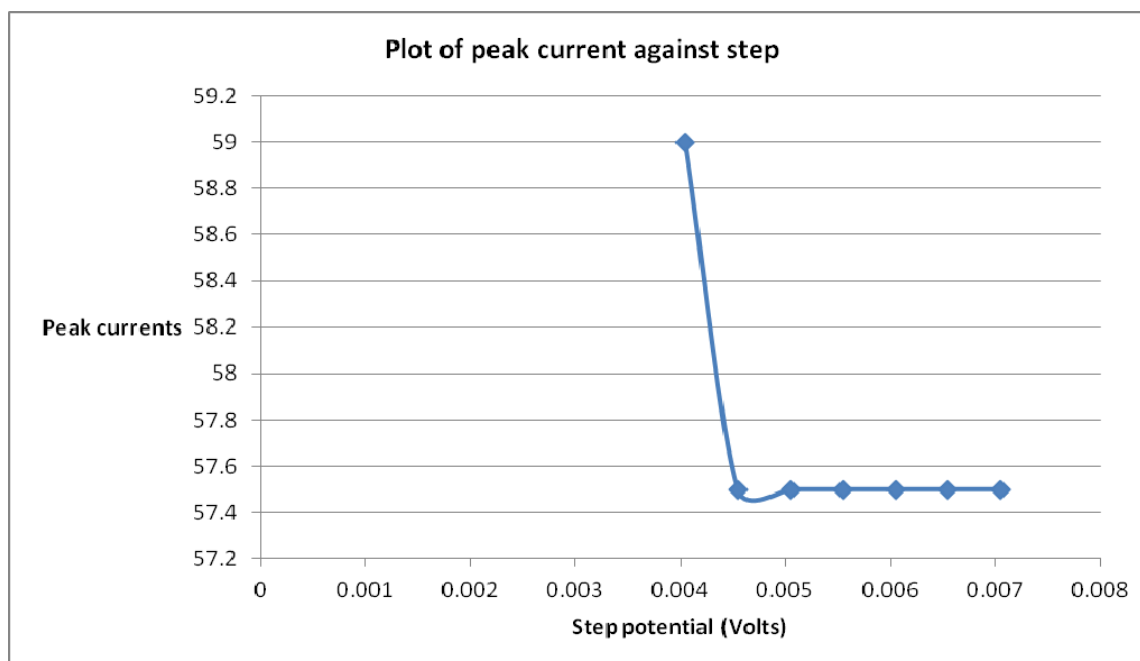
**Figure 4. 17: Square wave voltammogram for 30 ppm Lead nitrate solution obtained at step potential of 0.00605 Volts using un-modified Pyrolytic graphite as working electrode.**

Table 4–11 shows step potential and corresponding peak current obtained using un-modified pyrolytic graphite as working electrode.

**Table 4-11: Peak current and step potential.**

Step potential (Volts)	Current( $\mu$ A)
0.00405	59
0.00455	57.5
0.00505	57.5
0.00555	57.5
0.00605	57.5
0.00655	57.5
0.00705	57.5

Figure 4.18 shows a plot of peak current against step potential obtained using un-modified pyrolytic graphite as working electrode.



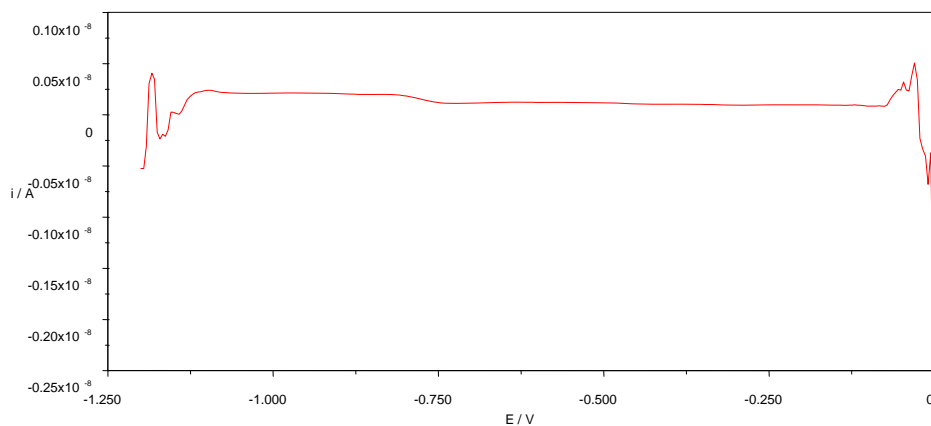
**Figure 4. 18: A plot of peak current against step potential.**

The step potential was varied from 0.00405 to 0.00705 V. The scan rate is related to the step potential. When the step potential is changed, the scan rate is also altered automatically by the instrument. Plot of peak current against step potential showed a drop in peak current as the scan rate was increased. At scan rate of 0.00605 the voltammogram appeared symmetrical. The subsequent scan rates did not result in increase in peak current, but the peak became broad with lower stability as shown. Therefore, step potential of 0.00605 V was chosen for further studies as an optimum value.

### 4.3 Anodic stripping-square wave voltammetry on cadmium bromide solution

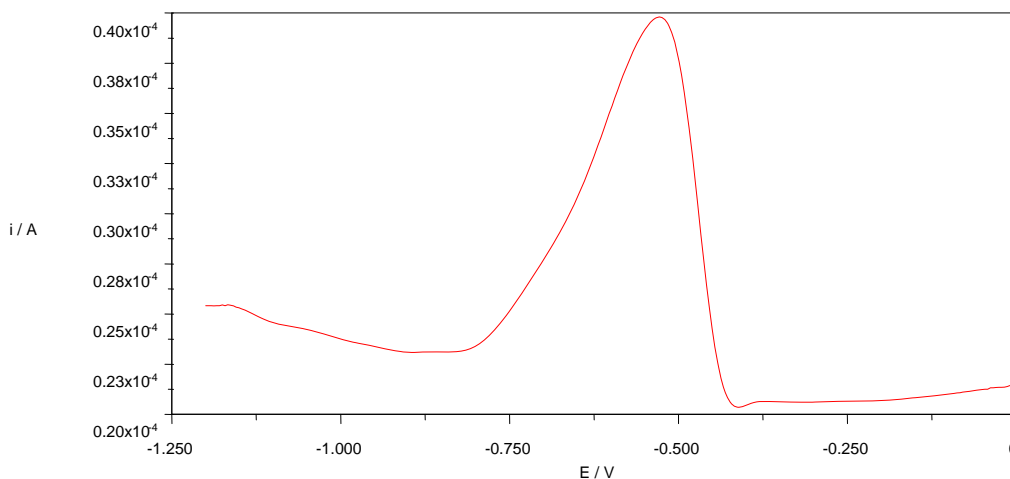
#### 4.3.1 The effect of deposition time on peak current obtained using Anodic stripping-square wave voltammetry on un-modified pyrolytic graphite electrode

The anodic stripping performed here was aimed at optimizing the deposition time in order to obtain maximum peak current for detection of cadmium ions in prepared solution while other parameters such as frequency, step potential, amplitude and deposition potential were held constant. The voltammogram obtained for the blank did not show a peak for reduction of cadmium ions, see Figure 4.19.



**Figure 4. 19: Voltammogram of 0.1M KCl (Blank) obtained at 120 seconds deposition time using un-modified Pyrolytic graphite as working electrode.**

Figure 4.20 shows voltammogram obtained when AS-SWV was carried out on 1 ppm Cadmium bromide solution at deposition time of 120 s using un-modified pyrolytic graphite electrode as working electrode. The electrolyte used was 0.1M KCl solution.



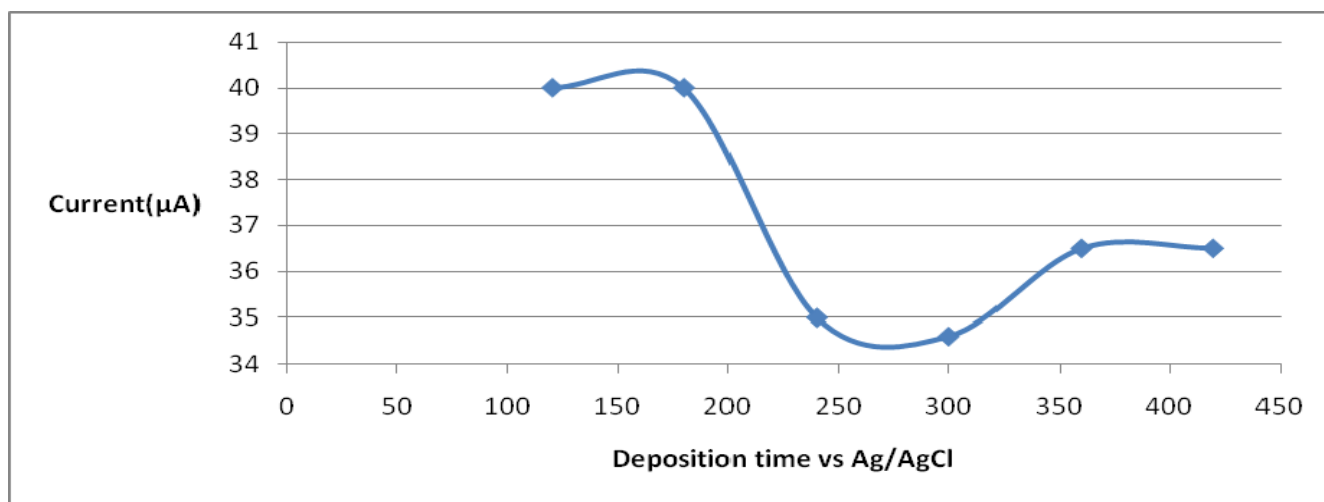
**Figure 4. 20: Square wave voltammogram for 1 ppm Cadmium bromide solution obtained at 120 seconds deposition time using un-modified Pyrolytic graphite as working electrode.**

Table 4.12 below shows deposition time and corresponding peak current obtained using un-modified pyrolytic graphite as working electrode.

**Table 4-12: Peak current and deposition time.**

Deposition time	Current( $\mu$ A)
120	40
180	40
240	35
300	34.6
360	36.5
420	36.5

Figure 4.21 shows a plot of peak current against deposition time obtained using un-modified pyrolytic graphite as working electrode.



**Figure 4. 21: A plot of peak current against deposition time for 1 ppm cadmium bromide solution.**

Deposition potential is an important parameter for stripping techniques and has a substantial influence on the sensitivity determination. The effect of deposition time on stripping current for  $\text{CdBr}_2$  was studied from 120 to 420 seconds and results are shown in Figure 4.21 above. From the cyclic Voltammetry carried on  $\text{CdBr}_2$  earlier in the research, the midpoint for the forward and backward wave was 0.57 V, this is a confirmation that peaks obtained using Anodic stripping-square wave voltammetry are for  $\text{CdBr}_2$  ions. The peak current remained constant for 120 and 180 s and thereafter dropped to lower level. As deposition time is increased more and more metals get deposited on the surface of the electrode, so the peak current greatly increases. However, when deposition time was beyond 180, the peak current started to drop indication that the amount of metal on the electrode surface tends to saturation. In this work 120 s was taken as deposition time.

#### **4.3.2 The effect of frequency on peak current obtained using Anodic stripping-square wave voltammetry on un-modified pyrolytic graphite electrode**

The anodic stripping performed here was aimed at optimizing the frequency in order to obtain maximum peak current for detection of cadmium ions in prepared solution, while other parameters such as deposition time, step potential, amplitude and deposition potential were held constant.

Figure 4.22 shows voltammogram obtained when AS-SWV was carried out on 1 ppm Cadmium bromide solution at frequency of 35Hz using un-modified pyrolytic graphite electrode as working electrode. The electrolyte used was 0.1M KCl solution

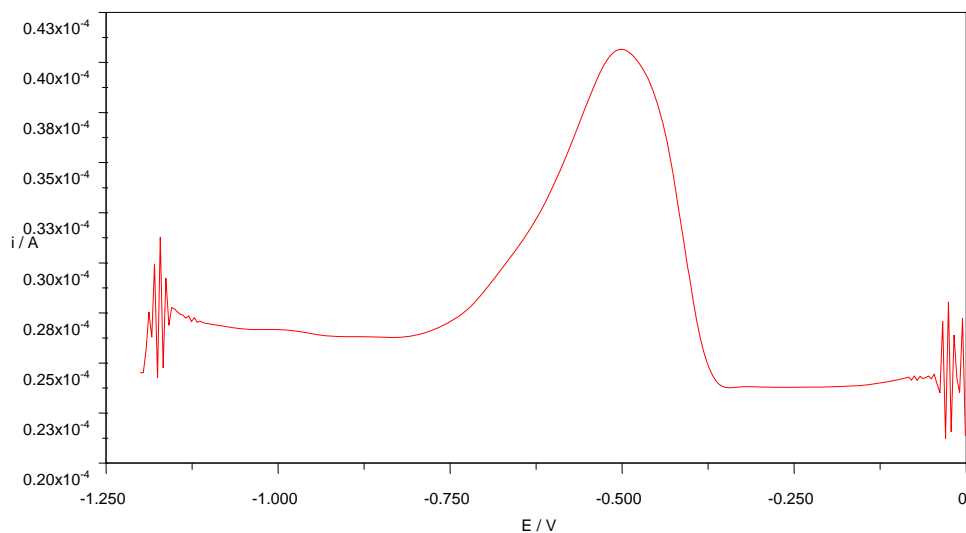


**Figure 4. 22: Square wave voltammogram for 1 ppm Cadmium bromide solution obtained at frequency of 35 Hz using un-modified Pyrolytic graphite as working electrode.**

Table 4.13 shows frequency and corresponding peak current obtained using un-modified pyrolytic graphite as working electrode.

**Table 4-13: Peak current and frequency.**

Frequency (Hz)	Current( $\mu$ A)
15	35
20	36.5
25	40
30	36.5
35	41.5
40	32.5
45	39



Figure 4.23 shows a plot of peak current against frequency in Hz obtained using un-modified pyrolytic graphite as working electrode.

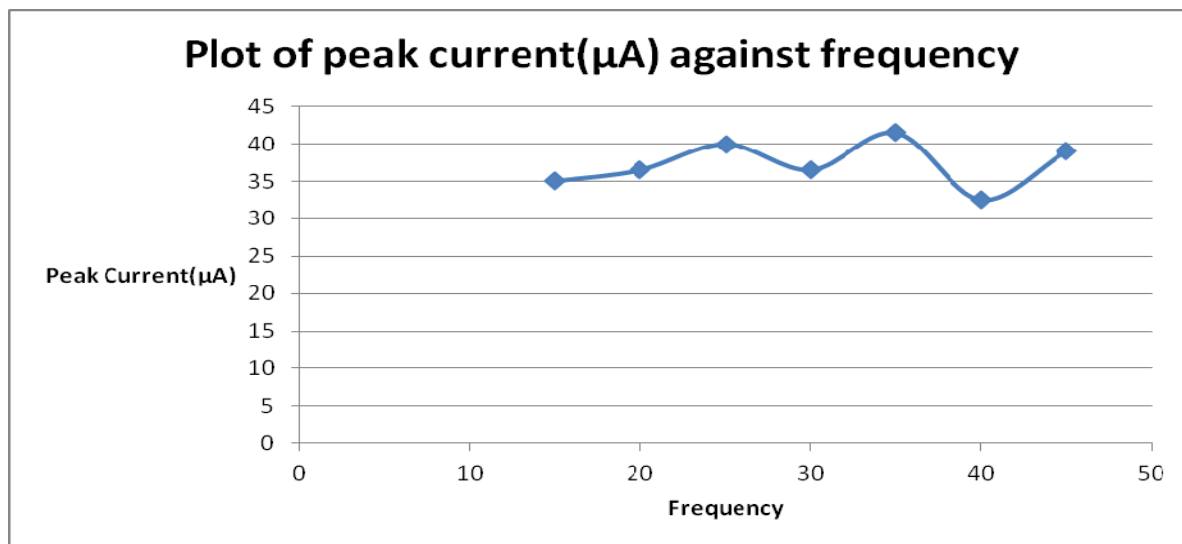


**Figure 4. 23: A plot of peak current against Frequency.**

From Figure 4.23 the frequency was varied from 15 to 45 Hz. The corresponding peak currents increased as frequency reached 25 Hz. The maximum peak current was obtained at a frequency of 35 Hz. This frequency was chosen for optimization of peak current. Beyond this frequency the peak current dropped and then increased. The stripping potential for this experiment was -0.57V vs. SCE. From the cyclic Voltammetry carried on  $\text{CdBr}_2$  earlier in the research, the midpoint for the forward and backward wave was -0.57 V vs. SCE, this is a confirmation that peaks obtained at same voltage using Anodic stripping-square wave voltammetry are for  $\text{CdBr}_2$  ions.

### 4.3.3 The effect of wave amplitude on peak current obtained using Anodic stripping-square wave voltammetry on un-modified pyrolytic graphite electrode

The anodic stripping performed here was aimed at optimizing the wave amplitude in order to obtain maximum peak current for detection of cadmium ions in prepared solution while other parameters such as deposition potential, deposition time, step potential and frequency were held constant. Figure 4.24 shows voltammogram obtained when AS-SWV was carried out on 1 ppm cadmium bromide solution at amplitude of 0.12V using un-modified pyrolytic graphite electrode as working electrode.

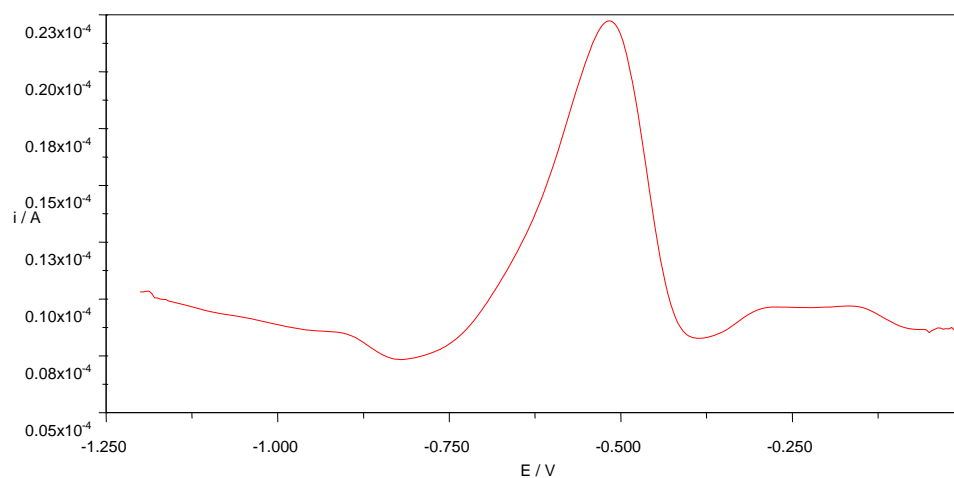


**Figure 4. 24: Square wave voltammogram for 1 ppm cadmium bromide solution obtained at amplitude of 0.12 Volts using un-modified Pyrolytic graphite as working electrode.**

Figure 4.25 shows a plot of peak current against amplitude obtained using un-modified pyrolytic graphite as working electrode

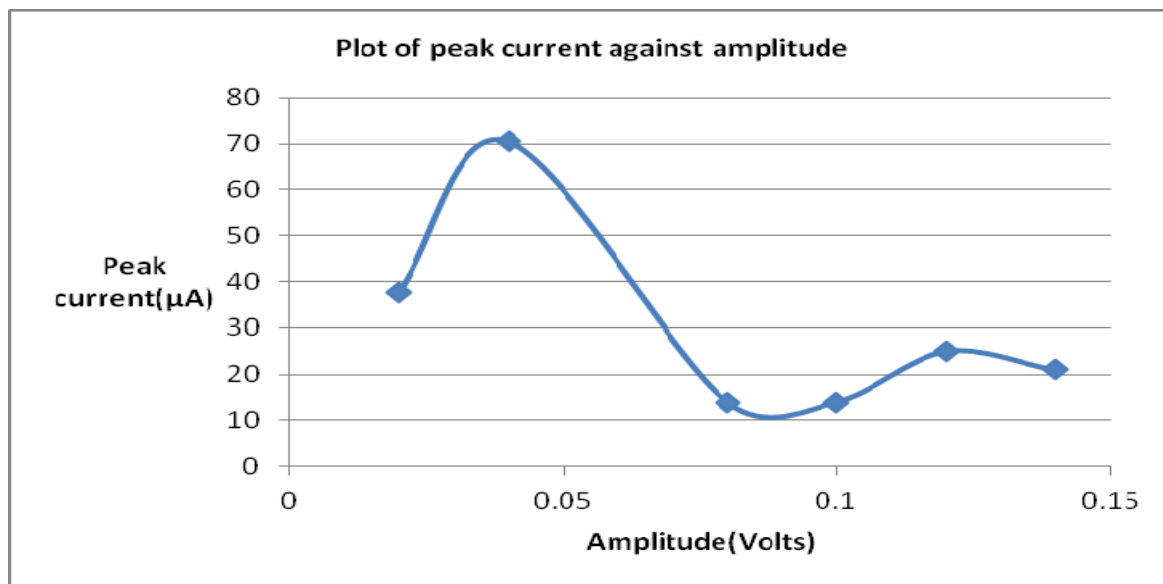


**Figure 4. 25: A plot of peak current against Change in phase amplitude.**

Table 4–14 shows amplitude and corresponding peak current obtained using un-modified pyrolytic graphite as working electrode.

**Table 4–14: Peak current and Phase amplitude.**

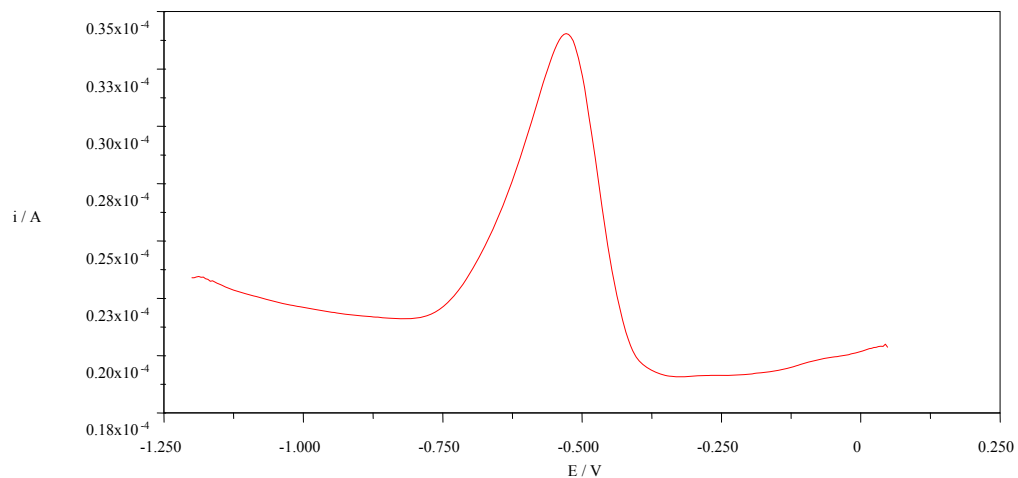
Phase amplitude(Volts)	Current(µA)
0.02	37.5
0.04	70.5
0.08	14
0.10	14
0.12	25
0.14	21

The Amplitude was varied from 0.02 to 0.14 volts. From the geometry of the voltammograms, the peak current increased as the phase amplitude was raised from 0.02 Volts to 0.2. The amplitude of 0.04 Volts gave the highest peak current. Beyond this amplitude the peak current dropped and remained constant and dropped again. Therefore, amplitude phase of 0.04 Volts was chosen for optimization of the peak current.

#### **4.3.4 The effect of deposition potential on peak current obtained using Anodic stripping-square wave voltammetry on un-modified pyrolytic graphite electrode**

The Electroanalysis performed here was aimed at optimizing the deposition potential in order to obtain maximum peak current for detection of Cadmium ions in prepared solution while other parameters such as amplitude, deposition time, step potential and frequency were held constant.

Figure 4.26 shows voltammogram obtained when AS-SWV was carried out on 1 ppm Cadmium bromide solution at deposition potential of 0.05V using un-modified pyrolytic graphite electrode as working electrode



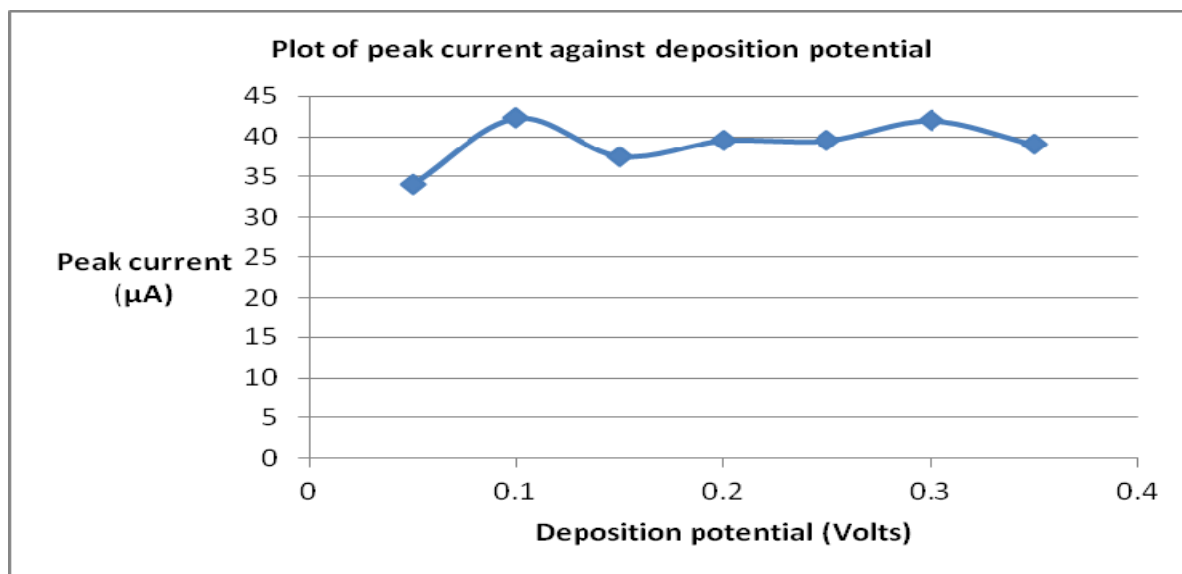
**Figure 4. 26: Square wave voltammogram for 1 ppm Cadmium bromide solution obtained at deposition potential of 0.05 Volts using bare Pyrolytic graphite as working electrode.**

Table 4-15 shows deposition potential and corresponding peak current obtained using unmodified pyrolytic graphite as working electrode.

**Table 4-15: Peak current and deposition potential.**

Deposition potential (Volts)	Current( $\mu$ A)
0.05	34
0.10	42.3
0.15	37.5
0.20	39.5
0.25	39.5
0.30	42
0.35	39

Figure 4.27 shows a plot of peak current against deposition potential obtained using un-modified pyrolytic graphite as working electrode.



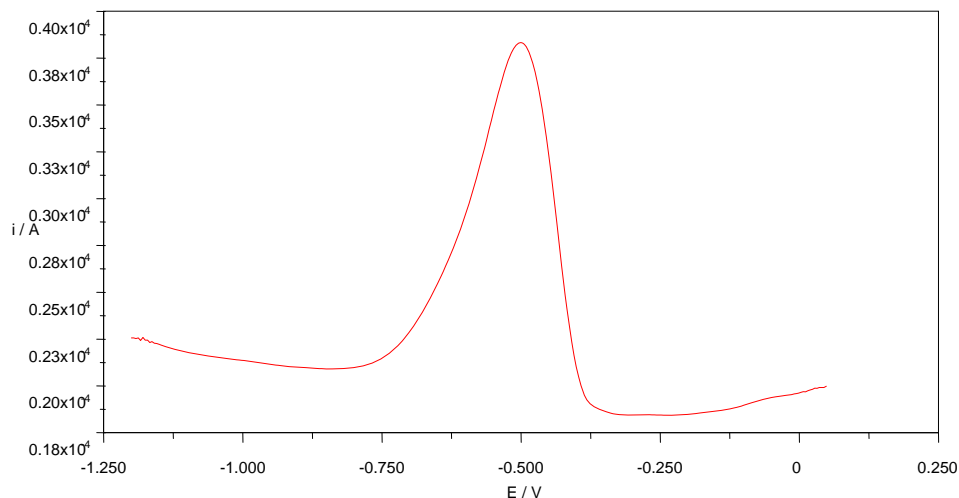
**Figure 4. 27: A plot of peak current against deposition potential.**

Deposition potential is an important parameter for stripping techniques and it has a substantial influence on the sensitivity for the determination of a given chemical species. The effect of deposition potentials on the stripping peak currents of  $\text{Cd}^{2+}$  is shown in Figure. 4.27. The deposition potential was varied from 0.05 to 0.35 V with a constant deposition time of 120 s. Therefore, the optimum value of the deposition potential used in this work is 0.10V. This voltage gave the highest peak current.

#### 4.3.5 The effect of step potential on peak current obtained using Anodic stripping-square wave voltammetry on un-modified pyrolytic graphite electrode

The stripping analysis performed here was aimed at optimizing the step potential in order to obtain maximum peak current for detection of Cadmium ions in prepared solution while other parameters such as deposition potential, deposition time, amplitude and frequency were held constant.

Figure 4.28 highlights the square wave voltammogram of 1 ppm Cadmium bromide solution obtained at step potential of 0.00405 V using un-modified pyrolytic graphite electrode as working electrode.



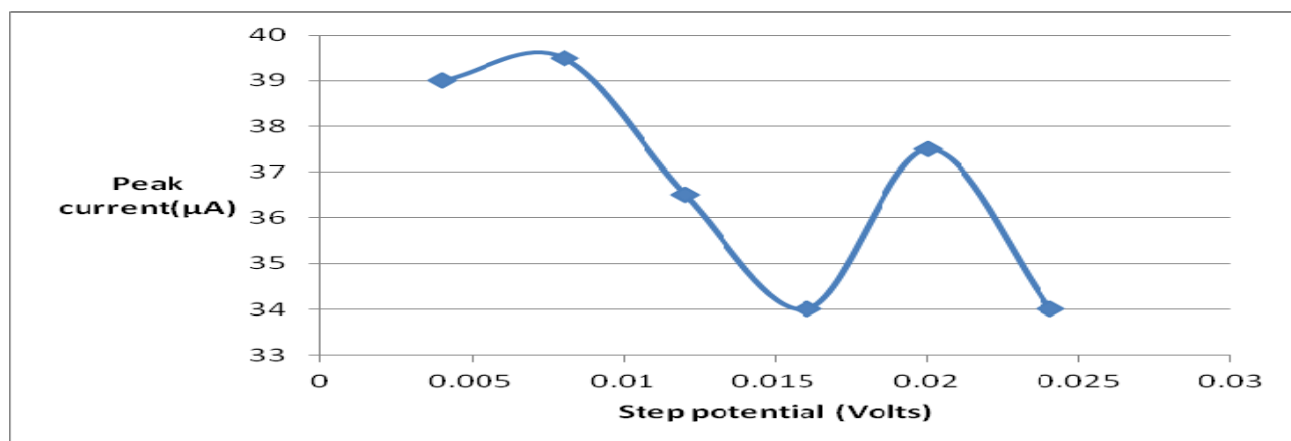
**Figure 4. 28: Square wave voltammogram for 1 ppm cadmium bromide solution obtained at scan rate 0.00405 Volts using un-modified Pyrolytic graphite as working electrode.**

Table 4-16 below shows step potential and corresponding peak current obtained using un-modified pyrolytic graphite as working electrode.

**Table 4-16: Peak current and step potential.**

Step potential (Volts)	Current( $\mu$ A)
0.00405	39
0.00805	39.5
0.01205	36.5
0.01605	34
0.02005	37.5
0.02405	34

Figure 4.29 illustrates a plot of peak current versus step potential obtained using un-modified pyrolytic graphite as working electrode.



**Figure 4. 29: A plot of peak current against step potential for 1 ppm cadmium bromide solution.**



The step potential was varied from 0.00405 to 0.02405 V. The scan rate is related to the step potential. When the step potential is changed the scan rate is also altered automatically by the instrument.

The plot of peak current against deposition potential showed an increase in peak current as the scan rate increased. The peak current suddenly dropped to the minimum of 34  $\mu$ A. The scan rate of 0.00805 V gave the highest peak current. Therefore, step potential of 0.00805 V was chosen for further studies as an optimum value.

#### **4.4 Anodic stripping-square wave voltammetry on a mixture of lead nitrate and cadmium bromide solution using un-modified pyrolytic graphite electrode.**

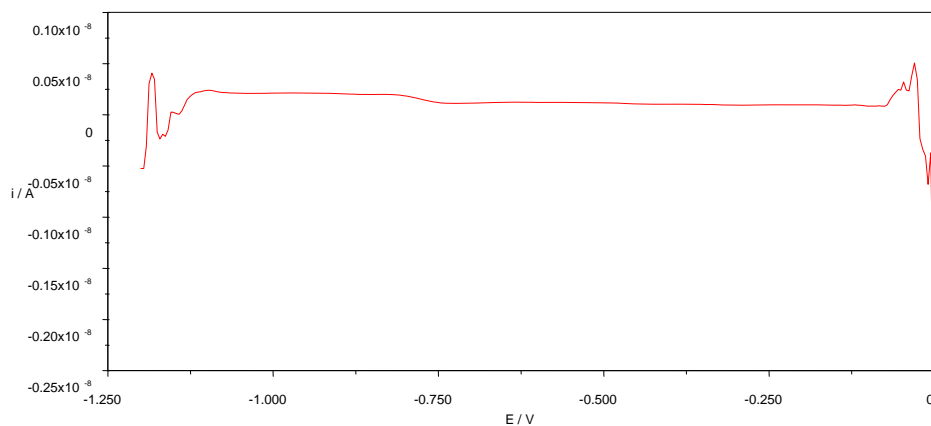
Detection of trace heavy metals need removal of dissolved oxygen by purging the system with Nitrogen gas or Argon gas. Detection of lead and cadmium using pyrolytic graphite electrode has not been reported in the literature in the department of Chemistry at The University of Nairobi to the best of my knowledge.

A similar experiment in Parts-per-billion levels of cadmium and lead were detected using square-wave anodic stripping voltammetry with a boron-doped diamond electrode [Carol Babyak et, al 2003] .In this work parameters that affect the peak current such as frequency, deposition potential, step potential and amplitude were investigated and optimized.

#### 4.4.1 The effect of deposition time on peak current obtained using Anodic stripping-square wave voltammetry on un-modified pyrolytic graphite electrode for 1 ppm mixture of lead nitrate and cadmium bromide

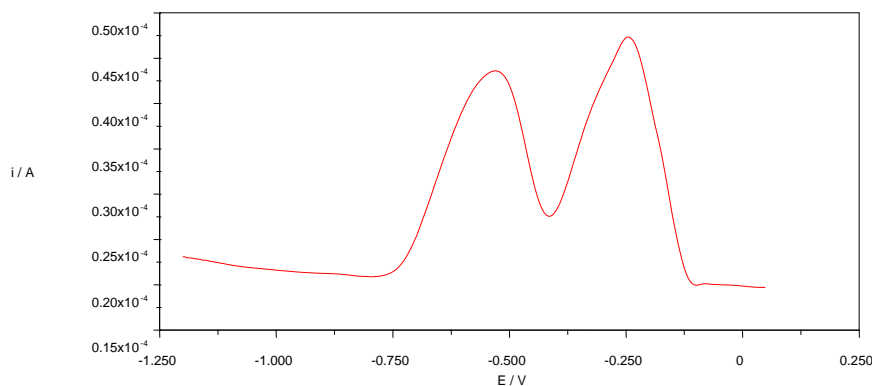
The stripping analysis performed here was aimed at optimizing the deposition time in order to obtain maximum peak current for detection of lead and Cadmium ions in prepared solution while other parameters such as deposition potential, step potential, amplitude and frequency were held constant.

Figure 4.30 highlights the square wave voltammogram of 0.1 M KCl (blank) solution obtained at deposition potential of 120 s using un-modified pyrolytic graphite electrode as working electrode



**Figure 4. 30: Square wave voltammogram of 0.1M KCl (Blank) obtained at 120 seconds deposition time using un-modified Pyrolytic graphite as working electrode.**

Figure 4.31 highlights the square wave voltammogram of 1 ppm mixture of lead nitrate and Cadmium bromide solution obtained at deposition potential of 120 s using un-modified pyrolytic graphite electrode as working electrode.



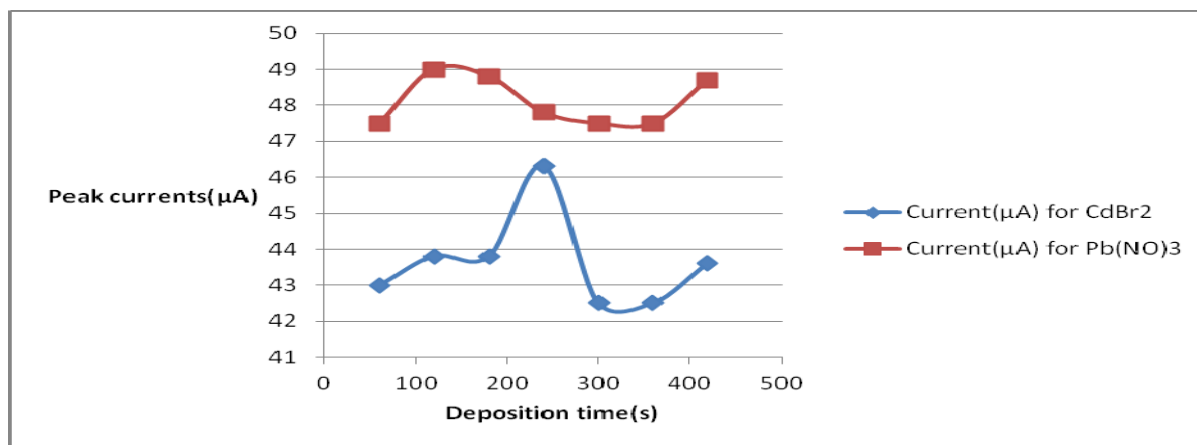
**Figure 4. 31: Square wave voltammogram for 1 ppm mixture of lead and cadmium bromide solution obtained at deposition potential of 120 s using un-modified Pyrolytic graphite as working electrode.**

Table 4-17 below shows deposition time and corresponding peak current obtained using un-modified pyrolytic graphite as working electrode.

**Table 4-17: Peak current and deposition time.**

Deposition time(s)	Current( $\mu$ A) for CdBr <sub>2</sub>	Current( $\mu$ A) for Pb(NO <sub>3</sub> ) <sub>3</sub>
60	43	47.5
120	43.8	49
180	43.8	48.8
240	46.3	47.8
300	42.5	47.5
360	42.5	47.5
420	43.6	48.7

Figure 4.32 shows a plot of peak current against deposition time obtained using un-modified pyrolytic graphite as working electrode.



**Figure 4. 32: A plot of peak current against deposition time for 1 ppm mixture of Lead nitrate and Cadmium Bromide solutions.**

The effect of deposition time on stripping current for cadmium bromide and lead Nitrate was studied from 120 to 420 seconds and results are shown in Figure 4.32.

From the Anodic stripping-square wave voltammetry carried on pure  $\text{CdBr}_2$  and  $\text{Pb}(\text{NO})_3$  earlier in the research, the peak appearing at  $-0.57\text{ V}$  is for  $\text{CdBr}_2$  while the second appearing at  $-0.313\text{ V}$  peak is for  $\text{Pb}(\text{NO})_3$ . From the two plots, it can be seen that the highest peak current for the mixture was  $49.0\ \mu\text{A}$  corresponding  $\text{Pb}(\text{NO})_3$  solution. The highest peak current obtained for  $\text{CdBr}_2$  solution was  $46.3\ \mu\text{A}$ .

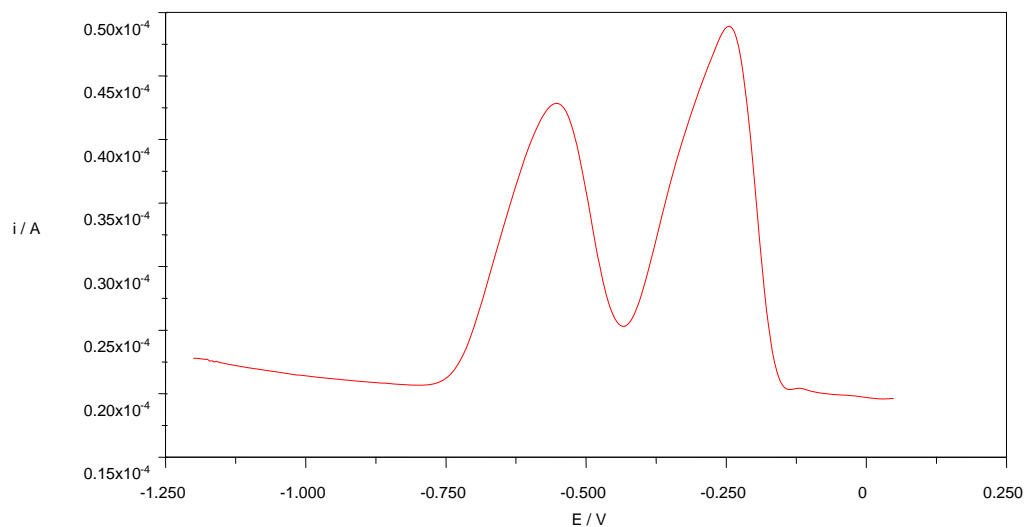
The effect of lead on cadmium stripping peak is shown in the Figure 4.32 . The peak current for Cadmium Bromide was less for the 1ppm mixture ,this suggests that inter-metallic bond formation between Cadmium and Lead could explain cadmium peak suppression by lead.

Competition between Lead and cadmium on active sites of modified pyrolytic graphite electrode may also explain the observed peak suppression of cadmium. Lead may out compete cadmium for active sites because of its larger diffusivity.

#### **4.4.2 The effect of frequency on peak current obtained using Anodic stripping-square wave voltammetry on un-modified pyrolytic graphite electrode on 1 ppm mixture of lead nitrate and Cadmium bromide solution**

The electrochemical analysis performed here was aimed at optimizing the frequency in order to obtain maximum peak current for detection of lead and Cadmium ions in prepared solution while other parameters such as deposition potential, step potential, amplitude and deposition time were held constant.

Figure 4.33 highlights the square wave voltammogram of 1 ppm mixture of lead nitrate and Cadmium bromide solution obtained at frequency of 15 Hz using un-modified pyrolytic graphite electrode as working electrode.



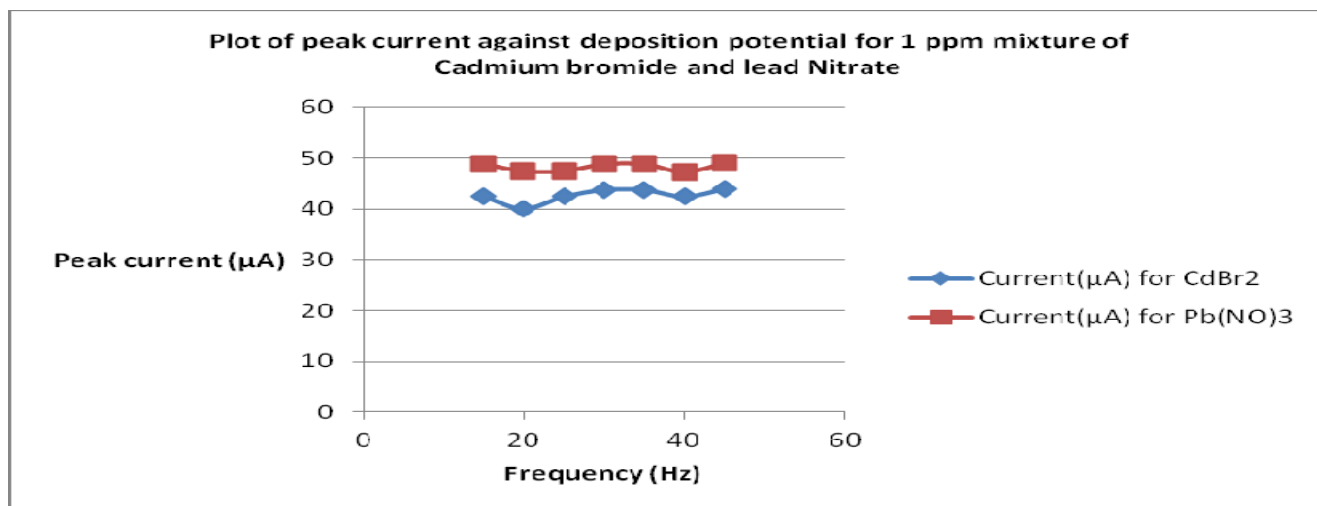
**Figure 4. 33: Square wave voltammogram for 1 ppm mixture of Cadmium bromide and Lead Nitrate solution obtained at frequency of 15 Hz using un-modified Pyrolytic graphite as working electrode.**

Table 4–18 shows frequency and corresponding peak current obtained using un-modified pyrolytic graphite as working electrode. By varying the frequency different values of current were obtained for Pb<sup>2+</sup> and Cd<sup>2+</sup> ions ( Figure 4.33).

**Table 4-18: Peak current and Frequency.**

Frequency	Current( $\mu$ A) for CdBr <sub>2</sub>	Current( $\mu$ A) for Pb(NO) <sub>3</sub>
15	42.5	48.8
20	40.1	47.5
25	42.5	47.5
30	43.8	48.8
35	43.8	48.8
40	42.5	47.3
45	44.0	49.0

Figure 4.34 shows a plot of peak current against frequency obtained using un-modified pyrolytic graphite as working electrode



**Figure 4. 34: A plot of peak current against Frequency.**

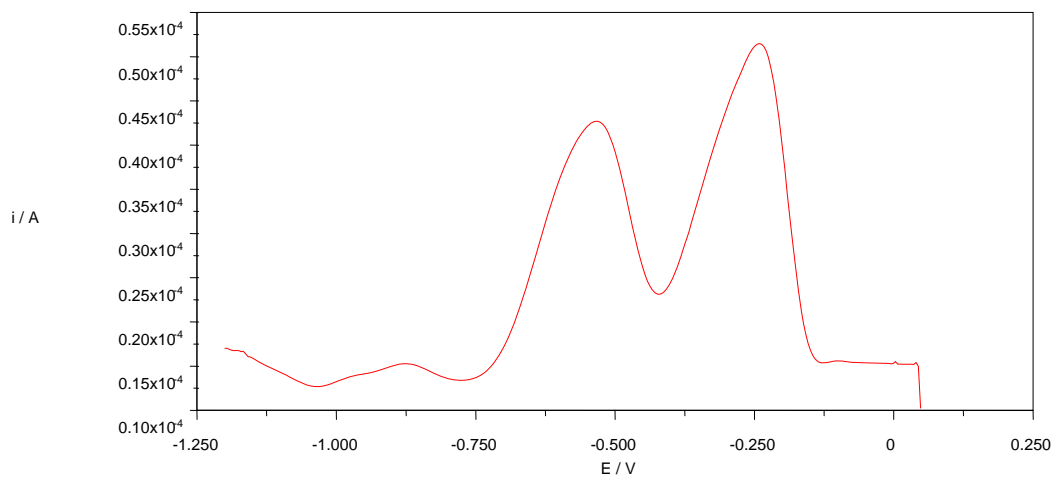
From Figure 4.34 the frequency was varied from 15 to 45 Hz. The corresponding peak currents were recorded as shown in Table 4-18. The maximum peak currents were obtained at a frequency of 45 Hz for both lead and Cadmium ions. This frequency was chosen for optimization of peak current.

#### **4.4.3 The effect of amplitude on peak current obtained using Anodic stripping-square wave voltammetry on un-modified pyrolytic graphite electrode of 1 ppm mixture of lead nitrate and Cadmium bromide solution**

The stripping analysis performed here was aimed at optimizing the amplitude in order to obtain maximum peak current for detection of lead and Cadmium ions in prepared solution while other parameters such as deposition potential, step potential, frequency and deposition time were held constant.

Figure 4.35 highlights the square wave voltammogram of 1 ppm mixture of lead nitrate and Cadmium bromide solution obtained at amplitude of 0.02 V using un-modified pyrolytic graphite electrode as working electrode.





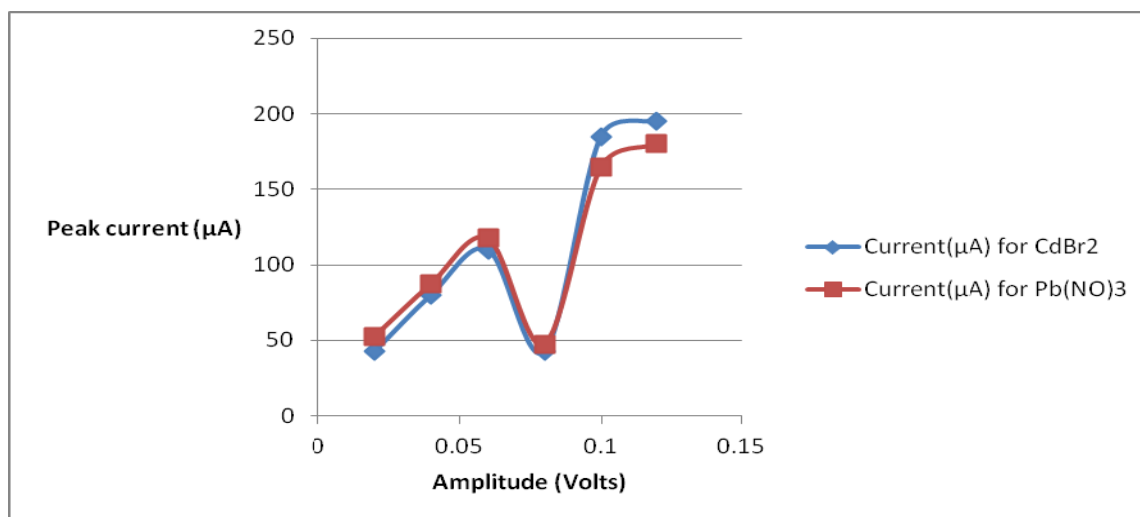
**Figure 4. 35: Square wave voltammogram for 1 ppm mixture of cadmium bromide and Lead Nitrate solution obtained at amplitude 0.02 Volts using un-modified Pyrolytic graphite as working electrode.**

Table 4-19 below show amplitude and corresponding peak current obtained using un-modified graphite as working electrode. By varying the amplitude different values of current were obtained for Pb<sup>2+</sup> and Cd<sup>2+</sup> ions (Figure 4.36)

**Table 4-19: Peak current and amplitude.**

Phase amplitude	Current( $\mu$ A) for CdBr <sub>2</sub>	Current( $\mu$ A) for Pb(NO <sub>3</sub> ) <sub>3</sub>
0.02	42.5	52.5
0.04	80	87.5
0.06	110	117.5
0.08	42.5	47.5
0.10	185	165
0.12	195	180

Figure 4.36 shows a plot of peak current against amplitude obtained using un-modified pyrolytic graphite as working electrode



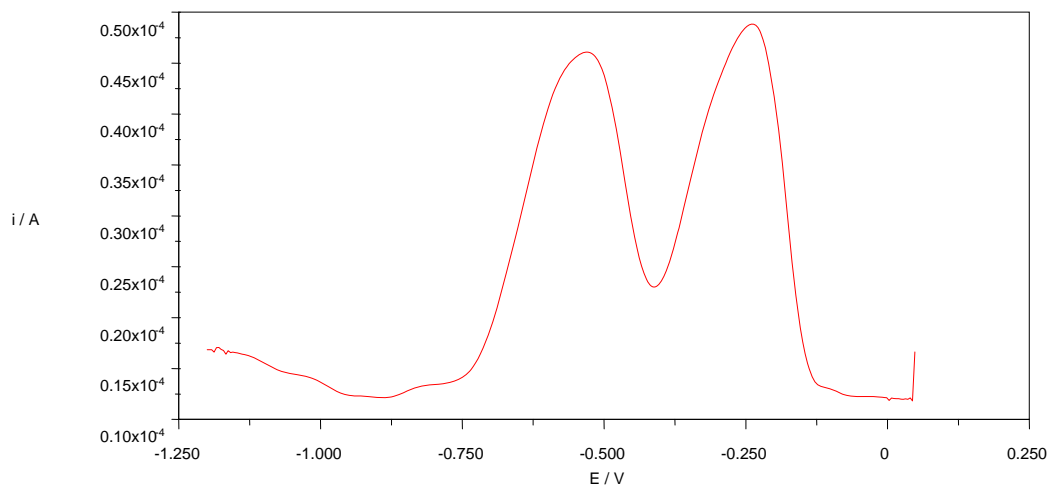
**Figure 4. 36: A plot of peak current against Change in phase amplitude.**

The amplitude was varied from 0.02 to 0.12 volts as shown in Figure 4.36. From the geometry of the voltammograms, the peak current increased as the phase amplitude was raised from 0.02 Volts to 0.6. The amplitude of 0.12 Volts gave the highest peak currents.

Beyond this amplitude the peak current dropped. Therefore, amplitude phase of 0.12 Volts was chosen for optimization for the peak current.

#### 4.4.4 The effect of deposition potential on peak current obtained using Anodic stripping-square wave voltammetry on un-modified pyrolytic graphite electrode of 1 ppm mixture of lead nitrate and Cadmium bromide solution

The electrochemical analysis performed here was aimed at optimizing the deposition potential in order to obtain maximum peak current for detection of lead and cadmium ions in prepared solution while other parameters such as amplitude, step potential, frequency and deposition time were held constant. Figure 4.37 highlights the square wave voltammogram of 1 ppm mixture of lead nitrate and cadmium bromide solution obtained at deposition potential of 0.02 V using un-modified pyrolytic graphite electrode as working electrode



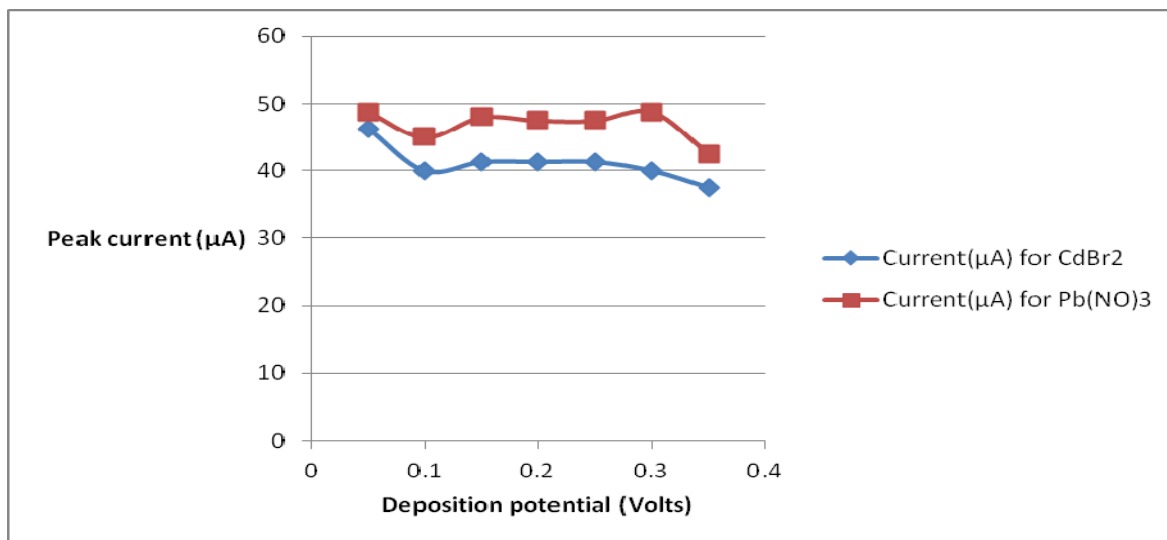
**Figure 4. 37: Square wave voltammogram for 1 ppm mixture Lead nitrate and Cadmium Bromide solution obtained at deposition potential 0.05 Volts using bare Pyrolytic graphite as working electrode.**

Table 4–20 below shows deposition potential and corresponding peak current obtained using un-modified pyrolytic graphite as working electrode .By varying the deposition potential different values of current were obtained for Pb<sup>2+</sup> and Cd<sup>2+</sup> ions ( Figure 4.37).

**Table 4-20: Peak current and deposition potential.**

Deposition potential	Current( $\mu$ A) for CdBr <sub>2</sub>	Current( $\mu$ A) for Pb(NO) <sub>3</sub>
0.05	46.3	48.8
0.10	40	45
0.15	41.3	48
0.20	41.3	47.5
0.25	41.3	47.5
0.30	40	48.8
0.35	37.5	42.5

Figure 4.38 shows a plot of peak current against deposition potential obtained using un-modified pyrolytic graphite as working electrode



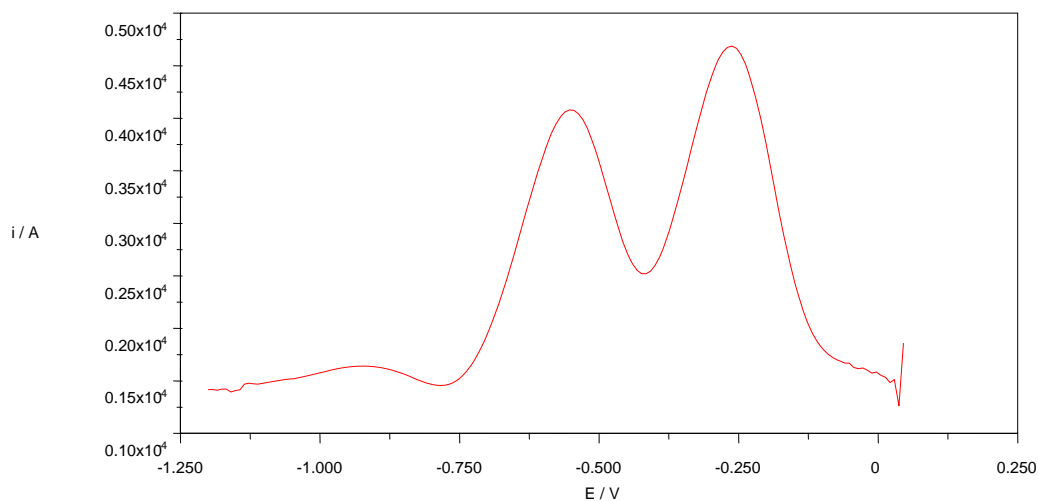
**Figure 4. 38: A plot of peak current versus deposition potential.**

The effect of deposition potentials on the stripping peak currents for a 1 ppm mixture of  $\text{Cd}^{2+}$  and  $\text{Pb}^{+}$  is shown in Figure. 4.38. The deposition potential was varied from 0.05 to 0.35 V with a constant deposition time of 120s. The highest stripping peak currents were obtained at deposition potential of 0.05 V. Therefore, the optimum value of the deposition potential used in this work is 0.05V. At this potential more and more complete reductions of  $\text{Cd}^{2+}$  and  $\text{Pb}^{+}$  ions to their neutral forms; beyond this potential the peak current drops due to hydrogen evolution that reduces on the surface of the electrode. This is in agreement with the literature [ Willy et, al (2009)].

#### 4.4.5 The effect of step potential on peak current obtained using Anodic stripping-square wave voltammetry on un-modified pyrolytic graphite electrode of 1 ppm mixture of lead nitrate and Cadmium bromide solution

The anodic stripping performed here was aimed at optimizing the step potential in order to obtain maximum peak current for detection of lead and cadmium ions in prepared solution while other parameters such as deposition potential, amplitude, frequency and deposition time were held constant.

Figure 4.39 highlights the square wave voltammogram of 1 ppm mixture of lead nitrate and Cadmium bromide solution obtained at step potential of 0.0805 V, using un-modified pyrolytic graphite electrode as working electrode.



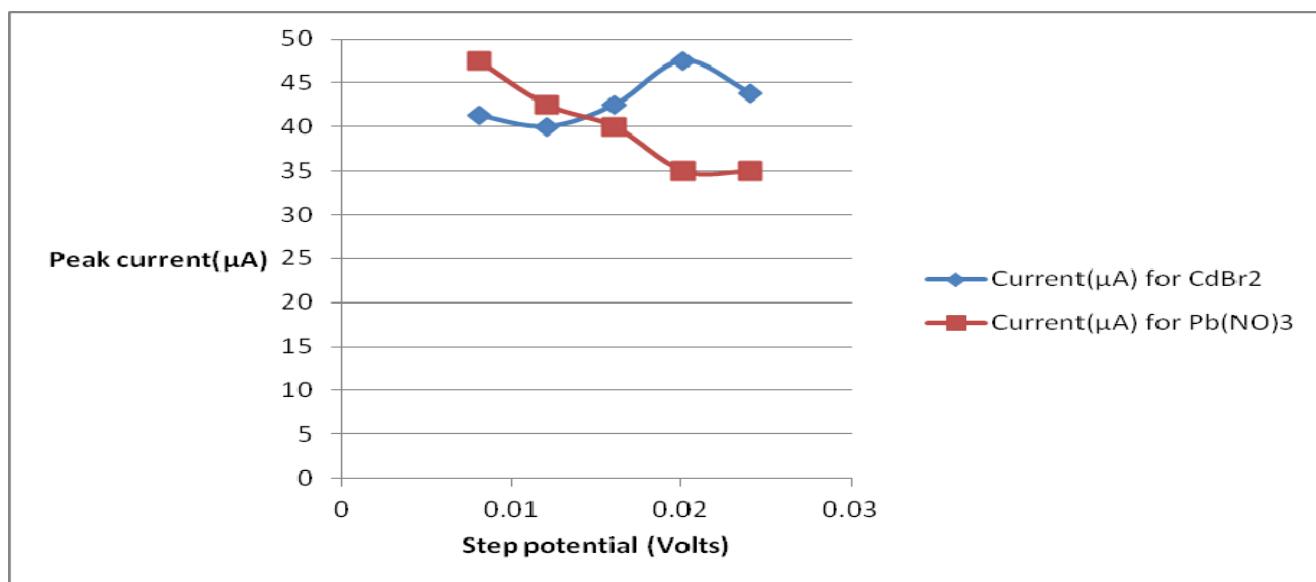
**Figure 4. 39: Square wave voltammogram for 1 ppm mixture Lead nitrate and Cadmium Bromide solution obtained at a step potential 0.0805 Volts, using non modified Pyrolytic graphite as working electrode.**

Table 4–21 below shows deposition potential and corresponding peak current obtained using un-modified pyrolytic graphite as working electrode .By varying the step potential different values of current were obtained for  $\text{Pb}^{2+}$  and  $\text{Cd}^{2+}$  ions ( Figure 4.38).

**Table 4-21: Peak current and Step potential.**

Step potential	Current( $\mu\text{A}$ ) for $\text{CdBr}_2$	Current( $\mu\text{A}$ ) for $\text{Pb}(\text{NO})_3$
0.00405	45	47.5
0.00805	41.3	47.5
0.01205	40.0	42.5
0.01605	42.5	40.0
0.02005	47.5	35.0
0.02405	43.8	35.0

Figure 4.40 shows a plot of peak current against step potential obtained using un-modified pyrolytic graphite as working electrode



**Figure 4. 40: A plot of peak current versus step potential for 1 ppm mixture of lead nitrate and cadmium bromide solution.**

The step potential was varied from 0.00405 to 0.02405 V. The scan rate is related to the step potential. When the step potential is changed, the scan rate is also altered automatically by the instrument. Plot of peak current against deposition potential, the highest peak current at scan rate of 0.00405 Volts. Therefore, step potential of 0.00405 V was chosen for further studies as an optimum value. At this potential more and more complete reductions of  $\text{Cd}^{2+}$  and  $\text{Pb}^{+}$  ions to their neutral forms occurred, beyond this potential the peak current drops due to hydrogen evolution on the surface of the electrode. This is in agreement with the literature [Willy et al (2009)].

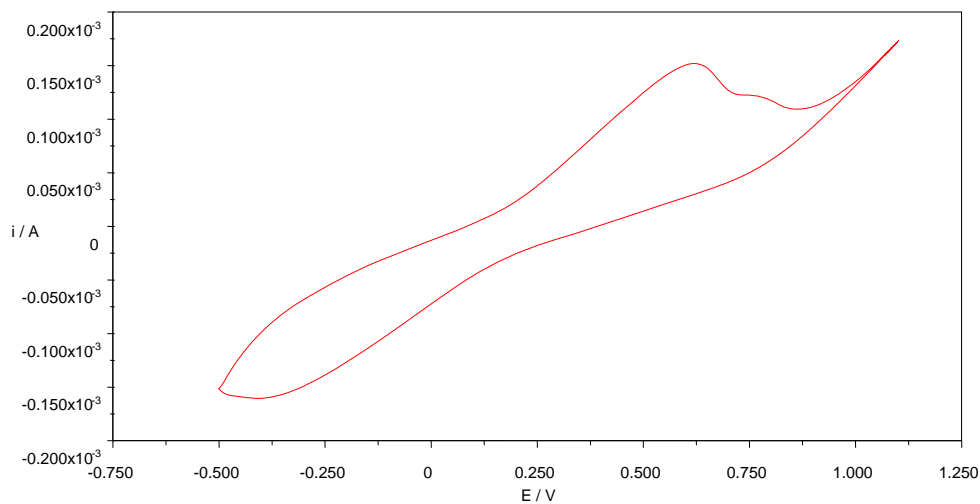


## **4.5 Anodic stripping-square wave voltammetry on lead nitrate solution using modified pyrolytic graphite polyaniline sensor**

### **4.5.1 The effect of deposition time on peak current obtained using Anodic stripping-square wave voltammetry on modified pyrolytic graphite electrode**

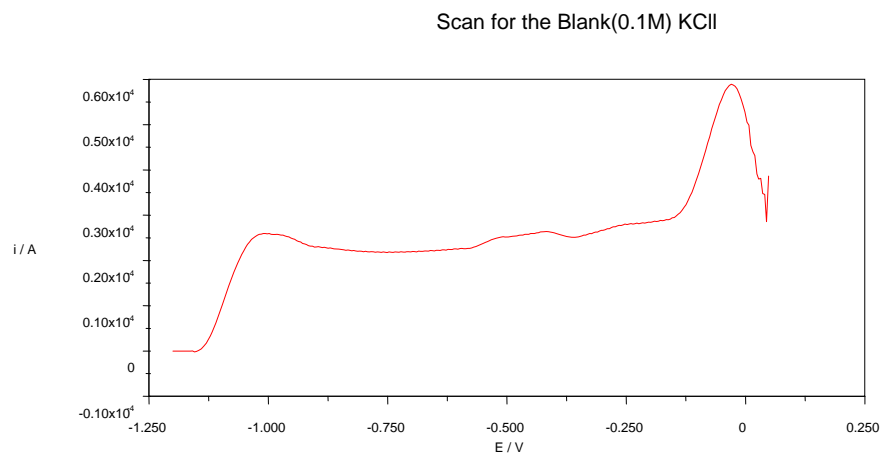
The electrochemical analysis performed here was aimed at optimizing the deposition time using modified pyrolytic electrode in order to obtain maximum peak current for detection of lead ions in prepared solution while other parameters such as amplitude, step potential, frequency and frequency were held constant.

Figure 4.41 highlights the cyclic voltammogram of aniline mixture obtained after electropolymerization of polyaniline on the surface of the electrode by multiple cyclic scanning at 100  $\text{mVs}^{-1}$  from -750 to 1250mV for 30 cycles at 25  $^{\circ}\text{C}$ .



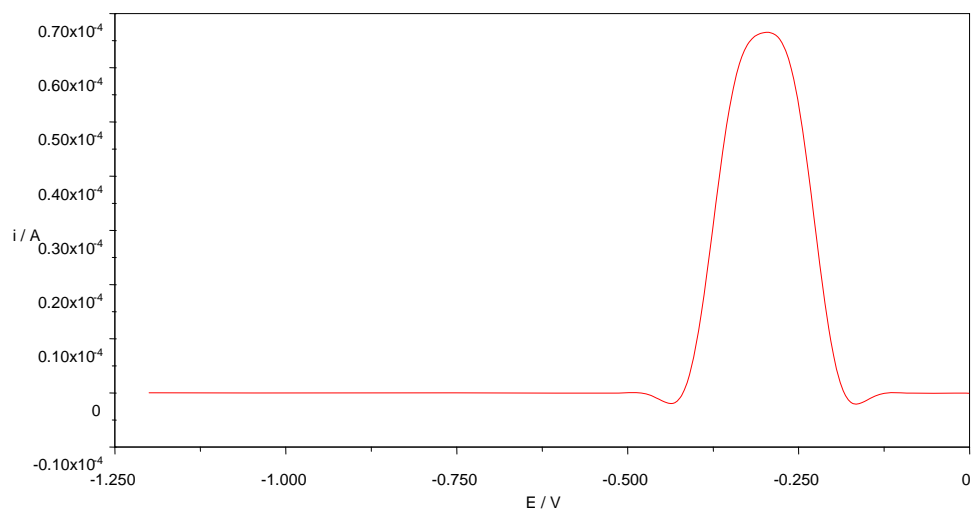
**Figure 4. 41: Cyclic voltammogram for aniline mixture using modified Pyrolytic graphite as working electrode.**

Figure 4.42 highlights the square wave voltammogram for 0.1 M KCl (blank) obtained at deposition potential of 120 S using modified pyrolytic graphite electrode as working electrode. No absorption was observed at reduction potential for lead and cadmium ions. The stripping peak observed at potential of 0 V was due to dissolved oxygen.



**Figure 4. 42: Square wave voltammogram for 0.1M KCl (Blank) obtained at 120 seconds deposition time using modified Pyrolytic graphite as working electrode.**

Figure 4.43 highlights the square wave voltammogram for lead nitrate solution obtained at deposition time of 420 s using modified pyrolytic graphite as working electrode.



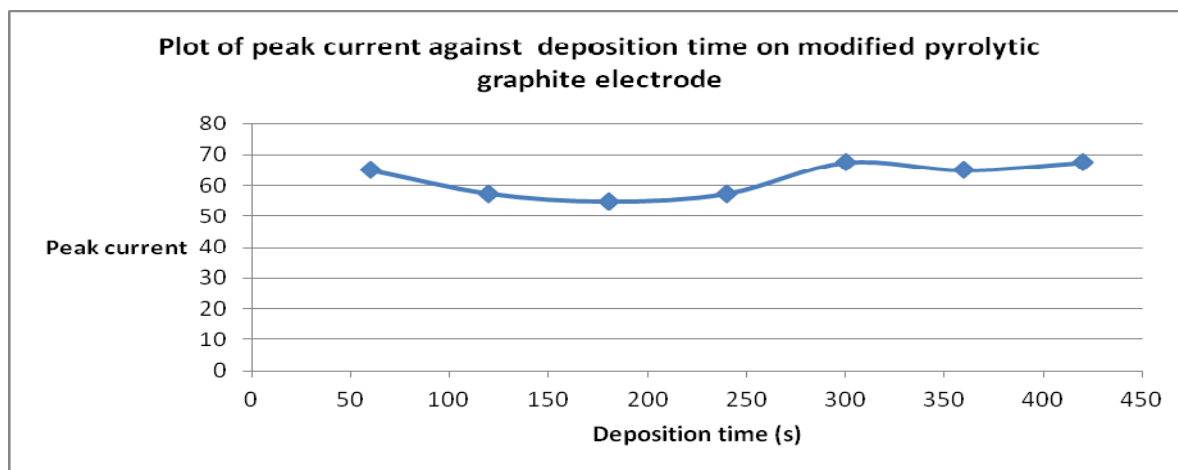
**Figure 4. 43: Square wave voltammogram for 30 ppm lead Nitrate obtained at 420 seconds deposition time using modified Pyrolytic graphite as working electrode.**

Table 4-22 below shows deposition time and corresponding peak current obtained using modified pyrolytic graphite as working electrode .By varying the deposition time different values of current were obtained for  $\text{Pb}^{2+}$  (Figure 4.44).

**Table 4-22: Peak and deposition time.**

Deposition time	Current( $\mu$ A)
60	65
120	57.5
180	55
240	57.5
300	67.5
360	65
420	67.5

Figure 4.44 shows a plot of peak current against deposition time obtained using modified pyrolytic graphite as working electrode



**Figure 4. 44: Plot of peak current against deposition time on modified pyrolytic graphite electrode.**

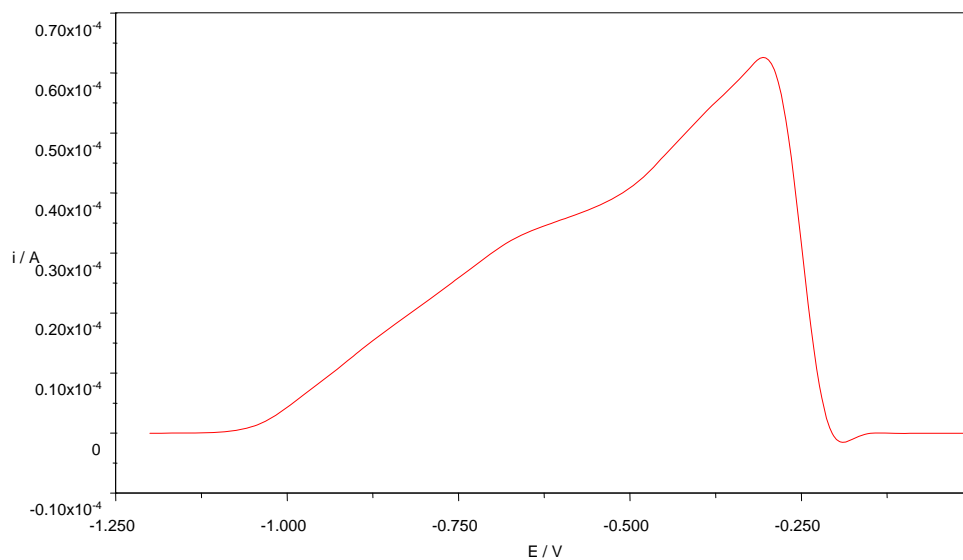
The effect of deposition time on stripping current for lead ions on modified graphite electrode was studied from 60 to 420 seconds and results are shown in the Figure 4.44. From the cyclic Voltammetry carried on lead (II) earlier in the research, the midpoint for the forward and backward wave was 0.313 V, this is a confirmation that peaks obtained at almost same V using Anodic stripping-square wave voltammetry are for Pb (II) ions.

It can be seen from Figure 4.42 that peak current obtained using the modified electrode was 67.5  $\mu\text{A}$  at deposition time of 300 seconds, there after it remained almost constant. This was due to the fact that all the active sites on the electrode surface had been occupied by lead. Any additional deposition did not result in increase of the peak currents.

#### **4.5.2 The effect of frequency on peak current obtained using Anodic stripping-square wave voltammetry on modified pyrolytic graphite electrode for 30 ppm lead Nitrate**

The anodic stripping performed here was aimed at optimizing the frequency in order to obtain maximum peak current using modified pyrolytic graphite electrode for detection of lead ions in prepared solution while other parameters such as deposition potential, amplitude, step and deposition time were held constant.

Figure 4.45 highlights the square wave voltammogram for lead nitrate solution obtained at frequency of 70 Hz using modified pyrolytic graphite as working electrode.



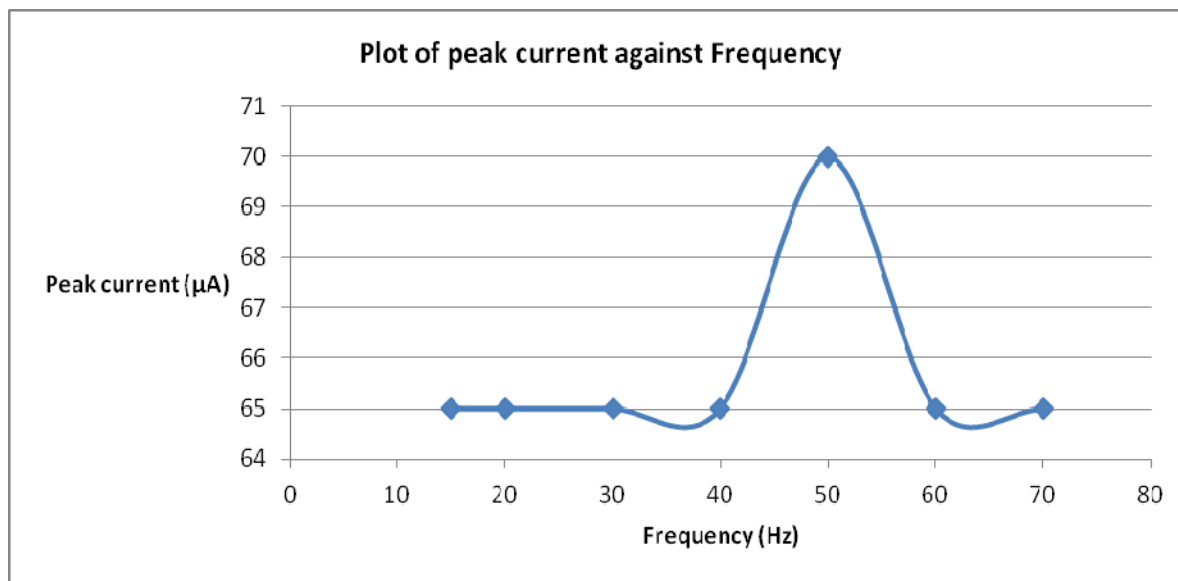
**Figure 4. 45: Square wave voltammogram for 30ppm lead nitrate solution obtained at 70 Hz frequency using modified Pyrolytic graphite as working electrode.**

Table 4-19 below shows frequency and corresponding peak current obtained using modified pyrolytic graphite as working electrode. By varying the frequency different values of current were obtained for  $\text{Pb}^{2+}$  (Figure 4.46).

**Table 4-23: Peak current and Frequency.**

Frequency(Hz)	Current( $\mu$ A)
15	65
20	65
30	65
40	65
50	70
60	65
70	65

Figure 4.46 shows a plot of peak current against frequency obtained using modified pyrolytic graphite as working electrode



**Figure 4. 46: A plot of peak current against Frequency.**

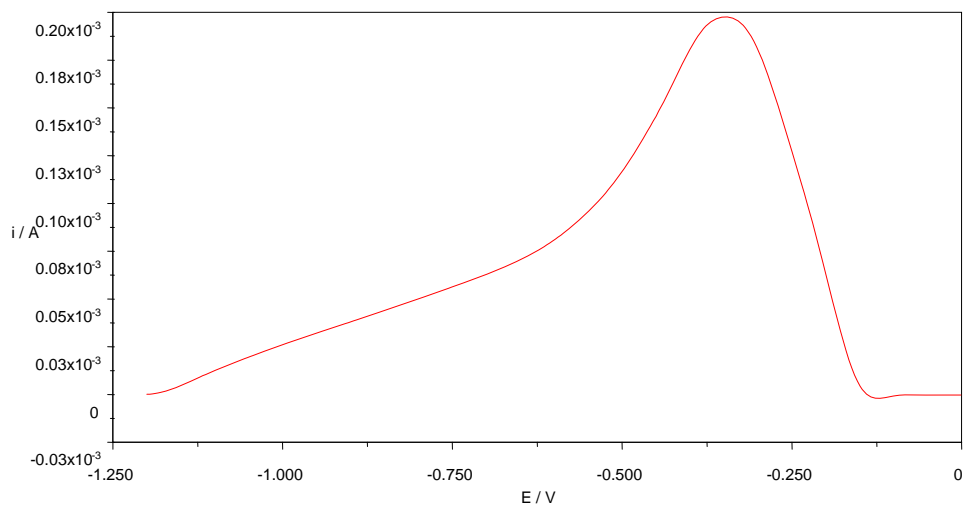


Figure 4.46 shows variation of frequency from 15 to 70 Hz. The corresponding peak currents remained constant up to 40Hz. It can be observed from the voltammograms that the peak size started broadening beyond frequency of 30 Hz. The maximum peak current was obtained at frequency of 50 Hz. This frequency was chosen for optimization of detection of lead ions in solution. Beyond this frequency the peak current dropped and then leveled off.

#### **4.5.3 The effect of deposition potential on peak current obtained using Anodic stripping-square wave voltammetry on modified pyrolytic graphite electrode**

The stripping analysis performed here was aimed at optimizing the deposition potential in order to obtain maximum peak current using modified pyrolytic graphite electrode for detection of lead ions in prepared solution while other parameters such as frequency, amplitude, step and deposition time were held constant.

Figure 4.47 highlights the square wave voltammogram for lead nitrate solution obtained at deposition potential of 0.075 V using modified pyrolytic graphite as working electrode



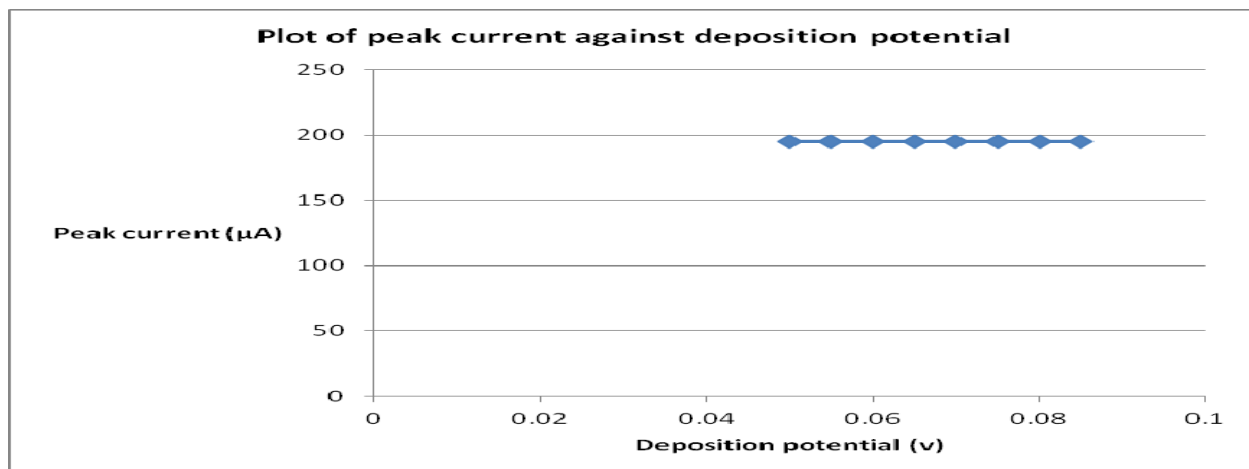
**Figure 4. 47: Square wave voltammogram for 30 ppm lead nitrate solution obtained at 0.075 V deposition potential using modified Pyrolytic graphite as working electrode.**

Table 4-24 shows frequency and corresponding peak current obtained using modified pyrolytic graphite as working electrode .By varying the deposition potential different values of current were obtained for  $\text{Pb}^{2+}$  (Figure 4.48).

**Table 4-24: Peak current and deposition potential.**

Deposition potential (Volts)	Current( $\mu$ A)
0.05	195
0.055	195
0.060	195
0.065	195
0.070	195
0.075	195
0.08	195
0.085	195

Figure 4.48 shows a plot of peak current against deposition potential obtained using modified pyrolytic graphite as working electrode



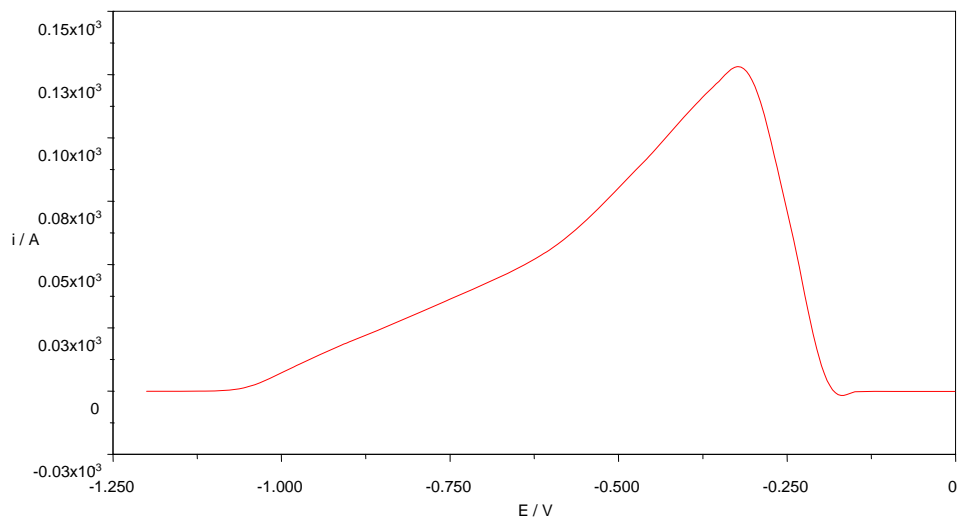
**Figure 4. 48: A plot of peak current against the deposition potential.**

The effect of deposition potentials on the stripping peak currents of  $\text{Pb}^{2+}$  is shown in Figure 4.47. The deposition potential was varied from 0.05 to 0.085 V with a constant deposition time of 120 s. The peak current obtained in this experiment remained constant despite the increase in deposition potential. This can be attributed to the fact that during the first scan of 0.05 Volts, all the active sites on the electrode were occupied by lead metal. Any further increase in deposition potential could not result in increase in peak current.

#### **4.5.4 The effect of Amplitude on peak current obtained using Anodic stripping-square wave voltammetry on modified pyrolytic graphite electrode.**

The anodic stripping performed here was aimed at optimizing the amplitude in order to obtain maximum peak current using modified pyrolytic graphite electrode for detection of lead ions in prepared solution while other parameters such as frequency, deposition time, step potential, deposition potential were held constant.

Figure 4.49 highlights the square wave voltammogram for lead nitrate solution obtained at amplitude of 0.04 V using modified pyrolytic graphite as working electrode.



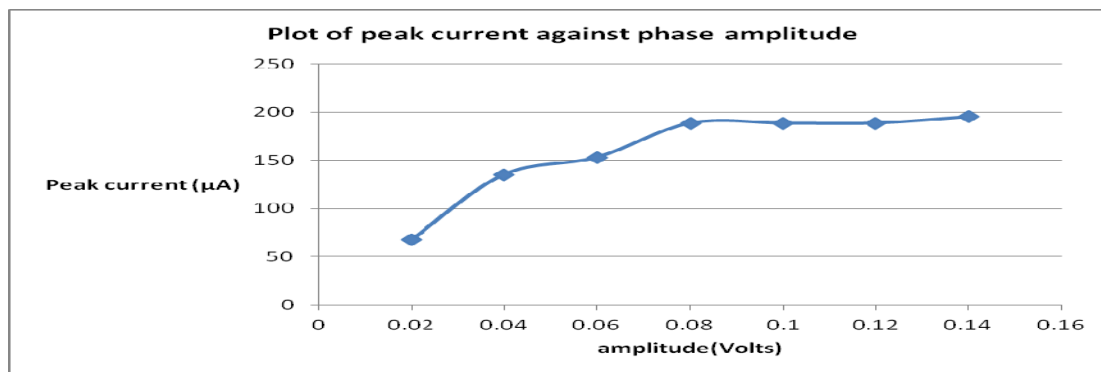
**Figure 4. 49: Square wave voltammogram for 30 ppm lead nitrate obtained at 0.04 Volts using modified Pyrolytic graphite as working electrode.**

Table 4-25 shows amplitude and corresponding peak current obtained using modified pyrolytic graphite as working electrode .By varying the amplitude different values of current were obtained for  $\text{Pb}^{2+}$  (Figure 4.50).

**Table 4-25: Peak current and Phase amplitude.**

Amplitude (Volts)	Current( $\mu$ A)
0.02	67.5
0.04	135
0.06	153
0.08	188.5
0.10	188.5
0.12	188.5
0.14	195.0

Figure 4.50 shows a plot of peak current against amplitude obtained using modified pyrolytic graphite as working electrode



**Figure 4. 50: A plot of peak current against amplitude on modified Pyrolytic graphite as working electrode.**

The amplitude was varied from 0.02 to 0.14 volts. From the geometry of the voltammograms, the peak current increased as the phase amplitude was raised from 0.02 Volts to 0.14. The peak current remained constant beyond 0.08 volts, suggesting that the electrode was saturated with lead such that an increase in phase amplitude did not result in increase in peak current. The amplitude of 0.08 Volts gave a fairly symmetrical peak. Beyond this amplitude the peak started to broaden with lower stability. Therefore, amplitude phase of 0.08 Volts was chosen for further studies.

#### **4.5.5 The effect of step potential on peak current obtained using Anodic stripping-square wave voltammetry on modified pyrolytic graphite electrode**

The electrochemical analysis performed here was aimed at optimizing the step potential in order to obtain maximum peak current using modified pyrolytic graphite electrode for detection of lead ions in prepared solution while other parameters such as frequency, deposition time, deposition potential and amplitude were held constant.

Figure 4.51 highlights the square wave voltammogram for lead nitrate solution obtained at step potential of 0.04 V using modified pyrolytic graphite as working electrode

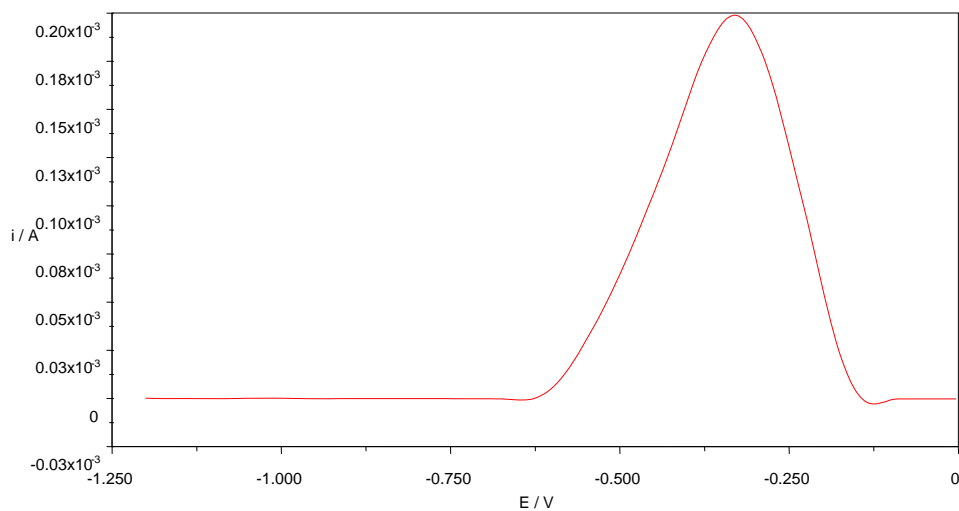


**Figure 4. 51: Square wave voltammogram for 30 ppm lead nitrate solution obtained at 0.00605 step up potential using modified Pyrolytic graphite as working electrode.**

Table 4.26 shows the step potential and corresponding peak current obtained using modified pyrolytic graphite as working electrode .By varying the amplitude different values of current were obtained for  $\text{Pb}^{2+}$  (Fig 4.52).



**Table 4-26: Peak current and step up potential.**

Step potential (Volts)	Current( $\mu\text{A}$ )
0.00405	195
0.00455	195
0.00505	195
0.00555	195
0.00605	195
0.00655	65
0.00705	65

Figure 4.52 shows a plot of peak current against step potential obtained using modified pyrolytic graphite as working electrode

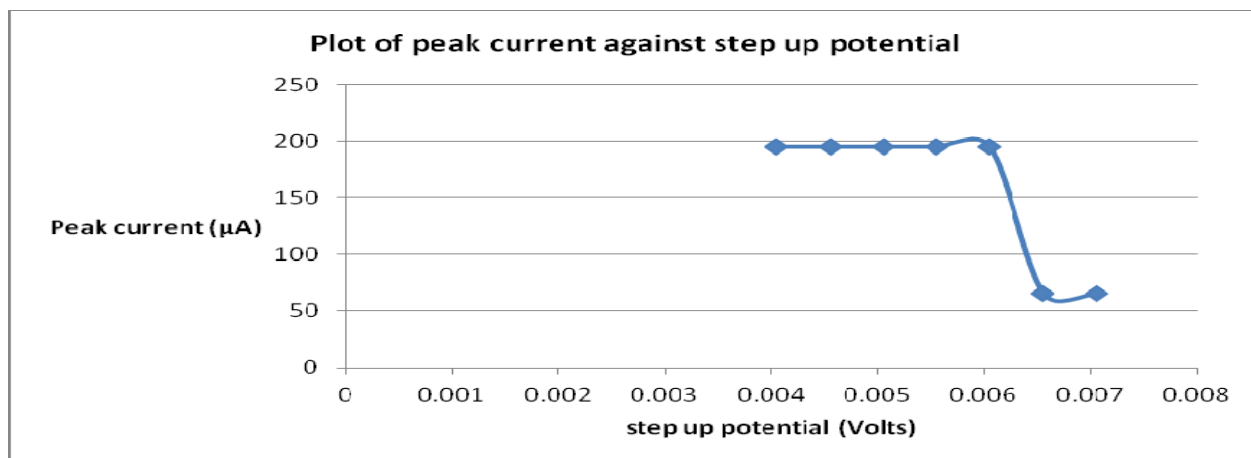


**Figure 4. 52: A plot of peak current against step potential on modified Pyrolytic graphite as working electrode.**

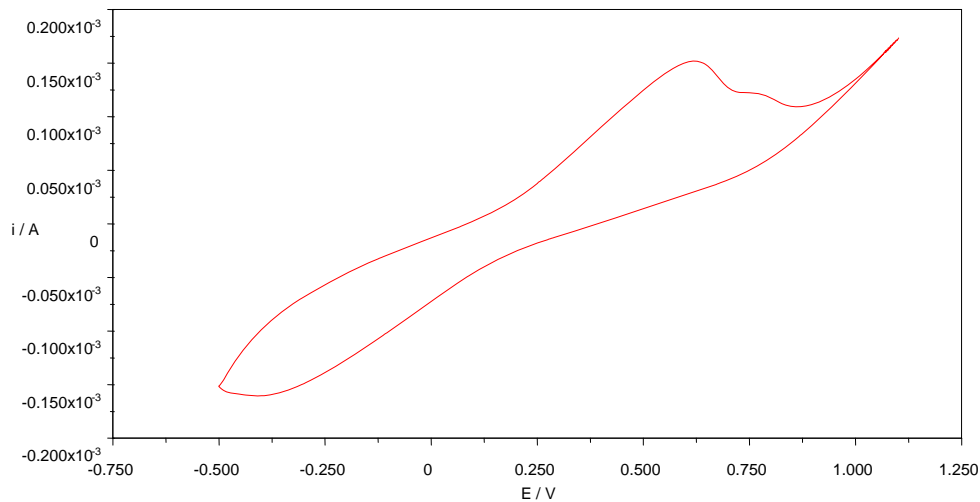
The step potential was varied from 0.00405 to 0.00705 V. The scan rate is related to the step potential. When the step potential is changed, the scan rate is also altered automatically by the instrument. From plot of peak current against step potential showed a constant peak current as step potential is increased up to 0.00705 Volts. However, the peak current dropped as the scan rate increased. The optimized step potential in this case was 0.00405 .

#### **4.6 Anodic stripping-square wave voltammetry on a mixture of lead nitrate and cadmium bromide solution carried out using modified pyrolytic graphite electrode**

##### **4.6.1 The effect of deposition time on peak current obtained using Anodic stripping-square wave voltammetry on modified pyrolytic graphite electrode for 1 ppm mixture of lead nitrate and Cadmium bromide solution**

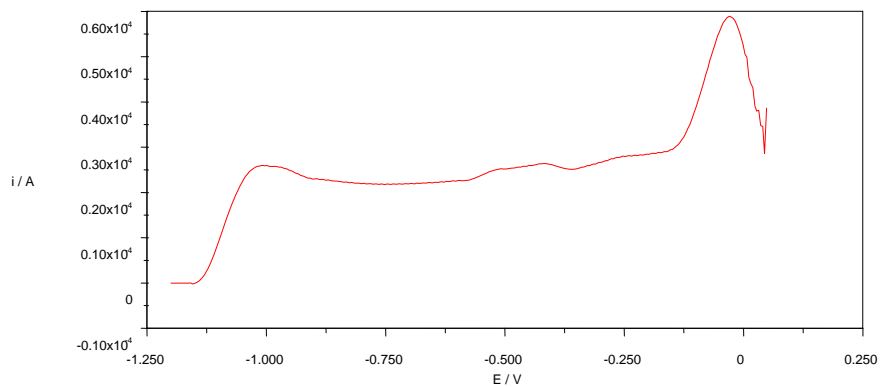
The stripping analysis performed here was aimed at optimizing the deposition time on modified electrode in order to obtain maximum peak current for detection of lead and Cadmium ions in prepared solution while other parameters such as deposition potential, step potential, amplitude and frequency were held constant.

Figure 4.53 highlights the cyclic voltammogram of aniline mixture obtained after electro-polymerization of polyaniline on the surface of the electrode by multiple cyclic scanning at 100  $\text{mVs}^{-1}$  from -750 to 1250mV for 30 cycles at 25  $^{\circ}\text{C}$  using modified electrode.



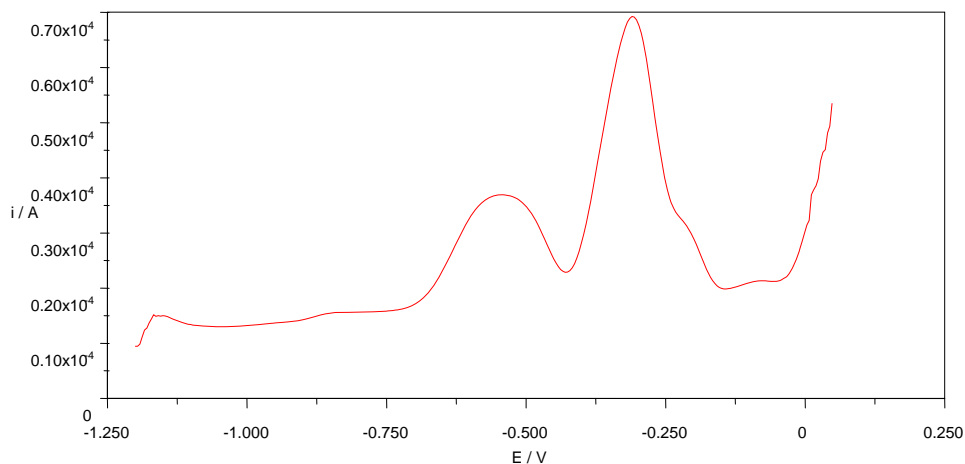
**Figure 4. 53: Voltammogram obtained after electropolymerization of polyaniline on the surface using modified Pyrolytic graphite as working electrode.**

Figure 4.54 highlights the square wave voltammogram for 0.1 M KCl (blank) obtained at deposition potential of 120 s using modified pyrolytic graphite electrode as working electrode. No stripping of ions was observed at reduction potential for lead and cadmium ions. The stripping peak observed at potential of 0 V was due to dissolved oxygen.



**Figure 4. 54: Square wave voltammogram for 0.1M KCl (Blank) obtained at 120 seconds deposition time using modified Pyrolytic graphite as working electrode.**

Figure 4.55 highlights the square wave voltammogram for 1 ppm mixture of lead nitrate and Cadmium bromide solution obtained at deposition time of 240 s using modified pyrolytic graphite as working electrode



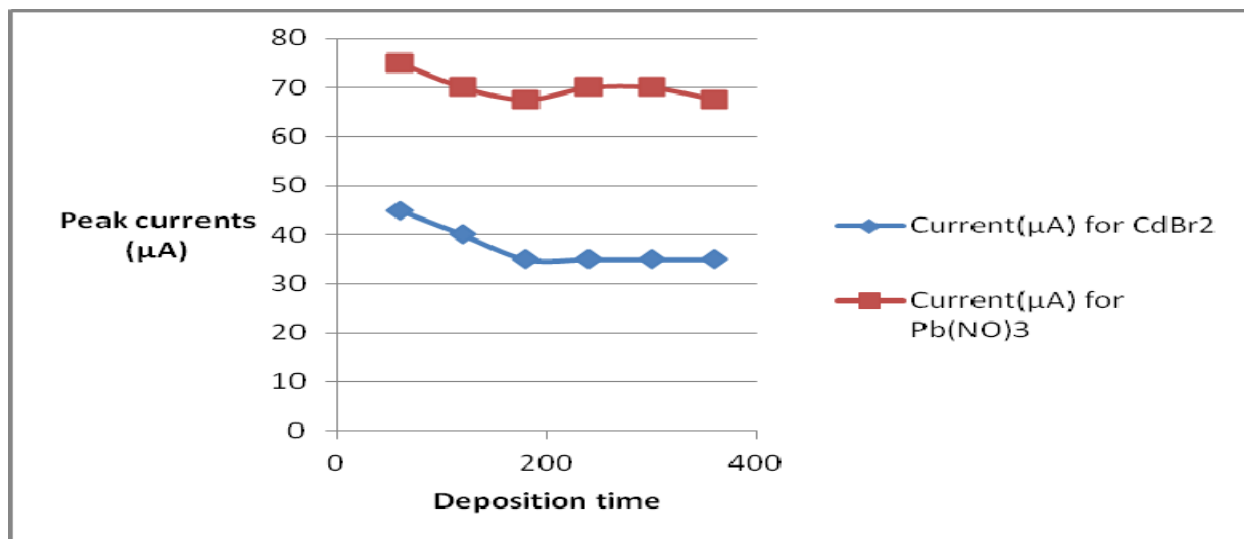
**Figure 4. 55: Square wave voltammogram for 1 ppm mixture of lead Nitrate and cadmium bromide mixture obtained at 240 seconds deposition time using modified Pyrolytic graphite as working electrode.**

Table 4-27 below shows the deposition time and corresponding peak current obtained using modified pyrolytic graphite as working electrode .By varying the deposition time different values of current were obtained for  $Pb^{2+}$  and  $Cd^{2+}$  ions (Figure 4.56).

**Table 4-27: Peak current and deposition time.**

Deposition time(s)	Current( $\mu A$ ) for $CdBr_2$	Current( $\mu A$ ) for $Pb(NO)_3$
60	45	75
120	40	70
180	35	67.5
240	35	70
300	35	70
360	35	67.5

Figure 4.56 shows a plot of peak current against deposition time obtained using modified pyrolytic graphite as working electrode



**Figure 4. 56: A plot of peak current against deposition time for Lead nitrate and Cadmium Bromide solution carried out on modified pyrolytic graphite.**

The effect of deposition time on stripping current on modified pyrolytic graphite electrode for cadmium bromide and lead nitrate was studied from 120 to 420 seconds and results are shown in Figure 4.56. From the Anodic stripping-square wave voltammetry carried on pure CdBr<sub>2</sub> and Pb(NO)<sub>3</sub> earlier in the research, the peak appearing at 0.57 V is for CdBr<sub>2</sub> while the second peak is for Pb(NO)<sub>3</sub>.

From Figure 4.56, it can be seen that the highest peak current for the mixture was 75  $\mu\text{A}$  corresponding  $\text{Pb}(\text{NO}_3)_2$  solution. The highest peak current obtained for  $\text{CdBr}_2$  solution was 45  $\mu\text{A}$ . The effect of lead on cadmium stripping peak is shown in the Fig 4.56 above. The peak current for cadmium bromide was less for the 1ppm mixture. This suggests that inter-metallic bond formation between cadmium and lead could explain cadmium peak suppression by lead.

Competition between lead and cadmium on active sites of modified pyrolytic graphite electrode may also explain the observed peak suppression of cadmium. Lead may out compete cadmium for active sites because of its larger diffusivity.

Deposition time of 60 s was chosen as ideal for optimization of the peak currents for the mixture of cadmium(II) and lead(II). As can be seen, the stripping response of cadmium(II) dropped rapidly with deposition time from 30 to 360 s. Lead(II) Anodic stripping-square wave voltammetry peak current dropped from 75 to 67.5  $\mu\text{A}$ , this was due to the saturation of the modified pyrolytic graphite electrode surface. A deposition of 60 s was used for subsequent experiments, as this was sufficient to obtain well-defined stripping peaks for cadmium and lead. Deposition longer than required can also deplete the metal ions in the bulk solution or lead to the formation of inter-metallic complexes, all of which will affect the definition and size of the stripping peaks [Wilson et, al (2001)]. The presence of break-point in the peak area vs. accumulation time plot may be due to the changes in the mechanism of deposition after longer periods [Honey et, al. 2002]. Such changes in the dynamics of deposition might be as a result of changes in the electrode surface during the accumulation period.

#### 4.6.2 The effect of frequency on peak current obtained using Anodic stripping-square wave voltammetry on modified pyrolytic graphite electrode for 1 ppm mixture of lead nitrate and Cadmium bromide solution

The electrochemical analysis performed here was aimed at optimizing the frequency in order to obtain maximum peak current for detection of lead and cadmium ions using modified electrode in prepared solution while other parameters such as deposition potential, step potential, amplitude and deposition time were held constant.

Figure 4.57 highlights the square wave voltammogram for 1 ppm mixture of lead nitrate and cadmium bromide solution obtained at frequency of 20 Hz using modified pyrolytic graphite as working electrode.

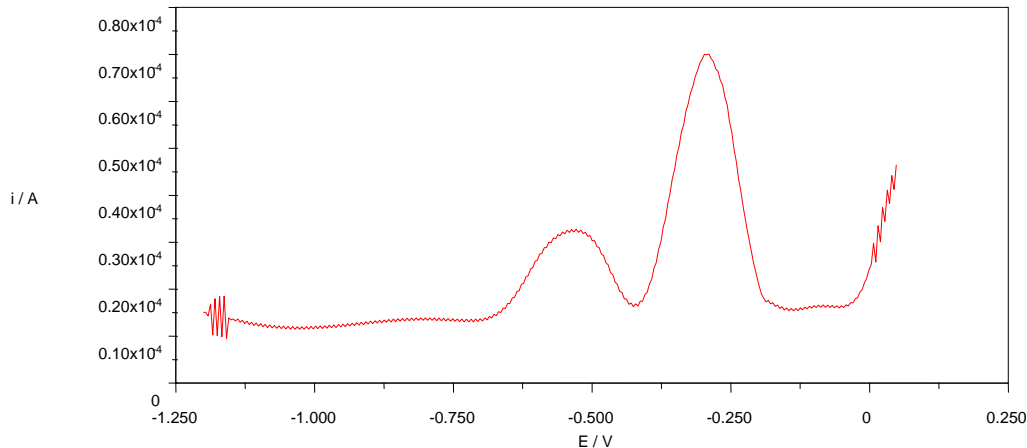


**Figure 4. 57: Square wave voltammogram for 1 ppm mixture of Cadmium bromide and Lead Nitrate solution obtained at frequency of 20 Hz using modified Pyrolytic graphite as working electrode.**

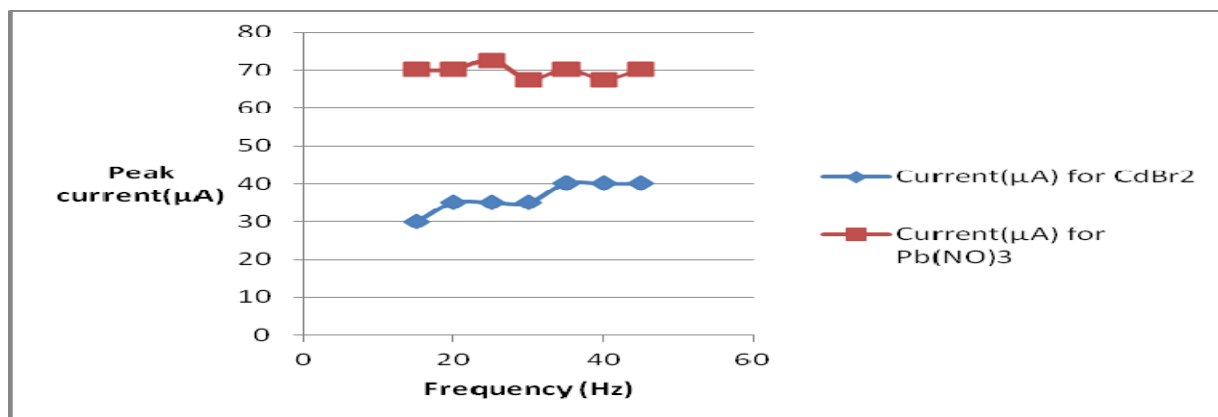


Table 4-28 below shows frequency and corresponding peak current obtained using modified pyrolytic graphite as working electrode .By varying the frequency different values of current were obtained for  $\text{Pb}^{2+}$  and  $\text{Cd}^{2+}$  ions (Figure 4.58).

**Table 4-28: Peak current and frequency.**

Frequency(Hz)	Current( $\mu\text{A}$ ) for $\text{CdBr}_2$	Current( $\mu\text{A}$ ) for $\text{Pb}(\text{NO})_3$
15	30	70
20	35	70
25	35	72.5
30	35	67.5
35	40	70
40	40	67.5
45	40	70

Figure 4.58 shows a plot of peak current against frequency obtained using modified pyrolytic graphite as working electrode



**Figure 4. 58: A plot of peak current against frequency.**

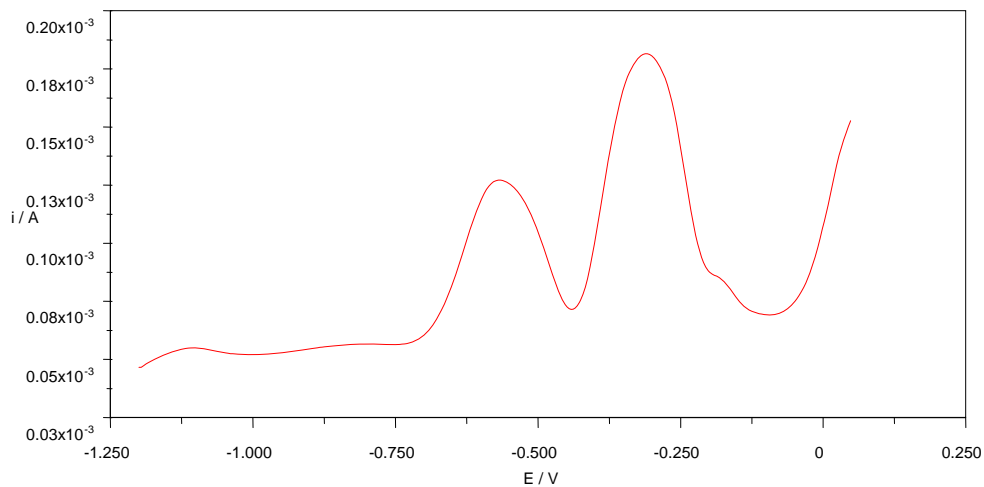
From figure 4.58 the frequency was varied from 15 to 45 Hz. The corresponding peak currents were recorded as shown in Table 4-28. The maximum peak currents obtained was 72.5  $\mu\text{A}$  for lead nitrate and 40  $\mu\text{A}$  for cadmium bromide.

For the effect of frequency on the stripping response, the SW-ASV signals for cadmium and lead decreased when the frequency proceeded to higher value as shown in the figure above. As a compromise among the two metals analyzed, frequency of 25 Hz was used as it provided the most stable peak shape and had the highest current for the simultaneous analysis of  $\text{Pb}^{2+}$  and  $\text{Cd}^{2+}$  ions.

#### **4.6.3 The effect of amplitude on peak current obtained using Anodic stripping-square wave voltammetry on modified pyrolytic graphite electrode of 1 ppm lead nitrate and cadmium bromide solution**

The stripping analysis performed here was aimed at optimizing the amplitude in order to obtain maximum peak current for detection of lead and Cadmium ions in prepared solution while other parameters such as deposition potential, step potential, frequency and deposition time were held constant.

Figure 4.59 highlights the square wave voltammogram for 1 ppm mixture of lead nitrate and cadmium bromide solution obtained at amplitude of 0.08 V using modified pyrolytic graphite as working electrode.



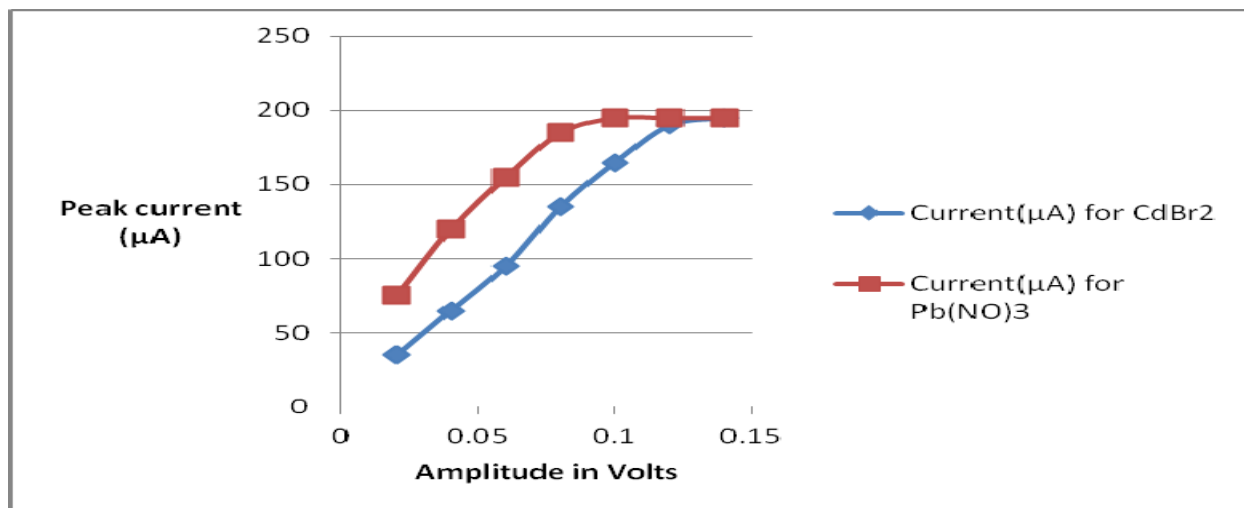
**Figure 4. 59: Square wave voltammogram for 1 ppm mixture of cadmium bromide and Lead Nitrate solution obtained at amplitude 0.08 Volts using Modified Pyrolytic graphite as working electrode.**

Table 4-29 shows amplitude and corresponding peak current obtained using modified pyrolytic graphite as working electrode .By varying the amplitude different values of current were obtained for  $\text{Pb}^{2+}$  and  $\text{Cd}^{2+}$  ions (Figure 4.60).

**Table 4-29: Peak current and Phase amplitude.**

Phase amplitude(Volts)	Current( $\mu$ A) for CdBr <sub>2</sub>	Current( $\mu$ A) for Pb(NO) <sub>3</sub>
0.02	35	75
0.04	65	120
0.06	95	155
0.08	135	185
0.10	165	195
0.12	190	195
0.14	195	195

Figure 4.60 shows a plot of peak current against amplitude obtained using modified pyrolytic graphite as working electrode



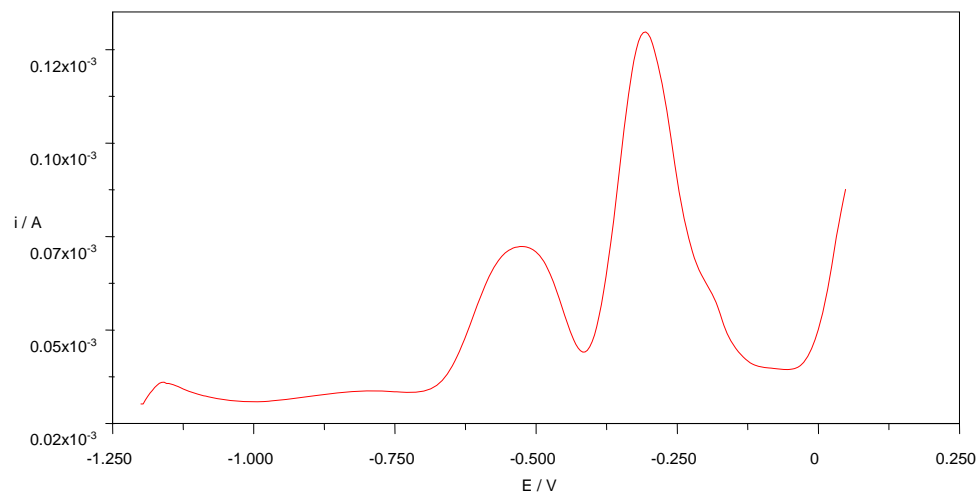
**Figure 4. 60: A plot of peak current against Change in phase amplitude.**

The phase amplitude was varied from 0.02 to 0.12 volts. From the geometry of the voltammograms, the peak current increased as the phase amplitude was raised from 0.02 Volts to 0.10. The amplitude of 0.14 Volts gave the highest peak currents. At the amplitude of 0.10 volts peaks of the voltammogram started to broaden.

#### **4.6.4 The effect of deposition potential on peak current obtained using Anodic stripping-square wave voltammetry on modified pyrolytic graphite electrode**

The electrochemical analysis performed here was aimed at optimizing the deposition potential using modified electrode in order to obtain maximum peak current for detection of lead and Cadmium ions in prepared solution while other parameters such as amplitude, step potential, frequency and deposition time were held constant.

Figure 4.61 highlights the square wave voltammogram for 1 ppm mixture of lead nitrate and Cadmium bromide solution obtained at amplitude of 0.08 V using modified pyrolytic graphite as working electrode.



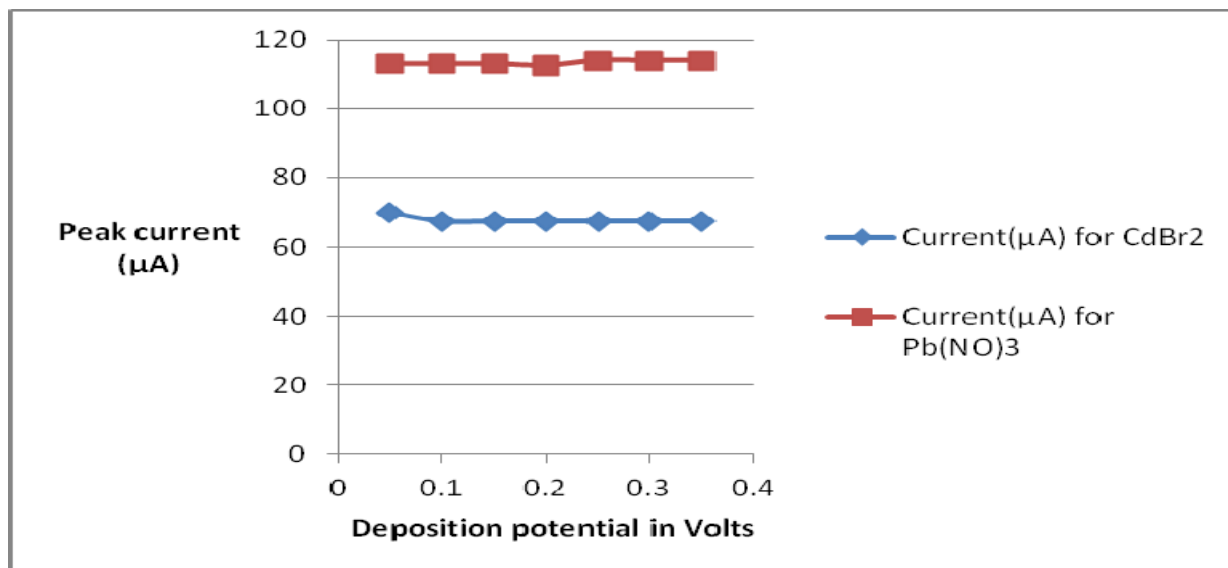
**Figure 4. 61: Square wave voltammogram for 1 ppm mixture Lead nitrate and Cadmium Bromide solution obtained at deposition potential 0.15 Volts using modified Pyrolytic graphite as working electrode.**

Table 4–30 below shows deposition potential and corresponding peak current obtained using modified pyrolytic graphite as working electrode. By varying deposition potential different values of current were obtained for  $\text{Pb}^{2+}$  and  $\text{Cd}^{2+}$  ions (Figure 4.62).

**Table 4-30: Peak current and Deposition potential.**

Deposition potential	Current( $\mu$ A) for CdBr <sub>2</sub>	Current( $\mu$ A) for Pb(NO <sub>3</sub> ) <sub>3</sub>
0.05	67.5	113
0.10	67.5	113
0.15	67.5	113
0.20	67.5	112.5
0.25	67.5	114
0.30	67.5	114
0.35	67.5	114

Figure 4.62 shows a plot of peak current against deposition potential obtained using modified pyrolytic graphite as working electrode



**Figure 4. 62: A plot of peak current against deposition potential.**

The effect of deposition potentials on the stripping peak currents of 1 ppm mixture of  $\text{Cd}^{2+}$  and  $\text{Pb}^{2+}$  is shown in Fig. 4.62. The deposition potential was varied from 0.05 to 0.35 V with a constant deposition time of 120s. The highest stripping peak currents were obtained at deposition potential of 0.25, 0.30, and 0.35 V. Therefore, the maximum peak current obtained was 114  $\mu\text{A}$  for lead nitrate and 67.5  $\mu\text{A}$  for cadmium bromide.

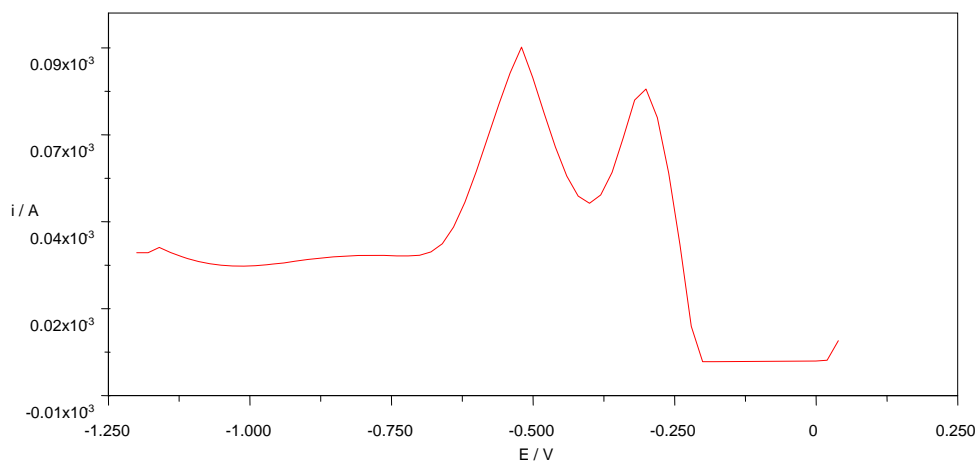
The effect of deposition potentials on the stripping peak currents of 1 ppm mixture of  $\text{Cd}^{2+}$  and  $\text{Pb}^{2+}$  is shown in Figure. 4.62. For cadmium, the SW-ASV signal remained constant even as the deposition potentials was varied. The response signal for lead dropped from 113 to 112.5 to and increased to 114 which is probably changed due to the electro-hydrolytic evolution of hydrogen [Choi et al. 2001]. A potential of 0.25 V was optimized for simultaneous detection of cadmium and lead because it provided the best compromise between sensitivity of the main peak and the background response.

#### **4.6.5 The effect of step potential on peak current obtained using Anodic stripping-square wave voltammetry on modified pyrolytic graphite electrode**

The anodic stripping performed here was aimed at optimizing the step potential in order to obtain maximum peak current using modified pyrolytic graphite electrode for detection of lead and Cadmium ions in prepared solution while other parameters such as deposition potential, amplitude, frequency and deposition time were held constant.



Figure 4.63 highlights the square wave voltammogram for 1 ppm mixture of lead nitrate and Cadmium bromide solution obtained at step potential 0.02 V using modified pyrolytic graphite as working electrode.



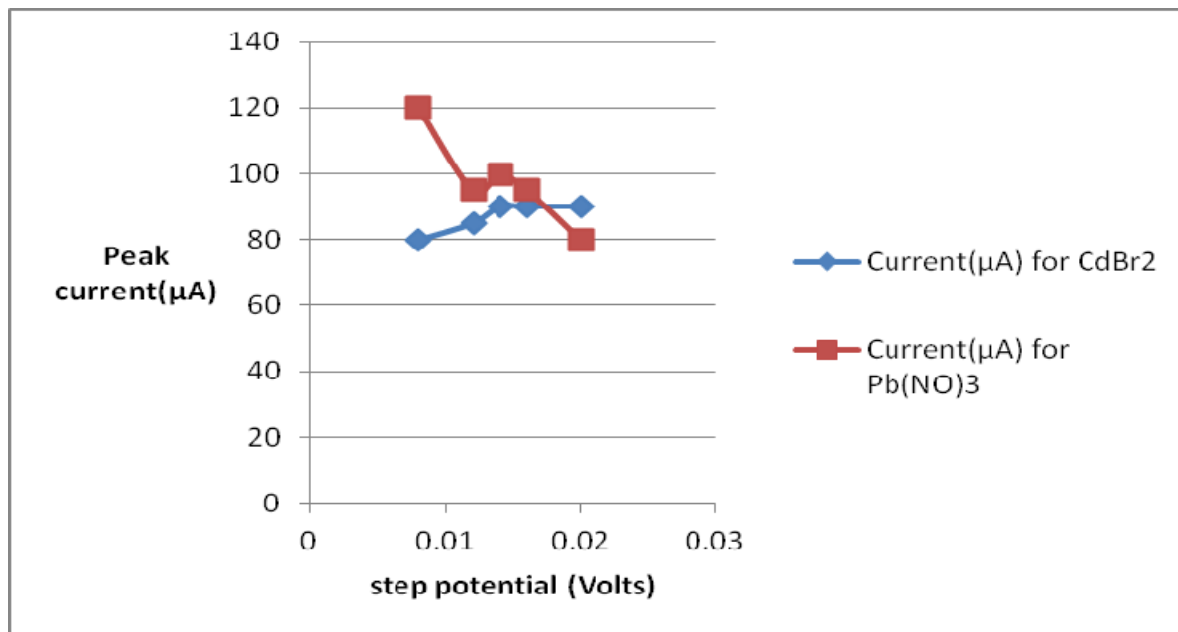
**Figure 4. 63: Square wave voltammogram for 1 ppm mixture of cadmium bromide and Lead Nitrate solution obtained at scan rate 0.02 Volts using modified Pyrolytic graphite as working electrode.**

Table 4-31 shows step potential and corresponding peak current obtained using modified pyrolytic graphite as working electrode .By varying step potential different values of current were obtained for Pb<sup>2+</sup> and Cd<sup>2+</sup> ions (Figure 4.64).

**Table 4-31: Peak current and Step potential.**

Step potential	Current( $\mu$ A) for CdBr <sub>2</sub>	Current( $\mu$ A) for Pb(NO <sub>3</sub> ) <sub>2</sub>
0.00405	70	130
0.00805	80	120
0.01205	85	95
0.01405	90	100
0.01605	90	95
0.02005	90	80

Figure 4.64 shows a plot of peak current against step potential obtained using modified pyrolytic graphite as working electrode.



**Figure 4. 64: A plot of peak current against step potential.**

The step potential was varied from 0.00405 to 0.02405 V. The scan rate is related to the step potential. When the step potential is changed, the scan rate is also altered automatically by the instrument. The Plot of peak current against step potential showed the highest peak current was obtained when scan rate was 0.01405 Volts. Therefore, step potential of 0.01405 V was chosen for further studies as an optimum value.

#### **4.7 Comparative analysis of peak currents obtained using modified and un-modified pyrolytic electrode for lead nitrate solutions**

##### **4.7.1 The effect of deposition time on peak current obtained using Anodic stripping-square wave voltammetry on modified and un-modified pyrolytic graphite electrode for lead nitrate solution**

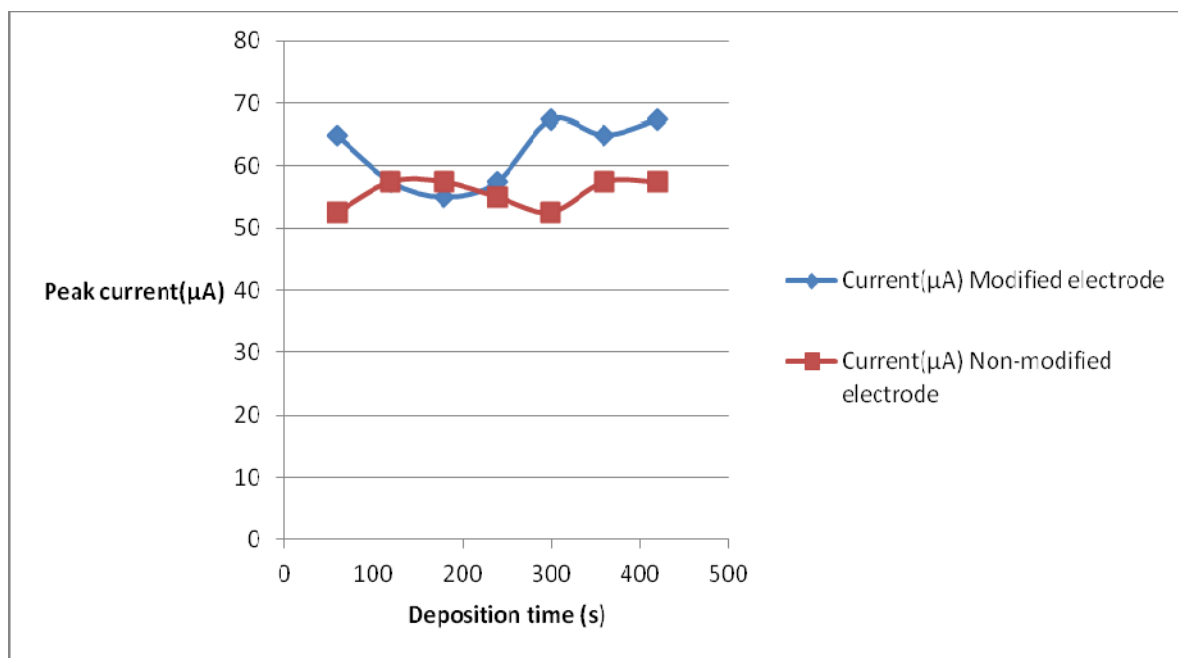
The comparative analysis done here was aimed at analyzing peak current obtained at different deposition time using modified and un-modified in order to determine whether the enhancement of sensitivity of the electrode had been achieved. Parameters such as deposition potential, amplitude, and frequency and deposition time were held constant.

Table 4-32 below shows deposition time and corresponding peak current obtained using modified and un-modified pyrolytic graphite as working electrode .By varying deposition time different values of current were obtained for  $\text{Pb}^{2+}$  ions.

**Table 4-32: Peak current and deposition time for modified and un-modified electrode.**

Deposition time	Current( $\mu\text{A}$ )	
	Modified electrode	Un-modified electrode
60	65	52.5
120	57.5	57.5
180	55	57.5
240	57.5	55
300	67.5	52.5
360	65	57.5
420	67.5	57.5

Figure 4.65 shows plots of peak current against deposition time obtained using modified and un-modified pyrolytic graphite as working electrode.



**Figure 4. 65: A plot of peak current against deposition time for modified and un-modified electrode.**

From Figure 4.65 the maximum peak current obtained in modified electrode was 67.5  $\mu\text{A}$  at 300 and 400 seconds, while for un-modified was 57.5  $\mu\text{A}$  at 120, 180, 360 and 420 seconds under same experimental conditions .i.e. the equipment set up was the same except for electrode modification. The highest peak current value for the modified electrode was larger than that obtained for un-modified. This can be explained that pyrolytic graphite electrode modified with polyaniline film exerts negative charges on the surface. The charges can favor accumulation of

increasing amounts of positively charged lead ions on the surface of the electrode. Hence, polyaniline films can be used as an excellent supporting material for heavy metal ion sensor. The enhanced peak current for lead ions is attributed to polyaniline film that exhibits a strong adsorptive power of heavy metals and hence an improved surface sensitivity

[S Anandhakumar et, al (2011)].

#### **4.7.2 The effect of frequency on peak current obtained using Anodic stripping-square wave voltammetry on modified and un-modified pyrolytic graphite electrode for lead nitrate solution**

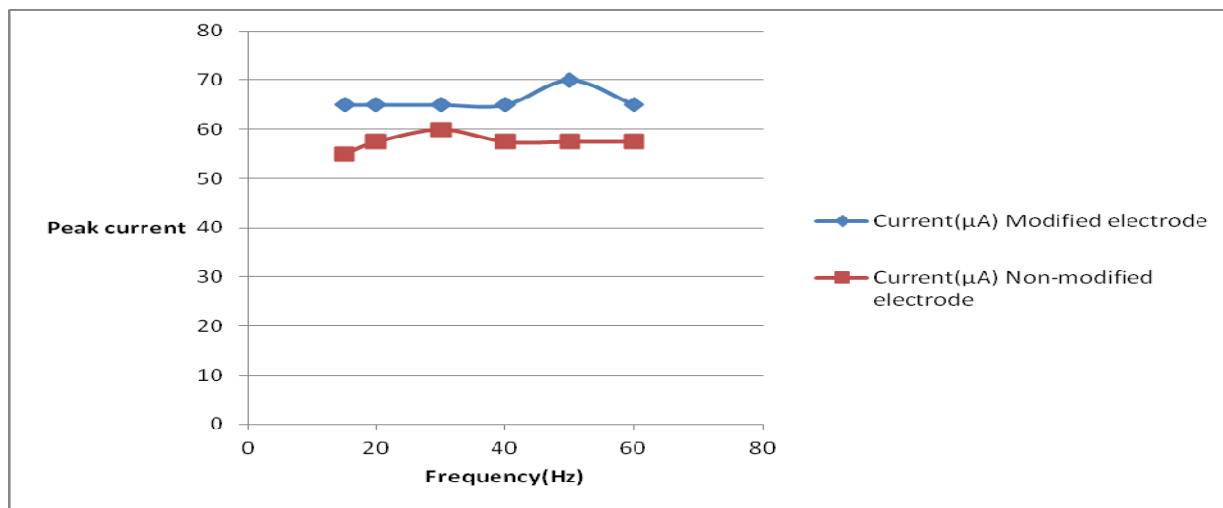
The comparative analysis done here was aimed at analyzing peak current obtained at different frequency using modified and un-modified in order to determine whether the enhancement of sensitivity of the electrode had been achieved. Parameters such as deposition potential, amplitude, step potential and deposition time were held constant.

Table 4-33 shows frequency and corresponding peak current obtained using modified and un-modified pyrolytic graphite as working electrode. By varying frequency different values of current were obtained for  $\text{Pb}^{2+}$  ions.

**Table 4-33: Peak current and Frequency for modified and un-modified electrode.**

Frequency(Hz)	Current( $\mu$ A)	
	Modified electrode	Un-modified electrode
15	65	55
20	65	57.5
30	65	60
40	65	57.5
50	70	57.5
60	65	57.5

Figure 4.66 shows plots of peak current against frequency obtained using modified and un-modified pyrolytic graphite as working electrode.



**Figure 4. 66: A plot of peak current against frequency for modified and un-modified electrode.**

From Figure 4.66 the maximum peak current obtained on modified electrode was 70  $\mu\text{A}$  at 50 Hz, while for un-modified was 60  $\mu\text{A}$  at 30 Hz under same experimental conditions .i.e. the equipment set up was the same except for electrode modification. The highest peak current value for the modified electrode is larger than that obtained for un-modified. This can be explained that pyrolytic graphite electrode modified with polyaniline film exerts negative charges on the surface. These charges can favor accumulation of increasing amounts of positively charged lead ions on the surface of the electrode.

#### **4.7.3 The effect of amplitude on peak current obtained using Anodic stripping-square wave voltammetry on modified and un-modified pyrolytic graphite electrode for lead nitrate solution**

The comparative analysis done here was aimed at analyzing peak current obtained at different amplitude using modified and un-modified in order to determine whether the enhancement of sensitivity of the electrode had been achieved. Parameters such as deposition potential, frequency, step potential and deposition time were held constant.

Table 4–34 below shows amplitude and corresponding peak current obtained using modified and un-modified pyrolytic graphite as working electrode, by varying amplitude different values of current were obtained for  $\text{Pb}^{2+}$  ions.



**Table 4-34: Peak current and amplitude for modified and un-modified electrode.**

Amplitude	Current( $\mu$ A)	
	Modified electrode	Un-modified electrode
0.02	67.5	67.5
0.04	135	135
0.06	153	153
0.08	188.5	188.5
0.10	188.5	188.5
0.12	188.5	188.5
0.14	195.0	195.0

From Table 4.34 the peak currents obtained using modified and non modified were same. This shows that electrode modification has no effect on sensitivity of the electrode for the parameter on lead ions.

#### **4.7.4 The effect of deposition potential on peak current obtained using Anodic stripping-square wave voltammetry on modified and un-modified pyrolytic graphite electrode for lead nitrate solution**

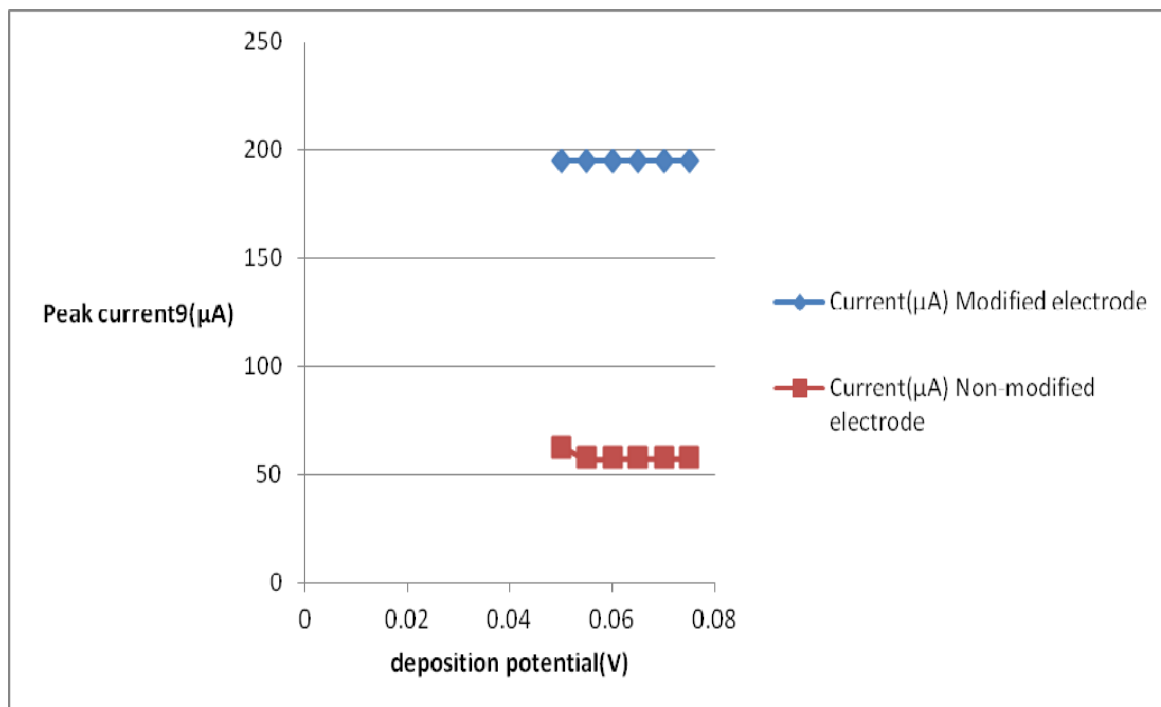
The comparative analysis done here was aimed at analyzing peak current obtained at different deposition potential using modified and un-modified electrode in order to determine whether the enhancement of sensitivity of the electrode had been achieved. Parameters such as amplitude, frequency, step potential and deposition time were held constant.

Table 4-35 below shows deposition potential and corresponding peak current obtained using modified and un-modified pyrolytic graphite as working electrode .By varying deposition potential different values of current were obtained for  $Pb^{2+}$  ions.

**Table 4-35: Peak current and deposition potential for modified and un-modified electrode.**

Deposition potential	Current( $\mu A$ )		Ratio(Modified/un-modified)
	Modified electrode	Un-modified electrode	
0.05	195	62.5	3.1
0.055	195	57.5	3.4
0.060	195	57.5	3.4
0.065	195	57.5	3.4
0.070	195	57.5	3.4
0.075	195	57.5	3.4

Figure 4.67 shows plots of peak current against deposition potential obtained using modified and un-modified pyrolytic graphite as working electrode.



**Figure 4. 67: A plot of peak current against deposition potential for modified and un-modified electrode.**

From Figure 4.67 the maximum peak current obtained using modified electrode was constant at  $195\mu\text{A}$  for all the deposition potential applied, while for un-modified the current was  $62.5\mu\text{A}$  at 0.5 volts, under same experimental conditions except for electrode modification. The highest peak current value for the modified electrode was 3.4 times larger than that obtained for un-modified. It can be explained that pyrolytic graphite electrode modified with polyaniline film exerts negative charges on the surface. These charges can favor accumulation of increasing amounts of positively charged lead ions on the surface of the electrode. There is a decrease in current at higher step potential (0.0065v).

**4.7.5 The effect of step potential on peak current obtained using Anodic stripping-square wave voltammetry on modified and un-modified pyrolytic graphite electrode for lead nitrate solution**

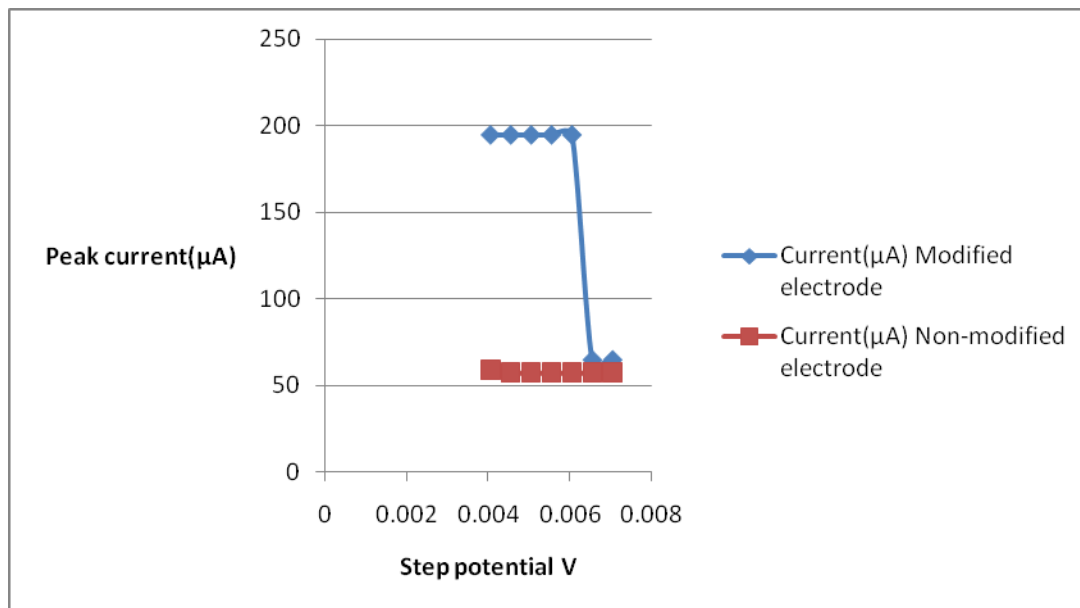
The comparative analysis done here was aimed at analyzing peak current obtained at different step potential using modified and un-modified electrode in order to determine whether the enhancement of sensitivity of the electrode had been achieved. Parameters such as amplitude, frequency, deposition potential and deposition time were held constant.

Table 4-36 below shows step potential and corresponding peak current obtained using modified and un-modified pyrolytic graphite as working electrode .By varying deposition potential different values of current were obtained for  $Pb^{2+}$  ions (Figure 4.68).

**Table 4-36: Peak current and step potential for modified and un-modified electrode.**

Step potential	Current( $\mu$ A)	
	Modified electrode	Un-modified electrode
0.00405	195	59
0.00455	195	57.5
0.00505	195	57.5
0.00555	195	57.5
0.00605	195	57.5
0.00655	65	57.5
0.00705	65	57.5

Figure 4.68 shows plots of peak current against step potential obtained using modified and un-modified pyrolytic graphite as working electrode



**Figure 4. 68: A plot of peak current against step potential for modified and un-modified electrode.**

From Figure 4.66 the maximum peak current obtained using modified electrode was  $195\mu\text{A}$  for lead ions while for un-modified was  $59\mu\text{A}$  at  $0.00405$  volts under same experimental conditions .i.e. the equipment set up set was same except for electrode modification. The highest peak current value for the modified electrode is larger than that obtained for un-modified. This can be explained that pyrolytic graphite electrode modified with polyaniline film exerts negative charges on the surface. These charges can favor accumulation of increasing amounts of positively charged lead ions on the surface of the electrode.

#### **4.8 Comparative analysis of peak currents obtained using modified and un-modified pyrolytic electrode for a mixture of 1 ppm lead nitrate and cadmium bromide solutions**

##### **4.8.1 The effect of deposition time on peak current obtained using Anodic stripping-square wave voltammetry on modified and un-modified pyrolytic graphite electrode for a mixture of 1 ppm lead nitrate and cadmium bromide solutions**

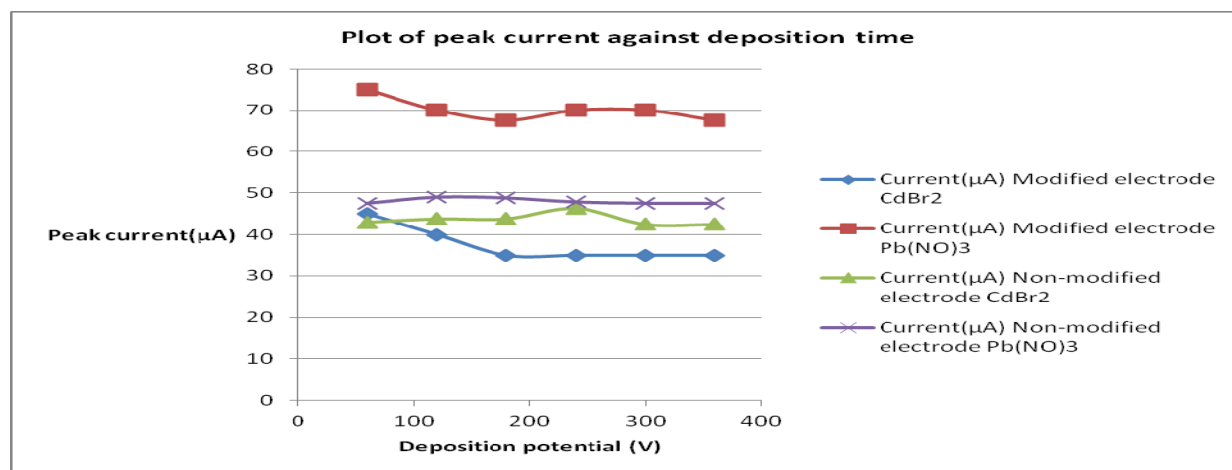
The comparative analysis done here was aimed at analyzing peak current obtained at different deposition time using modified and un-modified electrode in order to determine whether the enhancement of sensitivity of the electrode had been achieved. Parameters such as amplitude, frequency, deposition potential and step potential were held constant.

Table 4-37 below shows deposition time and the corresponding peak current obtained using modified and un-modified pyrolytic graphite as working electrode. By varying deposition time different values of current were obtained for  $\text{Pb}^{2+}$  and  $\text{Cd}^{2+}$  ions (Figure 4.69).

**Table 4-37: Deposition time for modified and un-modified electrode.**

Deposition time	Current( $\mu\text{A}$ )				Ratio (Modified/un-modified)	
	Modified electrode		Un-modified electrode			
	CdBr <sub>2</sub>	Pb(NO) <sub>3</sub>	CdBr <sub>2</sub>	Pb(NO) <sub>3</sub>	CdBr <sub>2</sub>	Pb(NO) <sub>3</sub>
60	45	75	43	47.5	1.1	1.6
120	40	70	43.8	49	0.9	1.4
180	35	67.5	43.8	48.8	0.8	1.4
240	35	70	46.3	47.8	0.8	1.5
300	35	70	42.5	47.5	0.8	1.5
360	35	67.5	42.5	47.5	0.8	1.4
<b>Total for the ratio</b>					<b>5.2</b>	<b>8.8</b>
<b>Average ratio for signal enhancement</b>					<b>0.9</b>	<b>1.5</b>

Figure 4.69 shows plots of peak current against deposition time obtained using modified and un-modified pyrolytic graphite as working electrode



**Figure 4. 69: A plot of peak current against deposition potential for modified and un-modified electrode.**

The peak current for cadmium bromide was less for the 1ppm mixture .This suggests that inter-metallic bond formation between cadmium and Lead could explain cadmium peak suppression .

From Figure 4.69 the values of peak currents for lead ions obtained using modified electrode was higher than the un-modified. However, the values of peak current obtained for cadmium ions using un-modified electrode are higher than for the modified electrode.

Table 4-37 average ratio of signal enhancement after electrode modification for lead increased by 1.5 while that for cadmium was suppressed to 0.9. This indicates that electro polymerization of polyaniline on the surface of the electrode increased sensitivity in detecting lead than cadmium ions .The increased deposit of the lead ions on the surface of the electrode occupies the active sites, leaving few active sites for cadmium ions to be reduced. This explains low detection for cadmium ions in solution in the presence of lead ions.

Competition between Lead and cadmium on active sites of modified pyrolytic graphite electrode may also explain the observed peak suppression of cadmium. Lead may out compete cadmium for active sites because of its larger diffusivity.

#### **4.8.2 The effect of frequency on peak current obtained using Anodic stripping-square wave voltammetry on modified and un-modified pyrolytic graphite electrode for a mixture of 1 ppm lead nitrate and cadmium bromide solutions.**

The comparative analysis done here was aimed at analyzing peak current obtained at different frequency using modified and un-modified electrode in order to determine whether the enhancement of sensitivity of the electrode had been achieved. Parameters such as amplitude, deposition time, deposition potential and step potential were held constant.

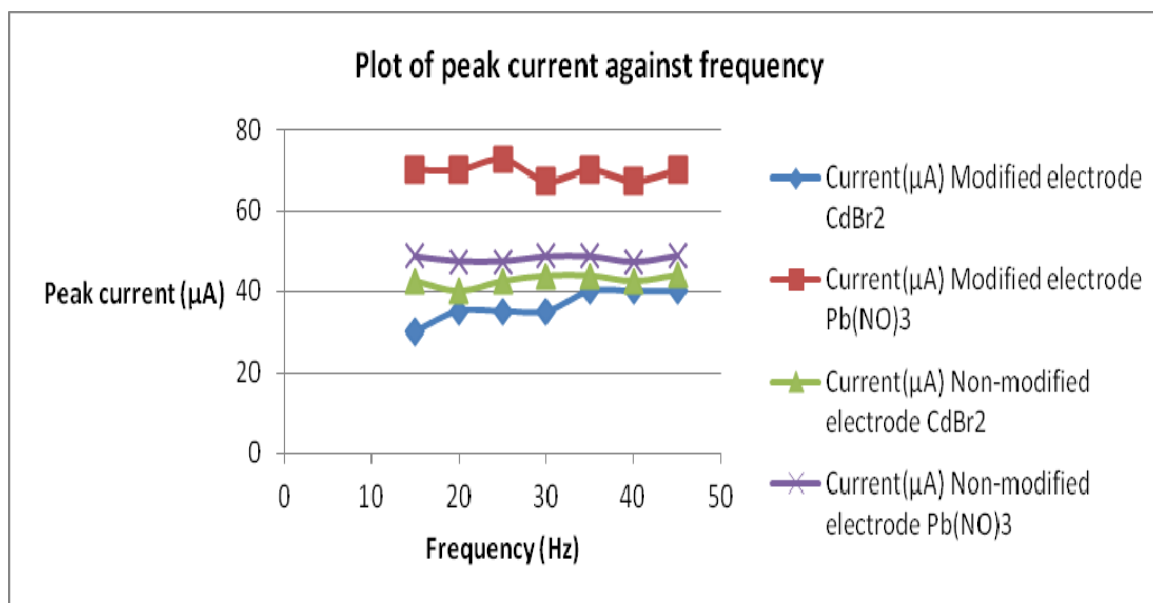


Table 4-38 below shows frequency and corresponding peak current obtained using modified and un-modified pyrolytic graphite as working electrode. By varying frequency different values of current were obtained for Pb<sup>2+</sup> and Cd<sup>2+</sup> ions (Figure 4.70).

**Table 4-38: Peak current and frequency for modified and un-modified electrode.**

Frequency	Current( $\mu$ A)				Ratio (Modified/un-modified)	
	Modified electrode		Un-modified electrode		CdBr <sub>2</sub>	Pb(NO) <sub>3</sub>
	CdBr <sub>2</sub>	Pb(NO) <sub>3</sub>	CdBr <sub>2</sub>	Pb(NO) <sub>3</sub>		
15	30	70	42.5	48.8	0.71	1.4
20	35	70	40.1	47.5	0.87	1.5
25	35	72.5	42.5	47.5	0.82	1.5
30	35	67.5	43.8	48.8	0.8	1.4
35	40	70	43.8	48.8	0.91	1.4
40	40	67.5	42.5	47.3	0.91	1.4
45	40	70	44.0	49.0	0.90	1.4
<b>Total for the ratio</b>					<b>5.92</b>	<b>10.0</b>
<b>Average ratio for signal enhancement</b>					<b>0.8</b>	<b>1.4</b>

Figure 4.70 shows plots of peak current against frequency obtained using modified and un-modified pyrolytic graphite as working electrode



**Figure 4. 70: A plot of peak current against frequency for modified and un-modified electrode.**

From figure 4.70 the values of peak currents for lead ions obtained using modified electrode was higher than that of the un-modified electrode. However, the values of peak current obtained for cadmium ions using un-modified electrode was higher than for the modified electrode. For cadmium ions, the highest peak current was obtained using un-modified electrode. This was expected because of competition between lead and cadmium on active sites of modified pyrolytic graphite electrode that explain the observed peak suppression of cadmium. Lead may out compete cadmium for active sites because of its larger diffusivity. This means that lead occupies most of the active sites on the surface of the electrode.

From Table 4-38 average ratio of signal enhancement after electrode modification for lead increased by 1.4 while that for cadmium was suppressed to 0.8. This indicates that electro polymerization of polyaniline on the surface of the electrode increased for sensitivity in detecting

lead than cadmium .The increased deposit of the lead ions on the surface of the electrode occupies the active sites, leaving few active sites for cadmium ions to be reduced. This explains low detection for cadmium ions in the solution.

#### **4.8.3 The effect of amplitude on peak current obtained using Anodic stripping-square wave voltammetry on modified and un-modified pyrolytic graphite electrode for a mixture of 1 ppm lead nitrate and cadmium bromide solutions**

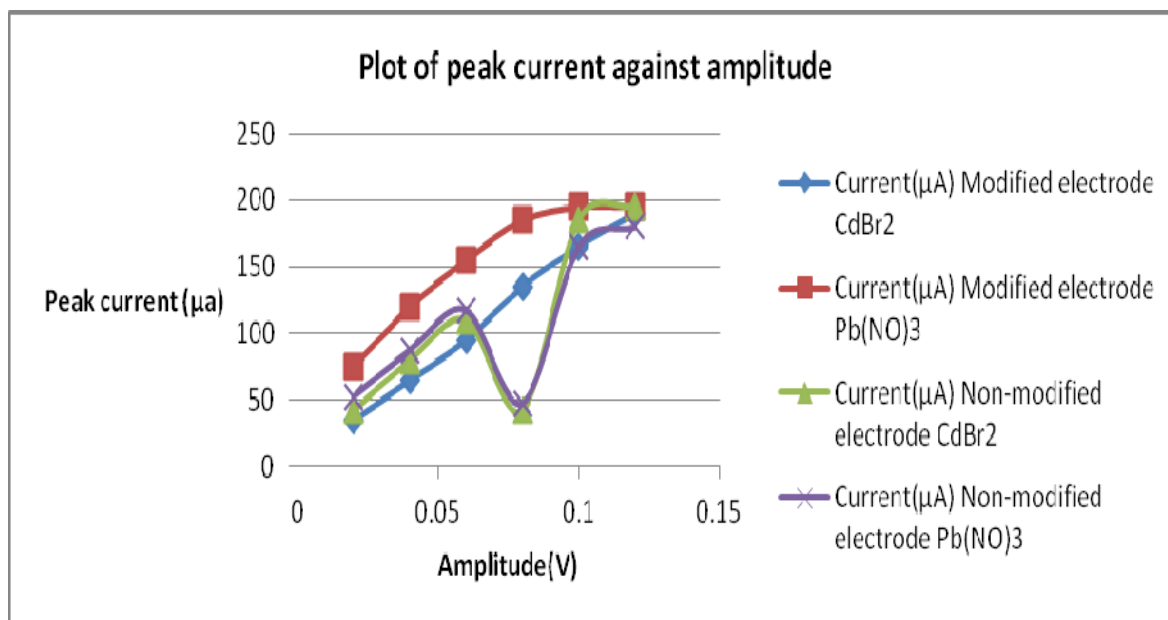
The comparative analysis done here was aimed at analyzing peak current obtained at different phase amplitude using modified and un-modified electrode in order to determine whether the enhancement of sensitivity of the electrode had been achieved. Parameters such as frequency, deposition time, deposition potential and step potential were held constant.

Table 4-39 shows frequency and corresponding peak current obtained using modified and un-modified pyrolytic graphite as working electrode .By varying frequency different values of current were obtained for  $\text{Pb}^{2+}$  and  $\text{Cd}^{2+}$  ions (Figure 4.71).

**Table 4-39: Peak current and phase amplitude for modified and un-modified electrode.**

Amplitude	Current( $\mu$ A)				Ratio (Modified/un-modified)	
	Modified electrode		Un-modified electrode		CdBr <sub>2</sub>	Pb(NO) <sub>3</sub>
	CdBr <sub>2</sub>	Pb(NO) <sub>3</sub>	CdBr <sub>2</sub>	Pb(NO) <sub>3</sub>		
0.02	35	75	42.5	52.5	0.8	1.43
0.04	65	120	80	87.5	0.81	1.37
0.06	95	155	110	117.5	0.86	1.32
0.08	135	185	42.5	47.5	3.2	3.90
0.10	165	195	185	165	0.89	1.18
0.12	190	195	195	180	0.97	1.08
<b>Total for the ratio</b>					<b>7.53</b>	<b>10.28</b>
<b>Average ratio for signal enhancement</b>					<b>1.04</b>	<b>1.5</b>

Figure 4.71 shows plots of peak current against amplitude obtained using modified and un-modified pyrolytic graphite as working electrode



**Figure 4. 71: A plot of peak current versus amplitude for modified and un-modified electrode.**

From Figure 4.71, the values of peak current for lead ions obtained using modified electrode were higher than the un-modified. However, the values of peak current obtained for cadmium ions using un-modified electrode were higher than modified. For cadmium ions, the highest peak current was obtained using modified electrode.

From the Table 4-39 average ratio of signal enhancement after electrode modification for lead increased by 1.5 while that for cadmium was 1.04. This indicates that electro polymerization of polyaniline on the surface of the electrode increased its sensitivity in detecting lead and cadmium ions in solution hence fulfilling one of the objectives of the research. However, The increased

deposit of the lead ions on the surface of the electrode occupies the active sites, leaving few active sites for cadmium ions to be reduced. This explains slight enhance of detection for cadmium ions in solution.

#### **4.8.4 The effect of deposition potential on peak current obtained using Anodic stripping-square wave voltammetry on modified and un-modified pyrolytic graphite electrode for a mixture of 1 ppm lead nitrate and cadmium bromide solutions**

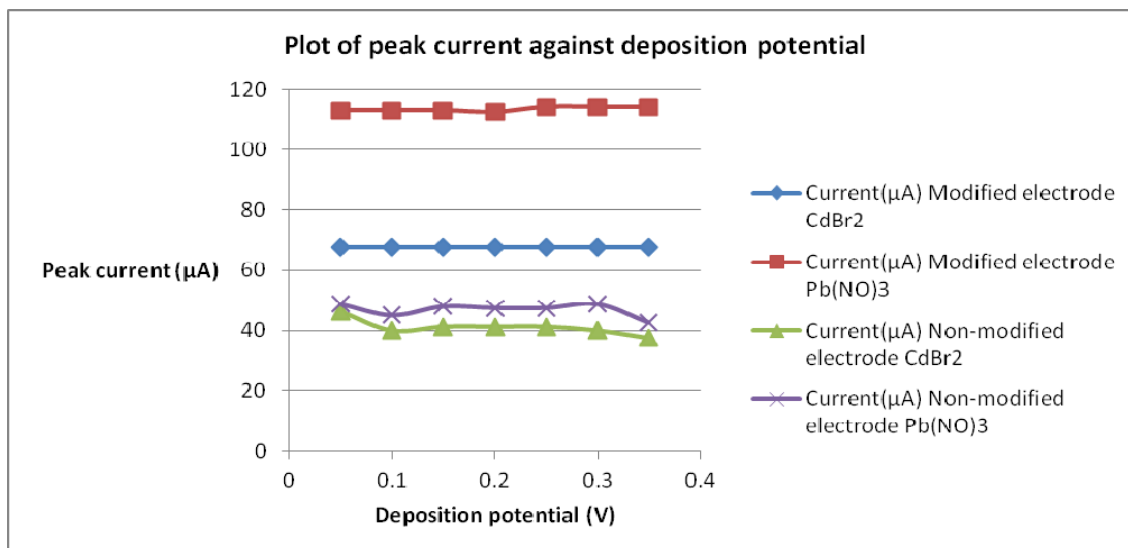
The comparative analysis done here was aimed at analyzing peak current obtained at different deposition potential using modified and un-modified electrode in order to determine whether the enhancement of sensitivity of the electrode had been achieved. Parameters such as amplitude, deposition time, frequency and step potential were held constant.

Table 4-40 below shows deposition potential and corresponding peak current obtained using modified and un-modified pyrolytic graphite as working electrode .By varying deposition potential different values of current were obtained for  $\text{Pb}^{2+}$  and  $\text{Cd}^{2+}$  ions (Figure 4.72).

**Table 4-40: Peak current and deposition potential for modified and un-modified electrode.**

Deposition potential	Current( $\mu\text{A}$ )				Ratio (Modified/un-modified)	
	Modified electrode		Un-modified electrode			
	$\text{CdBr}_2$	$\text{Pb}(\text{NO})_3$	$\text{CdBr}_2$	$\text{Pb}(\text{NO})_3$	$\text{CdBr}_2$	$\text{Pb}(\text{NO})$
0.05	67.5	113	46.3	48.8	1.5	2.31
0.10	67.5	113	40	45	1.7	2.5
0.15	67.5	113	41.3	48	1.6	2.4
0.20	67.5	112.5	41.3	47.5	1.6	2.4
0.25	67.5	114	41.3	47.5	1.6	2.4
0.30	67.5	114	40	48.8	1.7	2.3
0.35	67.5	114	37.5	42.5	1.8	2.7
<b>Total for the ratio</b>					11.5	14.61
<b>Average ratio for signal enhancement</b>					1.6	2.1

Figure 4.72 shows plots of peak current against deposition obtained using modified and un-modified pyrolytic graphite as working electrode



**Figure 4.72: A plot of peak current against amplitude for modified and un-modified electrode.**

From Table 4-40 the sensitivity was enhanced by 2.1 for Lead and 1.6 for Cadmium.

**4.8.5 The effect of step potential on peak current obtained using Anodic stripping-square wave voltammetry on modified and un-modified pyrolytic graphite electrode for a mixture of 1 ppm lead nitrate and cadmium bromide solutions.**

The comparative analysis done here was aimed at analyzing peak current obtained at different step potential using modified and un-modified electrode in order to determine whether the enhancement of sensitivity of the electrode had been achieved. Parameters such as amplitude, deposition time, frequency and deposition potential were held constant.

Table 4-41 below shows step potential and corresponding peak current obtained using modified and un-modified pyrolytic graphite as working electrode. By varying step potential different values of current were obtained for Pb<sup>2+</sup> and Cd<sup>2+</sup> ions (Figure 4.73).



**Table 4-41: Peak current and step potential for modified and un-modified electrode.**

Step potential	Current( $\mu$ A)				Ratio (Modified/un-modified)	
	Modified electrode		Un-modified electrode		CdBr <sub>2</sub>	Pb(NO) <sub>3</sub>
	CdBr <sub>2</sub>	Pb(NO) <sub>3</sub>	CdBr <sub>2</sub>	Pb(NO) <sub>3</sub>		
0.00405	70	130	45	47.5	1.6	2.7
0.00805	80	120	41.3	47.5	1.9	2.5
0.01205	85	95	40.0	42.5	2.1	2.2
0.01405	90	100	42.5	40.0	2.1	2.5
0.01605	90	95	47.5	35.0	1.9	2.7
0.02005	90	80	43.8	35.0	2.1	2.3
0.00405	70	130	45	47.5	1.6	2.7
<b>Total for the ratio</b>					<b>13.3</b>	<b>17.6</b>
<b>Average ratio of signal enhancement</b>					<b>1.9</b>	<b>2.5</b>

Figure 4.73 shows plots of peak current against step potential obtained using modified and un-modified pyrolytic graphite as working electrode.

From figure 4.73 the values of peak currents for lead and cadmium ions obtained using modified electrode were higher than the un-modified. This demonstrates that pyrolytic graphite electrode modified with polyaniline film exerts negative charges on the surface. These charges can favor accumulation of increasing amounts of positively charged lead and cadmium ions. From the Table 4-41 the average ratio of signal enhancement after electrode modification for lead increased by 2.5 while that for cadmium was 1.9. This indicates that electro polymerization of polyaniline on the surface of the electrode increased its sensitivity in detecting lead and cadmium ions in solution.

Competition between lead and cadmium on active sites of modified pyrolytic graphite electrode may also explain the observed peak suppression of cadmium. Lead may out compete cadmium for active sites because of its larger diffusivity.

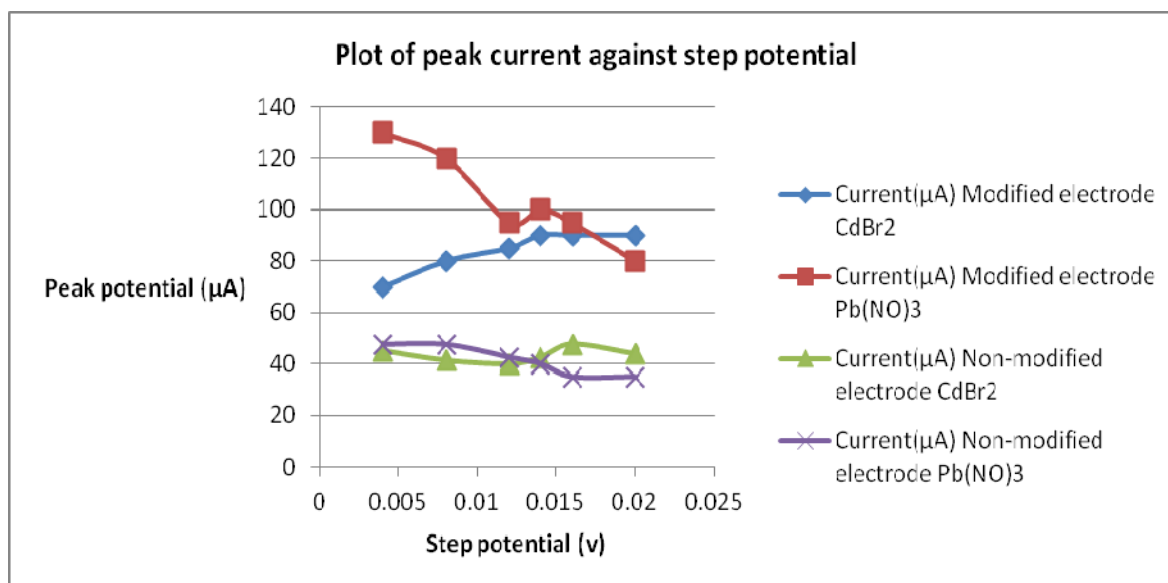


**Figure 4. 73: A plot of peak current against step for modified and un-modified electrode.**

#### 4.9 Determination of Limits of Detection (LOD) and Limits of Quantitation (LOQ)

The LOD of an analyte is that concentration of the analyte which gives an instrumental signal (y) significantly different from the "blank" or "background" signal. Limit of quantitation /Limit of determination(LOQ) is regarded as the lower limit for precise quantitative measurements.

The calculation done here was aimed at determining limits of detection and limits of quantitation from data obtained using anodic stripping-square wave voltammetry on modified pyrolytic graphite electrode for a mixture of cadmium bromide and lead nitrate solution.

Table 4-42 shows concentration and corresponding peak current obtained using modified pyrolytic graphite as working electrode by varying concentration, different values of current were obtained for  $\text{Pb}^{2+}$  and  $\text{Cd}^{2+}$  ions (Figure 4.73).

**Table 4-42: Peak current and concentration.**

Concentration (ppm)	Current( $\mu\text{A}$ ) for $\text{CdBr}_2$	Current( $\mu\text{A}$ ) for $\text{Pb}(\text{NO}_3)_2$
0.1	45.7	55.7
0.2	57	64
0.3	45.7	65.7
0.4	60	70
0.5	55	75

#### 4.9.1 LOD and Limits of Quantitation (LOQ) for cadmium bromide

Figure 4.74 shows plots of peak current against concentration obtained using modified pyrolytic graphite as working electrode

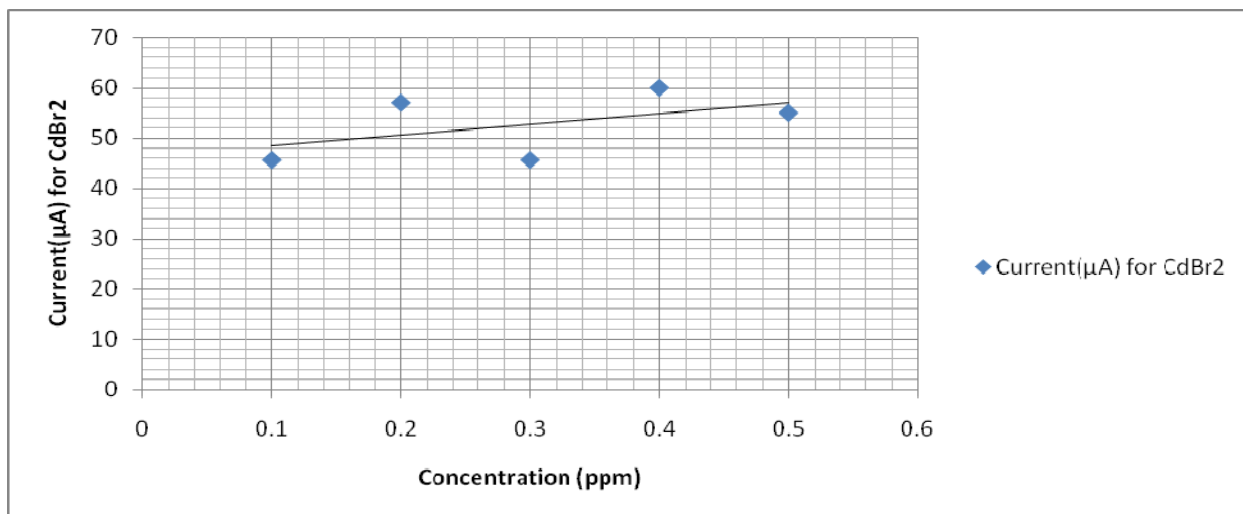


**Figure 4. 74: A plot of peak current against concentration for CaBr<sub>2</sub>.**

Table 4–.43 below shows statistical parameters obtained when an a plot of peak current against concentration was done.

**Table 4-43: Summary output for CdBr<sub>2</sub>.**

<b>Regression Statistics</b>	
Multiple R	0.516238471
R Square	0.266502159
Adjusted R Square	0.022002879
Standard Error	6.542476595
Intercept	46.2
Concentration (ppm)	21.6

**4.9.1.1 Limits of detection (LOD)**

$$Y_{LOD} = a + 3(S_{Y/X}) \dots\dots\dots(4.1)$$

Where: a is the y-Intercept,  $S_{Y/X}$  is the calibration standard error,  $Y_{LOD}$  is the minimum signal that can be detected by the equipment given the standard range.

$$Y_{LOD} = 46.2 + 3(6.54) = 65.82 \dots\dots\dots(4.2)$$

$$\text{Linear } Y = a + b x \dots\dots\dots(4.3)$$

$$Y_{LOD} = a + b X_{LOD}$$

$$65.82 = 46.2 + 21.6 X_{LOD}$$

$$\frac{65.82 - 46.2}{21.6} = 0.908 \text{ ppm} = X_{LOD}$$

According to this calculation the LOD for  $CdBr_2$  was 0.908 ppm. A similar experiment was done by Carol Babyak, 2003 where parts-per-billion levels of cadmium were detected using square-wave anodic stripping voltammetry with a boron-doped diamond electrode. The LOD in this case was 15 ppb. This value is smaller than in this study because other factors affecting the detection limit such as pH and use of other electrolytes and surfactants needs to be exploited further.

**4.9.1.2 Limits of Quantitation (LOQ)**

$$Y_{LOQ} = a + 10 (S_{Y/X}) \dots\dots\dots(4.4)$$

$$= 46.2 + 65.2$$

$$Y_{LOQ} = 111.62$$

$$Y_{LOQ} = a + bX_{LOQ}$$

$$111.62 = 46.2 + 21.6 \times X_{LOQ}$$

$$X_{LOQ} = 3.03 \text{ ppm}$$

According to this calculation the LOQ for  $\text{CdBr}_2$  was 3.03 ppm. A similar experiment was done by Babyak et,al 2003 where Parts-per-billion levels of cadmium were detected using square-wave anodic stripping voltammetry with a boron-doped diamond electrode. The LOQ in that case was 50 ppb. This value is smaller than that obtained in this study because other factors such as pH and electrolyte were not investigated.

#### 4.9.2 Limits of detection (LOD) and Limits of Quantitation (LOQ) for lead nitrate solution

Figure 4.75 shows plots of peak current against concentration obtained using modified pyrolytic graphite as working electrode

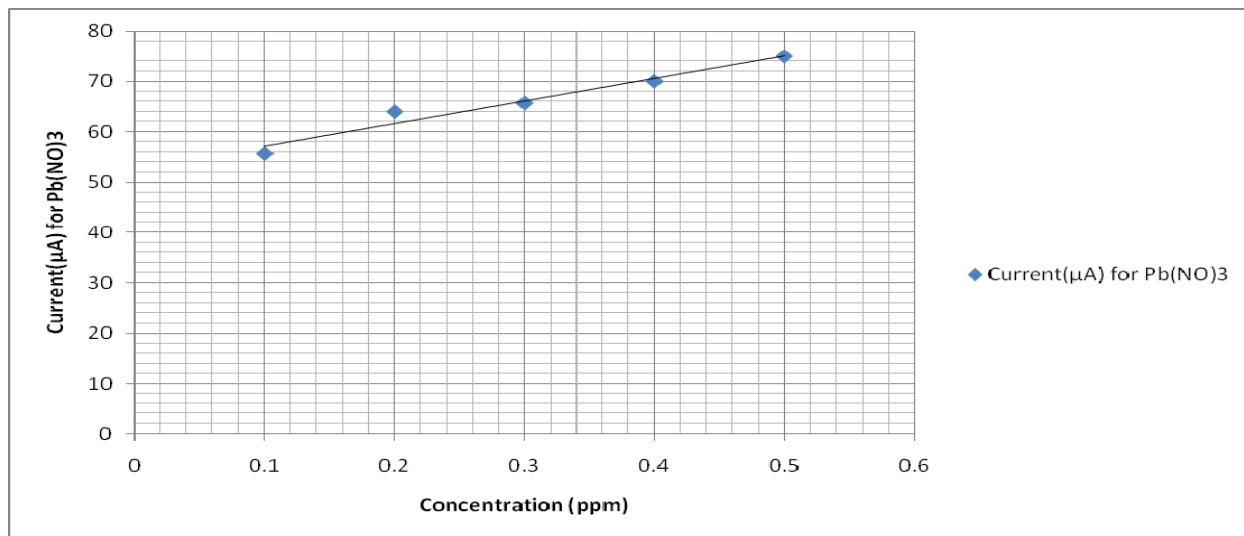


**Figure 4. 75:** A plot of peak current against concentration for  $\text{Pb}(\text{NO})_3$ .

Table 4–44 below shows statistical parameters obtained when an a plot of peak current against concentration was done.

**Table 4-44: Summary Output for Pb(NO)<sub>3</sub>.**

<b>Regression Statistics</b>	
Multiple R	0.97992872
R Square	0.960260297
Adjusted R Square	0.947013729
Standard Error	1.656502339
Intercept	52.7
Concentration (ppm)	44.6

Linearity  $r = 0.9799$

$$r^2 = 0.96$$

$$f = 72.49$$

The values of  $r$  and  $r^2$  tending towards 1, and the values of f-anova are pointing towards perfect linearity.

#### 4.9.2.1 Limits of detection (LOD)

$$Y_{LOD} = a + 3(S_{Y/X}) \dots \dots \dots (4.5)$$

$$= 52.7 + 3(1.65)$$

Linear equation

$$Y = a + bx \dots \dots \dots (4.6)$$

$$Y_{LOD} = a + bx_{LOD} \dots \dots \dots (4.7)$$

$$57.65 = 52.7 + 44.6x_{LOD}$$

$$x_{LOD} = 0.11 \text{ ppm}$$

According to this calculation the LOD for  $Pb(NO)_3$  was 0.11 ppm. A similar experiment was done by Babyak et al 2003 where parts-per-billion levels of lead were detected using square-wave anodic stripping voltammetry with a boron-doped diamond electrode. The LOD in that case was 10 ppb. This value is smaller than our results because other factors affecting the detection limit such as pH, other electrolytes, use of surfactants and presence of other dissolved ions were not optimized.

#### 4.9.2.2 Limits of Quantitation (LOQ)

$$Y_{LOQ} = a + 10(S_{Y/X}) \dots \dots \dots (4.8)$$

$$= 52.7 + 16.56$$

$$Y = a + bx_{LOD} \dots \dots \dots (4.9)$$

$$69.26 - 52.7 = 11.6 x_{LOQ} \dots \dots \dots (4.10)$$

$$x_{LOQ} = 0.37 \text{ ppm} \dots \dots \dots (4.11)$$

According to this calculation the LOQ for  $Pb(NO)_3$  was 0.37 ppm. A similar experiment was done by Babyak, et al 2003 where Parts-per-billion levels of cadmium were detected using square-wave anodic stripping voltammetry with a boron-doped diamond electrode. The LOQ in this case was 10 ppb. This value is smaller than our result because other factors affecting the detection limit such as pH and electrolyte were supposed to be exploited.



Competition between lead and cadmium on active sites of modified pyrolytic graphite electrode may also explain the calculated higher values of LOD and LOQ for cadmium. Lead may out compete cadmium for active sites because of its larger diffusivity.

# CHAPTER FIVE

## CONCLUSIONS AND RECOMMENDATIONS

### 5.1 CONCLUSIONS

#### 5.1.1 Cyclic voltammetry

The results from cyclic voltammetry demonstrated that voltammograms obtained depend on the electrolyte and the solvent used. Ferrocene was used as standard and values of the parameters such as the ratio of anodic peak current to cathodic peak current was unity ( $i_{pa}/i_{pc}=1$ ), plot of peak current versus square root of scan rate gave a straight line which agrees with the literature. The solvent of choice must dissolve the chemical species of interest fully. For the present research work the best electrolyte was found to be 0.1 M KCl for dissolving of lead nitrate and cadmium bromide salts.

#### 5.1.2 Anodic stripping-square wave voltammetry

Anodic stripping-square wave voltammetry was used with pyrolytic graphite electrode to detect cadmium and lead in prepared solutions of lead and cadmium. This research work presented the results obtained for electrochemical stripping voltammetric analysis of cadmium and lead using in-house fabricated electrode. The three-electrode configuration system coupled with AS- SWV has provided a means of a relatively inexpensive on-site detector for trace levels of trace metals. Detection of these metals was carried out on modified pyrolytic graphite electrode using the optimized procedures developed for measurements in this work. The un-modified electrode acted

as supports for the electro-deposition of polyaniline film. With the optimized working conditions, the results obtained indicate that the modified electrochemical sensors are sensitive enough for the SV-SWA determination of cadmium and lead in solution.

The use of modified pyrolytic graphite electrode for the simultaneous detection of lead and cadmium ions has been presented.

Electro polymerization of polyaniline on the surface of the electrode increased sensitivity in detecting lead than cadmium. The increased deposit of the lead ions on the surface of the electrode occupies the active sites, leaving few active sites for cadmium ions to be reduced. This explains low detection for cadmium ions in solution.

The enhanced electrode sensitivity has been achieved by optimizing various parameters such as deposition potential, deposition time, frequency, step potential and amplitude. In this study the LOD for  $\text{Pb}(\text{NO})_3$  was 0.11 ppm while that of cadmium bromide was 0.908 ppm. The maximum signal enhancement for lead ions was 2.5 times while for cadmium bromide it was 1.6 times.

Modified pyrolytic graphite electrode can be a suitable candidate for detection of heavy metals. Further optimization of the modified pyrolytic graphite electrode can be carried out to detect nanomolar /sub-nanomolar level of heavy metals by investigating other factors such as pH and use of surfactants.

## 5.2 Recommendations

Based on the conclusions made from the results of this study the following are the recommendations for further work:

- 1) Modification of the electrode can further be carried out on materials such as glassy carbon and bismuth electrodes.
- 2) Other Polymeric materials than can be used as conducting polymers such polypyrroles and polythiophenes should be investigated for sensitivity enhancement.
- 3) Non-Instrumental factors such as the effect of other ions,  $Mg^{2+}$ ,  $Ca^{2+}$ ,  $Ni^{2+}$ ,  $Fe^{2+}$  on peak current should also be investigated.
- 4) The effect of electrolytes such as  $KNO_3$ ,  $NaCl$  and related salts on the peak currents should be investigated.
- 5) I have developed a sensor which can be used to determine lead and cadmium in solution simultaneously in solution.
- 6) The AS-SWV is an environmentally friendly and uses less energy compared to AAS ,hence its green technology that has less impact on the surrounding and conserves energy.

## REFERENCES

**Alegret, S., Merkoci A.,(2003).** Composite and Biocomposite Materials for Electrochemical Sensing in Integrated Analytical Systems. 377 –412.

**Allen J.; Bard Larry R. Faulkner(2000).**Electrochemical methods: Fundamentals and applications 2<sup>nd</sup> Ed. Wiley ISBN 0471043729.

**Allen J.; Bard, Larry R. Faulkner (2000).**Electrochemical methods: Fundamentals and applications 2<sup>nd</sup> ed.Wiley.ISBN 0471043729 .

**Anandhakumar, S., Mathiyarasu, J., (2010).** Simultaneous Determination of Cadmium and Lead Using PEDOT/PSS Modified Glassy Carbon Electrode American Journal of Analytical Chemistry, 2011, 2, 470-474.

**Bard A.J and Faulkner L.R(1980).**Electrochemical methods: Fundamentals and applications John wiley and sons,Newyork.

**Bard and Faulkner L.R(2001).**Electrochemical methods: Fundamentals and applications 2 Edition , wiley Newyork,ISBN 0-471-04372-9.

**Bosch R.W.,Ferron D.,and Cells J.P. (2007).**"Electrochemistry in light body reactors",CRC press,Vol. 6 pp 45-48.

**Brown,T.L;Eugene L.H.,Jr.,Bruce E.B, Julia.R.B (2003).**"Electrochemistry Chemistry".9th edition US:Pearson Education.ISBN 0-13-066997-0.OCLC 47953855.

**Carol Babyak, Ronald B. Smart (2003).**Electrochemical Detection of Trace Concentrations of Cadmium and Lead with a Boron-Doped Diamond Electrode: Effect of KCl and KNO<sub>3</sub> Electrolytes, Interferences and Measurement in River Water. Electroanalysis 2004, 16, No3.

- Christopher M.A and Ana Maria O.B (1993).** Electrochemistry: Principles ,methods applications, oxford science publications.
- Cook D.R.,Watkin D.J.,Bushnel D.W.(1999).**"Long term follow-up of pyrolytic carbon metacarpophalangeal Implants".J Bone. Joint surg.81.
- Cotton F.A.;Wilkinson G.;Murillo C.A (1999).**Advanced Inorganic Chemistry (6<sup>th</sup> ed), New york Wiley.
- Dalibor Stankovic,;Dragan Manojlovic,Goran Roglic ( 2011).** Simultaneous Determination of Pb and Cd Traces in Water Samples by Anodic Stripping Voltammetry Using a Modified GC Electrode. Electroanalysis , 23, No. 8, 1928 – 1933.
- Greely R.S.(1960).**Electrochemistry of inorganic compounds. Phys.Chemistry, vol 64,652
- Gritzer,G.,Kuta J.(1984).**"Recommendations on reporting electrode potentials in non aqueous solvents".Pure Appl. Chem 56 (4):461-466.
- Hinman A.S.,Pons S. and Cassidy J. (1985).** Voltammetry and coulometry with Immersed thin layer electrode-1.Model effect of solution sensitivity in linear sweep voltammetry. Electrochimica.Acta 30,89-94.
- Hobart H. Willard;lynne and John AD(1988).**Instrumental method of analysis 7<sup>th</sup> edition.Belmont california.pp118-148.
- Iwunze M.O.,Sucheta A. and Russling J.F. (1990).**Bicontinuous microemulsions as a media for electrochemical studies. Anal. Chem 62,644-649.
- Kamau,G.N.,Willis,W.S and Rusling,J.F(1985).**Electrochemical and electro spectroscopic studies of highly polished carbon electrodes.Anal. Chem.Vol 57 545-551.

**Kiratu M. J., (2009).**Msc thesis "Electrochemical and spectroscopic characterization of ferrocene thiosemicarbazone ligand and copper complexes".

**Kissinger, Peter,William R.Heineman (1996).**Laboratory techniques in electroanalytical chemistry,2<sup>nd</sup> edition,Revised and expanded (2<sup>ed</sup>) CRC.ISBN 0824794451.

**Larry L Faulkner (1983).**Electrochemical characterization of chemical systems ,Academic press, Vol. 3pages 137-248

**Lee JD.(1996).**Concise Inorganic chemistry 5<sup>th</sup> edition, pp 51,952.

**Miriam Masila K. (1996)** .Electrochemical catalytic Dehalogenation of Organohalide pollutant  
Msc thesis university of Nairobi cho.Q.D.C 15 PP 85.

**Mohd fairulnizal and Ibtisam e. Tothill/2011.**Determination of Lead(II), Cadmium(II) and Copper(II) in Waste-Water and Soil Extracts on Mercury Film Screen-Printed Carbon Electrodes Sensor,Sains Malaysiana 40(10)(2011)1153–1163.

**Nicholson,R.S.;Irving. Shain (1964),**"Theory of stationery electrode polarography.single scan and Cyclic methods applied to reversible,Irreversible and kinetic systems.Anal Chem 37 1351-1355".

**Pavlishchuk,Vitaly V.,Antony W. Addison (2000).**"Conversion constants for Redox potential measured versus different electrodes in acetonitrile solutions at 25<sup>0</sup>C.Inorganic chemica Acta 298 (1).

**Pipat Chooto, P., Puchong (2010).** Determination of trace levels of Pb(II) in tap water by anodic stripping voltammetry with boron doped diamond electrode. Anal. Chem., 1998, 35, 345–348 .

**Pletcher,D (1975).**Application of electrochemical techniques to the study of homogeneous chemical reactions,chemical society reviews,14.

pp 2-8.

**Sawyer,D.T and Robert,J.L.Roberts Jr (1995).**"Electrochemistry for Chemist". John Willey and sons,Inc 205.

**Scogg, D.A, West, D.M, Holler, F.J,(1988).**Fundamentals of analytical chemistry,5<sup>th</sup> edition,saunders publishers college,New York.

**Sukeri Anandhakumar, Jayaraman Mathiyarasu,(2011).**Simultaneous Determination of Cadmium and Lead Using PEDOT/PSS Modified Glassy Carbon Electrode. American Journal of Analytical Chemistry, 2011, 2, 470-474.

**Swain GM, Sonthalia P, McGaw E, Show Y (2004).** Metal Ion Analysis in contaminated water samples using anodic stripping voltammetry and a nano crystalline diamond thin-film electrode. Anal Chim Acta522, 35–44.

**Wiley-VCH Verlag GmbH&Co., Weinheim (2004)** .Nanostructured Polyaniline Sensors, Chem. Eur. J. 2004, 10, 1314-1319.

**Willard,H.H.,Merrit,L.L.,Dean,J.A and Frank,S.A(1986).**,Instrumental methods of analysis. Sixth edition.CBPS publishers,Delhi-India.

**William Hill. J,Ralph H.Petruci,Terry McCreary,Scott.S. Perry (2004).**General Chemistry: An integrated Approach (7<sup>th</sup> Edition).Pearson Education publishers.pp 1200.

**Y. Bonfil, E. Kirowa-Eisner (2009).** Determination of nanomolar concentrations of lead and cadmiumby anodic-Anodic stripping-Anodic stripping-square wave voltammetry at the silver electrode. Analytica Chimica Acta 457 (2002) 285–296.



**Z. M. Wang, H. W. Guo, E. Liu, G. C. Yang,(2009).** Determination of Trace Cd and Pb in Solutions Having Surfactants *Electroanalysis* 2005 ,17,No.10.

**Znoeva Anna Viladmirovna (2006),** " The Improvement of anodic stripping voltammetric (ASV) method of cadmium and mercury determination" Msc thesis Lulea University of technology ,Russia 2006:117 pp 4-16.

**Zoski, cynthia G.(2007).**Handbook of electrochemistry. Elsevier science. ISBN 0444519580.